

35
11-27-62

MASTER

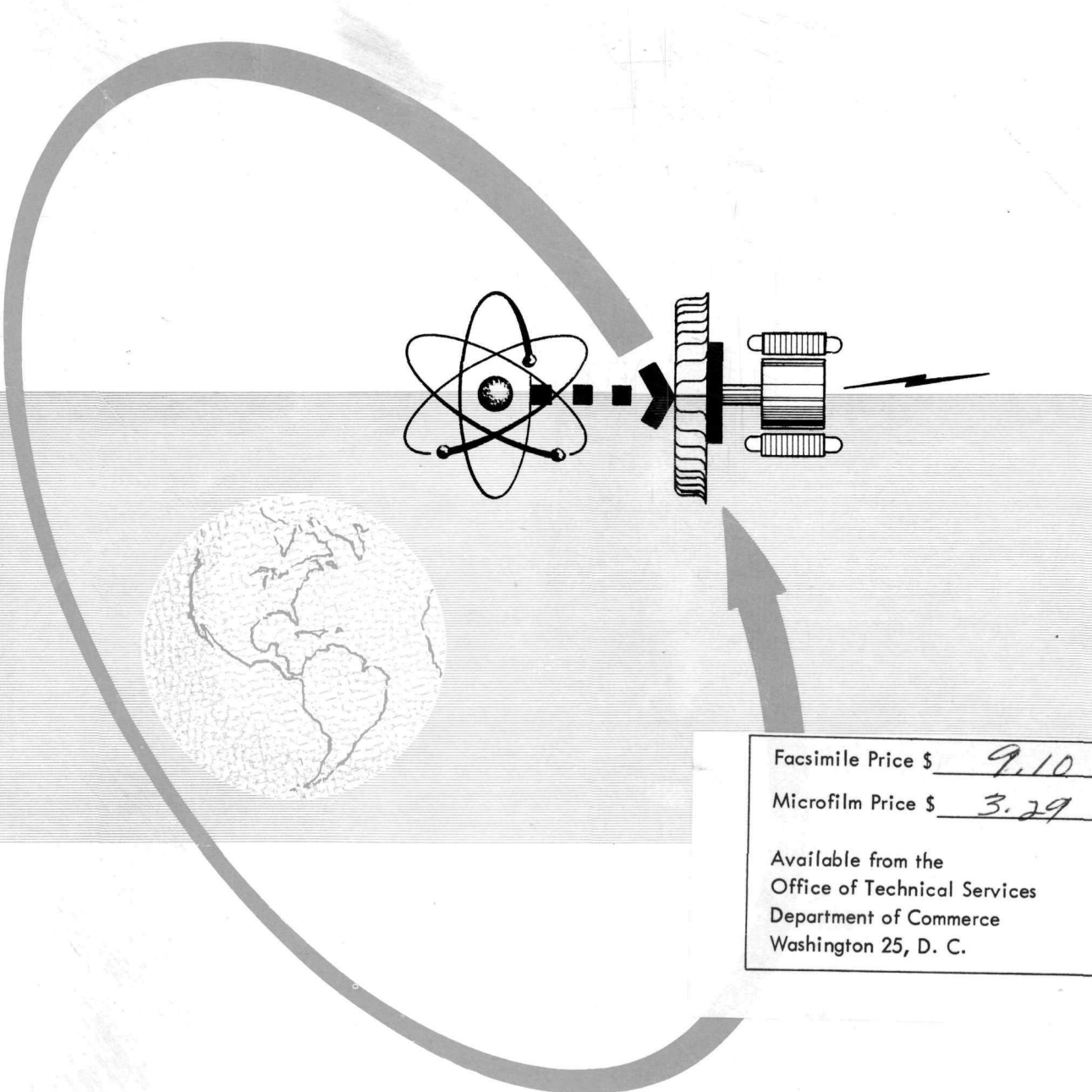
NAA-SR-6307

TRW REPORT No. ER-4108

THE SNAP II POWER CONVERSION SYSTEM

TOPICAL REPORT No. 15

CRU DESIGN AND DEVELOPMENT



AEC RESEARCH AND DEVELOPMENT REPORT

PREPARED UNDER SUBCONTRACT
N 843 FS - 101221 FOR ATOMICS
INTERNATIONAL, A DIVISION OF
NORTH AMERICAN AVIATION, INC.



TAPCO a division of
Thompson Ramo Wooldridge Inc.
CLEVELAND, OHIO

DISCLAIMER

This report was prepared as an account of work sponsored by an agency of the United States Government. Neither the United States Government nor any agency Thereof, nor any of their employees, makes any warranty, express or implied, or assumes any legal liability or responsibility for the accuracy, completeness, or usefulness of any information, apparatus, product, or process disclosed, or represents that its use would not infringe privately owned rights. Reference herein to any specific commercial product, process, or service by trade name, trademark, manufacturer, or otherwise does not necessarily constitute or imply its endorsement, recommendation, or favoring by the United States Government or any agency thereof. The views and opinions of authors expressed herein do not necessarily state or reflect those of the United States Government or any agency thereof.

DISCLAIMER

Portions of this document may be illegible in electronic image products. Images are produced from the best available original document.

PROJECT

512-078252-08

NAA-SR-6307
THE SNAP II POWER CONVERSION
SYSTEM TOPICAL REPORT NO. 15
CRU DESIGN AND DEVELOPMENT
TRW REPORT NO. ER-4108

PREPARED BY:

Rankine Power Systems Dept.

CHECKED BY:

D. L. Southam

D. L. Southam
Senior Project Engineer

APPROVED BY:

G. Y. Ono

G. Y. Ono
Senior Project Engineer

E. G. Rapp

E. G. Rapp
Chief Engineer

C. G. Martin

C. G. Martin
Associate Director, Engr.

Prepared under Subcontract N843FS-101221 for Atomics International
A Division of North American Aviation Inc.

DATE

Prepared: July, 1961

Published: October, 1962

DEPARTMENT

0868

Thompson Ramo Wooldridge Inc.

CLEVELAND, OHIO, U. S. A.

LEGAL NOTICE

This report was prepared as an account of Government sponsored work. Neither the United States, nor the Commission, nor any person acting on behalf of the Commission:

- A. Makes any warranty or representation, express or implied, with respect to the accuracy, completeness, or usefulness of the Information contained in this report, or that the use of any Information, apparatus, method, or process disclosed in this report may not Infringe privately owned rights; or
- B. Assumes any liabilities with respect to the use of or for damages resulting from the use of Information, apparatus, method, or process disclosed in this report.

As used in the above, "person acting on behalf of the Commission" includes any employee or contractor of the Commission to the extent that such employee or contractor prepares, handles, or distributes, or provides access to, any information pursuant to his employment or contract with the Commission.

ABSTRACT

SNAP II is the designation for a 3 kw nuclear auxiliary power unit to be used in a satellite vehicle. This system consists of a reactor heat source, a mercury Rankine engine and an alternator. The alternator, mercury pump, turbine, and reactor coolant pump are mounted on a common shaft supported by mercury lubricated bearings. Design details and test results of combined rotating unit (CRU) development are described in this report. The work was performed under a subcontract to Atomics International as part of the Atomic Energy Commission Contract AT (11-1) GEN-8.

TABLE OF CONTENTS

	Page No.
1.0 Summary	1
2.0 Introduction	2
3.0 CRU Design Evolution	7
3.1 Conceptual Design	7
3.2 CRU I Design	11
3.2.1 Housing	17
3.2.2 Shaft	21
3.2.3 Bearings	22
3.2.4 Turbine	22
3.2.5 Alternator	23
3.2.6 Mercury Pump	23
3.2.7 Sodium Pump	24
3.2.8 Fabrication	24
3.3 CRU II Design	25
3.3.1 Housing	25
3.3.2 Shaft	25
3.3.3 Bearings	25
3.3.4 Turbine	26
3.3.5 Alternator	26
3.3.6 Mercury Pump	26
3.3.7 Sodium Pump	26
3.4 CRU III Design	27
3.4.1 Housing	27
3.4.2 Shaft	28
3.4.3 Bearings	34
3.4.4 Turbine	34
3.4.5 Alternator	34
3.4.6 Mercury Pump	35
3.4.7 NaK Pump	35



TABLE OF CONTENTS (Continued)

	Page No.
4.0 CRU Test and Development	37
4.1 Test Equipment	37
4.2 Data Analysis Techniques	45
4.3 CRU I Tests	49
4.3.1 Critical Speed Test Results	54
4.3.2 Vibration Testing	57
4.3.3 CRU Component Testing (Alternator Stator Assembly)	72
4.3.4 Shock Testing (Alternator Stator)	76
4.4 CRU II Tests	78
4.5 CRU Test Summary	85
5.0 Conclusions	95

LIST OF ILLUSTRATIONS

Figure No.	Page No.	
1	SNAP I Turbomachinery Package	8
2	Design I	9
3	Design II	10
4	Design III	12
5	Design IV	13
6	Design V	14
7	Design VI	15
8	Design VII	16
9	Cross-Sectional View of SNAP II CRU	18
10	External View of CRU	19
11	Turbo-generator Parts Prior to Assembly	20
12	Curves for CRU III	33
13	Performance Test Rig Schematic	38
14	View of Components Located in CRU Booth	40
15	View of Components Located in Condenser Booth	41
16	Control Console for SNAP II Performance Rig	42
17	Mercury Loop Thermocouple Locations	46
18	Data Categories	47
19	Performance Test Rig Flow Diagram	50
20	View of CRU Test Enclosure	51
21	Location of CRU Internal Temperature Probes	52
22	Location of CRU External Temperature Probes	53
23	Vibration Amplitude vs Shaft Speed	56
24	Plot of Significant Parameters CRU I-1B	58
25	Statistical Results of CRU I-1B-1	59
26	Statistical Housing Temperature Results (CRU I-1B-1)	60
27	Vibration Test Flow Schematic	65
28	View of MB Console and Exciter Test Facility	66
29	Test Recording Equipment	67
30	Lateral Fixturing Required for CRU I	68
31	Longitudinal Fixturing Required for CRU I	69
32	Historical Summary of CRU I	71
33	View of Turbine Bearing Surface	73
34	Vibration Test of Alternator Stator	74
35	Vibration Test of Alternator Stator (Constant Displacement Portion)	75
36	Stator Shock Test Oscilloscope Pattern	77
37	Alternator Stator Shock Test Fixture	80
38	Component Power Losses at No Load Versus Speed	82
39	Willans Line CRU II 2-2	83
40	Computer Flow Diagram	86
41	Performance Map CRU II	87
42	Shaft Power vs Turbine Inlet Pressure for CRU II	88



LIST OF TABLES

	Page No.
I Initial SNAP II Operating Requirements	3
II Weight, Mass Moment, and Critical Speeds For CRU's I, II, and III	29
III Distribution of CRU III Shaft Assembly Weight and Corresponding Static Deflection for a Typical Critical Speed Determination	30
IV Representative Shaft Conditions and Critical Speeds	32
V Performance Test Rig Capabilities	44
VI Operating Conditions CRU I 20-Day Endurance Run	55
VII Summary of CRU I-1B-1 Test Results	61
VIII CRU II Altered Input Parameters	79
IX Component Power Consumption	79
X Summary of CRU I-II Testing	90
XI Summary of CRU I-II-III Testing	92

1.0 SUMMARY

Design objectives and features of combined rotating units (CRU) I, II, and III are described and illustrated. In addition, a comparison of test results with design objectives is presented for one CRU I and two CRU II units. Test results of CRU I and II units have indicated the feasibility of operating a CRU for long periods of time at the required design point. Preliminary environmental tests of CRU I have indicated that the rotating unit can withstand the launch environments of vibration and shock.

Modifications and improvements in the CRU components are currently under development to more exactly meet performance objectives for the flight systems. The future CRU units and the remainder of the power conversion system will be utilized for extensive system development, including nuclear and orbital start testing.

2.0 INTRODUCTION

The SNAP II auxiliary power unit for 3 kw of electrical output consists of a reactor heat source and a power conversion system. The power conversion system is a mercury Rankine engine composed of:

A mercury boiler heated by NaK reactor coolant

An axial flow impulse turbine, which extracts energy from the superheated mercury vapor

A condenser which returns the vapor to a liquid state

A mercury pump which returns the condensate to the boiler

The turbine directly drives the alternator, the mercury pump, and a permanent magnet induction NaK pump which is designed to circulate the NaK between the mercury boiler and the reactor.

At the initiation of the SNAP II program, packaging of mercury environment CRU's had already been accomplished for the SNAP I program (which preceded SNAP II by approximately one year). SNAP I also employed a mercury Rankine engine for a 500 watt electrical output using the heat energy from the decay of an isotope.

Selection of the cycle conditions, which established the operating conditions for the SNAP II CRU were reported in Topical Report No. 1 entitled "Design Point Determination" (Thompson Ramo Wooldridge Engineering Report No. 3619, Document AE-61 A). These initial operating requirements are summarized in Table I.



TABLE I
INITIAL SNAP II OPERATING REQUIREMENTS

Alternator

Net Electrical Output	3 kw
Frequency	2000 cps
Frequency Regulation	1%
Voltage	110 volts
Voltage Regulation	5%
Power Factor	1 to .8 lagging
Shaft Power Required	3.88 kw

Reactor Coolant Pump (Na Pump)

Operating Temperature	1000°F
Flow	45.2 lb/min
Pressure Rise	3 psi
Shaft Power Requirement	.443 kw

Mercury Pump

Maximum Inlet Temperature	420°F
Inlet Pressure	5.5 psia min
Outlet Pressure	138 psia
Flow Rate	37 lb/min
Shaft Power Requirement	.24 kw

TABLE I (continued)

Mercury Bearings

Inlet Temperature	430°F maximum
Flow Rate	20 lb/min
Shaft Power Required	.600 kw

Mercury Turbine

Shaft Power Output	5.16 kw
Inlet Temperature	1150°F
Inlet Pressure	105 psia
Outlet Temperature	600°F
Outlet Pressure	6.5 psia
Flow Rate	17 lb/min
Efficiency	55%

Selection of optimum components to meet the SNAP II objectives has been described in previous topical reports. This component selection is summarized as follows:

Alternator

A radial gap permanent magnet alternator was selected because of the inherent reliability and light weight of such a machine. The stator was wound two phase to provide maximum slot fill and efficiency. External connections provided the required single phase operation. In order to improve operating efficiency, the alternator output was later modified to two phase operation. The rotor magnet of Alnico V was magnetized with six poles to provide the required 2,000 cycle operation at 40,000 rpm.

Reactor Coolant Pump

A shaft-driven rotating magnet pump was selected as the method of circulating the reactor coolant. With this pump, a shaft mounted permanent magnet was used to induce a flow of sodium or NaK by electromagnetic reactions. Both radial gap and axial gap-type pumps were evaluated. In the radial gap design, the stator consisted of a coil of tubing surrounding the magnetic rotor. Rotation of the magnetic rotor then induced a flow of sodium in the stator coil. In the axial gap design, rotor motion induced a rotation of the reactor coolant in a pumping annulus. The pumping action was then developed by centrifugal means similar to a centrifugal pump. The axial gap pump was ultimately selected because of improved efficiency and the ease of CRU integration.

Mercury Pump

The mercury pump consisted of a shaft-driven centrifugal pump and a jet type booster pump.

The jet pump utilized a portion of the centrifugal pump discharge to boost the condensed mercury pressure. In this manner centrifugal pump cavitation could be avoided with the high shaft speed and low net positive suction head of 6 psia.

Mercury Bearings

Several types of mercury lubricated bearings are currently being evaluated for the SNAP II application. Both the hydrosphere and the combination of two journal bearings with a double acting thrust bearing were evaluated in the design evolution leading to the CRU I and II units.

Mercury Turbine

A two-stage axial flow impulse turbine was selected to best meet the SNAP II requirements. An impulse machine was selected to avoid excessive shaft thrust loads. The turbine wheels were shrouded to prevent tip leakage and to allow a design wherein separable turbine blades of optimum materials could be used. The 250° F of superheat at the turbine inlet avoided excessive mercury condensation and eliminated the need for complicated separation devices between stages.

3.0 CRU DESIGN EVOLUTION

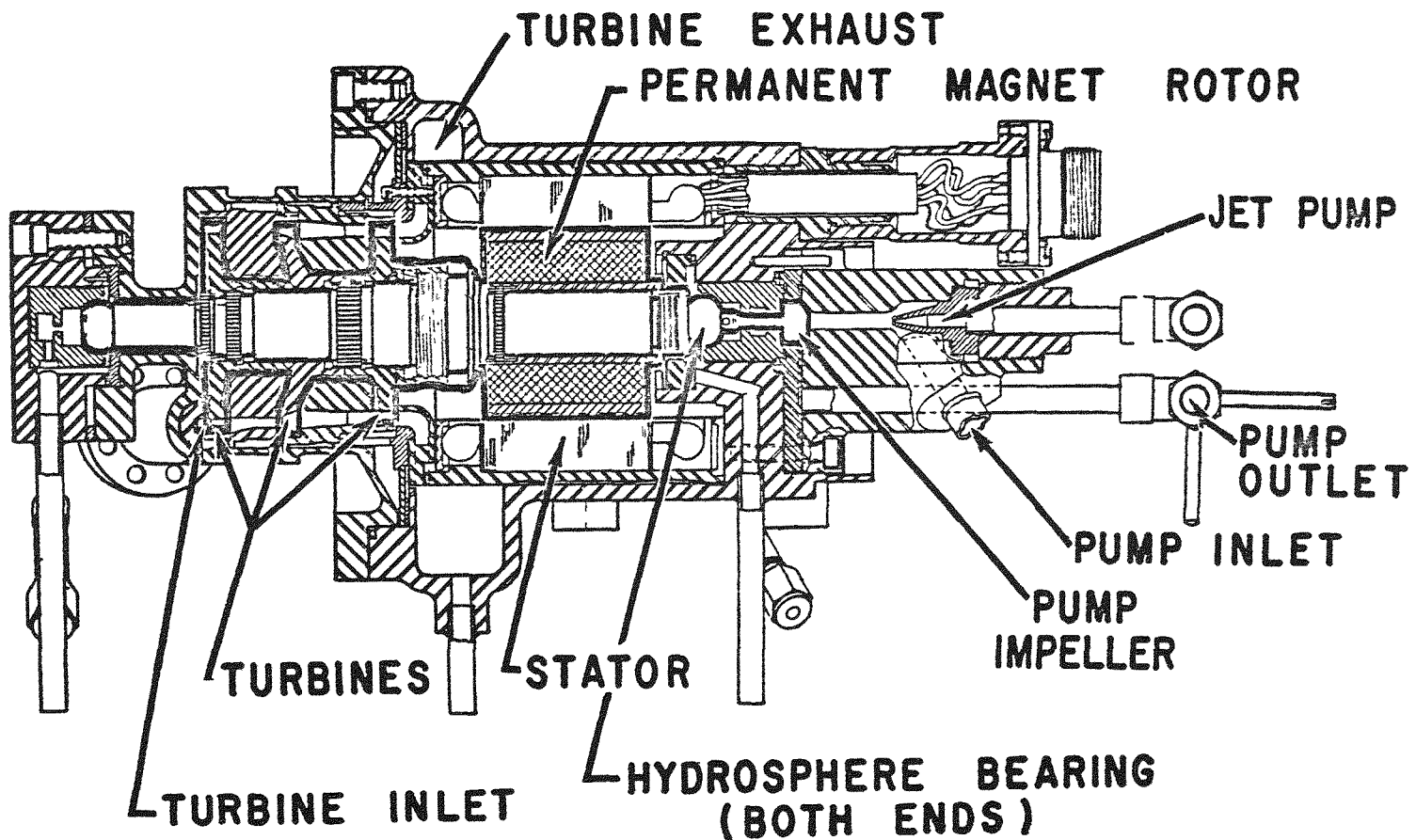
3.1 Conceptual Design

SNAP II CRU design was developed on the foundation of SNAP I technology, which had reached the point of conversion from specification to hardware at the time the SNAP II CRU design was initiated. Figure 1 shows the basic design features of the SNAP I rotating unit. The SNAP I program provided an understanding of turbine, alternator, mercury pump, and mercury bearing performance while operating in an integrated rotating unit.

The first step in SNAP II CRU development was the integration of initial component designs to attain a package which could be converted to hardware. Seven design drawings have been selected from the drawings prepared during this period to illustrate evolution of the SNAP II CRU. Design I (Figure 2) gave priority to optimum component design, deferring the resolution of compromises dictated by component relationships to later development. The turbine dynamometer test unit furnished the design for the turbine, its inlet and exit scrolls, and the interstage seal. The alternator design met the electrical requirements, the expected stress capability of the rotor, and the dimensional limitations of the gap. The SNAP I program provided the base lines for the bearings, the mercury pump design, and the rotating unit configuration. The first sodium pump was a radial gap design.

Design II approached a solution to the critical speed problem created by the size, position, and need for thermal isolation of the radial gap sodium pump. As shown in Figure 3, Design II provided an overhung axial gap sodium pump and increased shaft diameter. This change increased the alternator shaft diameter and the turbine interstage seal and required a shaft extension from the hydrosphere bearing at the sodium pump end.

SNAP I TURBOMACHINERY PACKAGE



DESIGN I

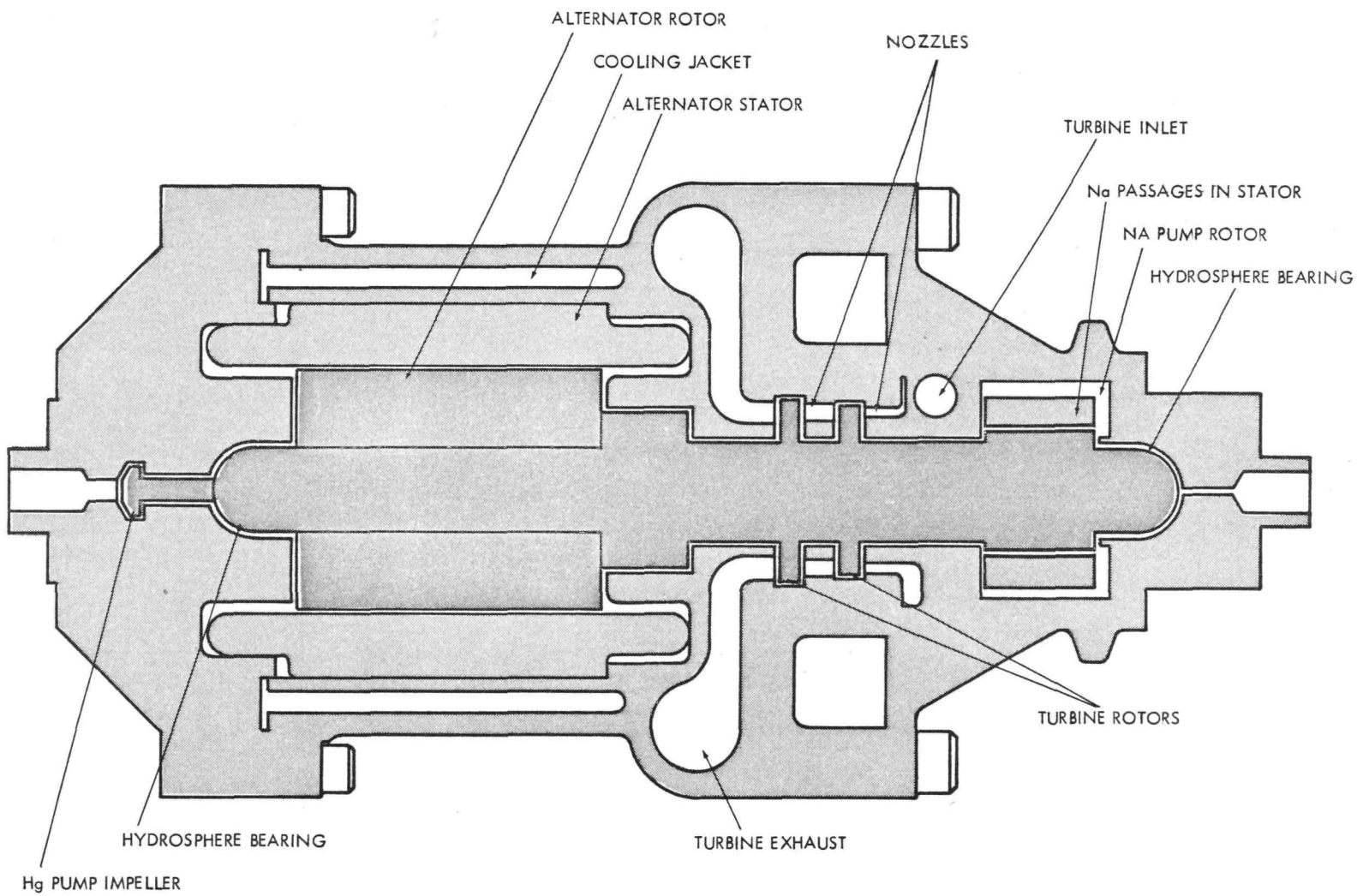
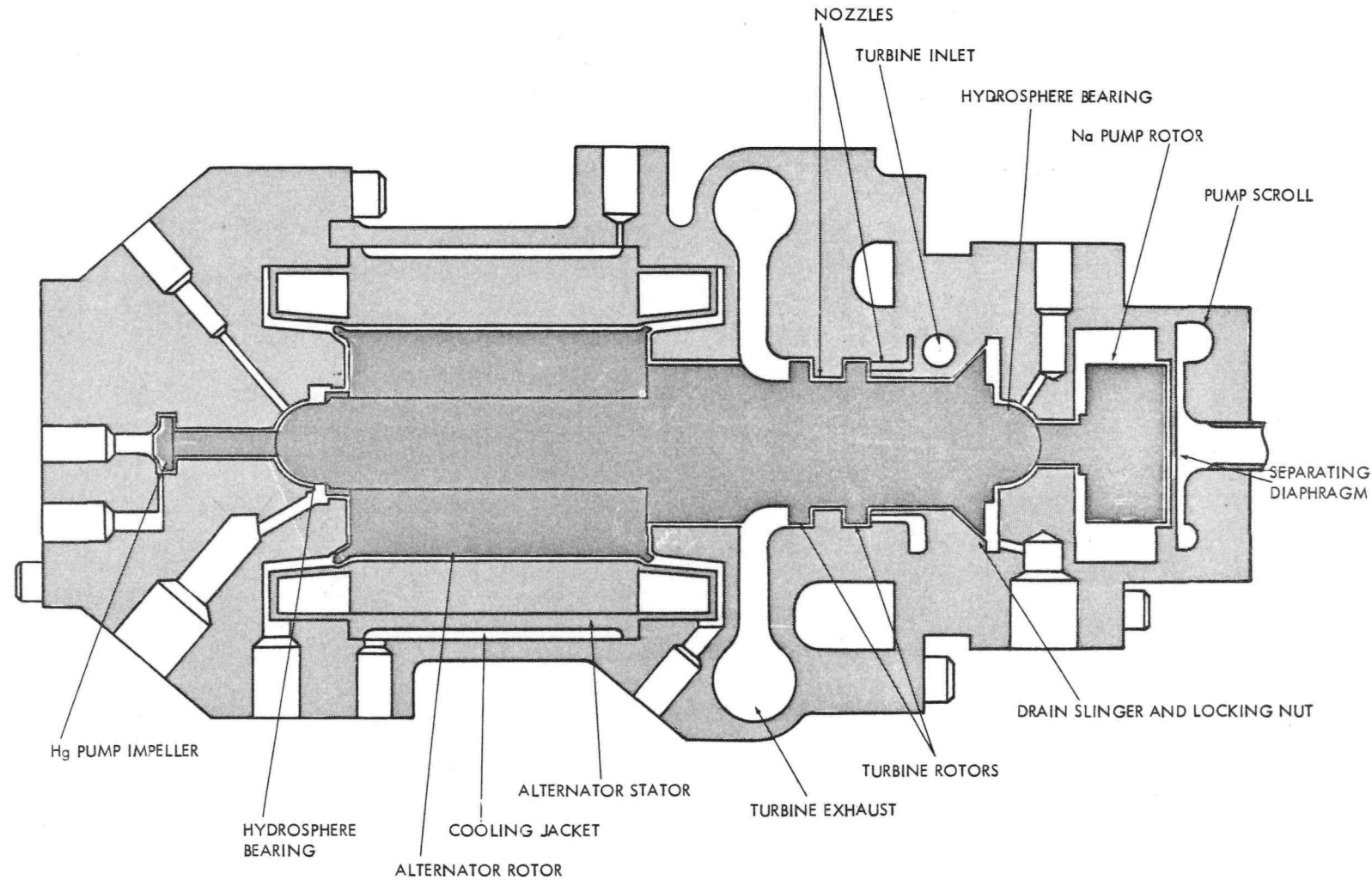


FIGURE 2

DESIGN II



The shaft extension required in Design II implied reduction of bearing surface, complex fabrication and assembly, an intensified seal problem, and an intricate arrangement for providing bearing supply and drain. Design III, therefore, changed to a journal bearing at the sodium pump end, as shown in Figure 4. Design IV, Figure 5, using an overhung radial gap sodium pump extended from a journal bearing, was also investigated.

Further analytical efforts, coupled with initial component test data, provided more information about expected power losses, thermal effects and material requisites. In addition, the seals and shaft geometry were modified to decrease power losses as well as increase the critical speed of the rotating unit to 46,500 rpm. Initial calculations indicated a 38,000 rpm critical speed, which was extremely close to the desired operating speed of 40,000 rpm.

The CRU housing was modified to provide improved temperature controls, particularly in the critical bearing areas. Designs V and VI (Figures 6 and 7) were a result of these changes. These designs, however, were not completely satisfactory, since the combination of a hydrosphere and a journal bearing complicated the mercury pump assembly. Furthermore, this bearing combination required a thrust balance between the hydrosphere bearing and the other CRU components. To improve CRU reliability for all possible thrust load requirements, two journal bearings, combined with a double-acting thrust bearing, were designed, as shown in Figure 8.

3.2 CRU I Design

Study of system characteristics, thermal maps, stress, critical speed, rotating seals, static

DESIGN III

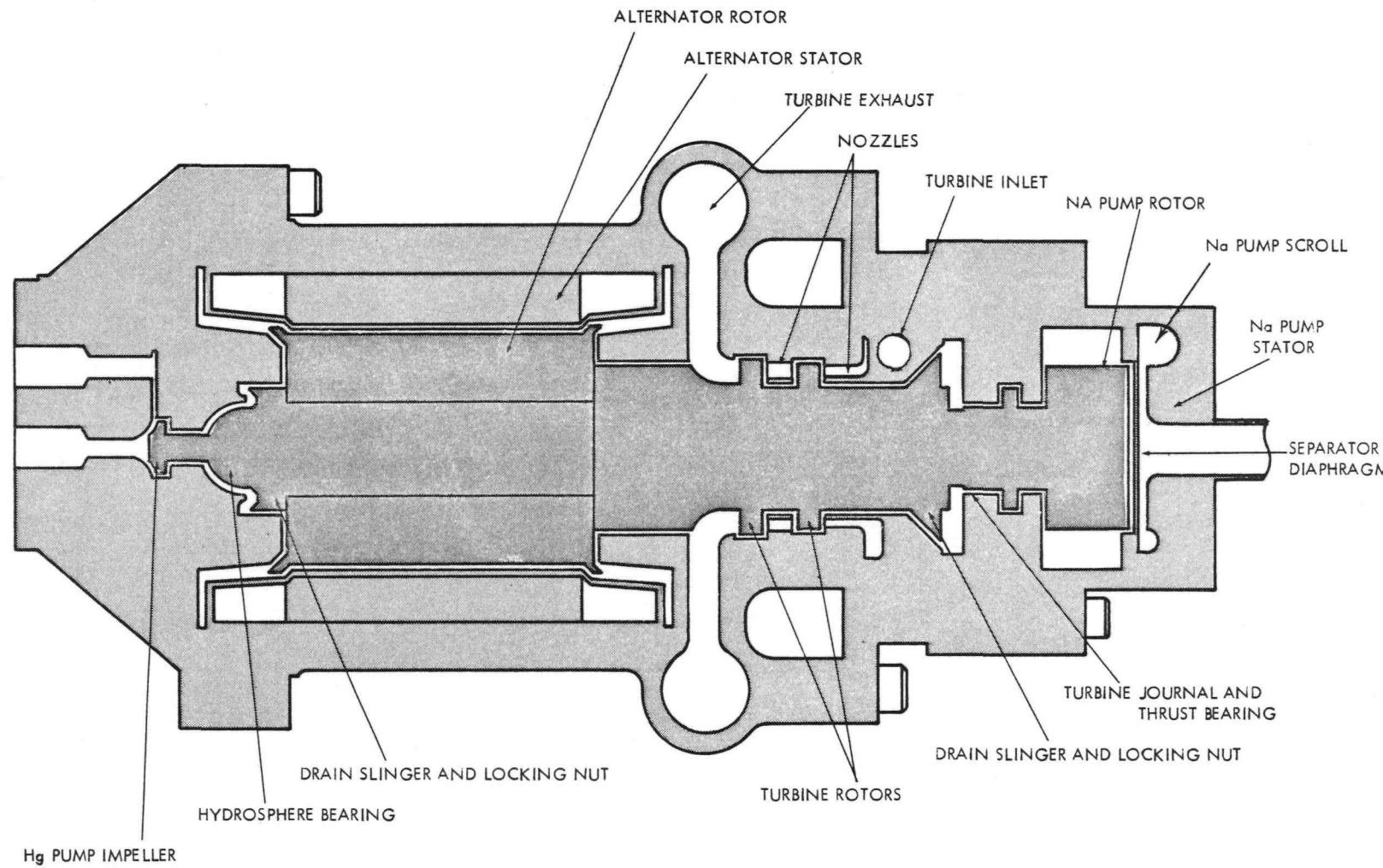
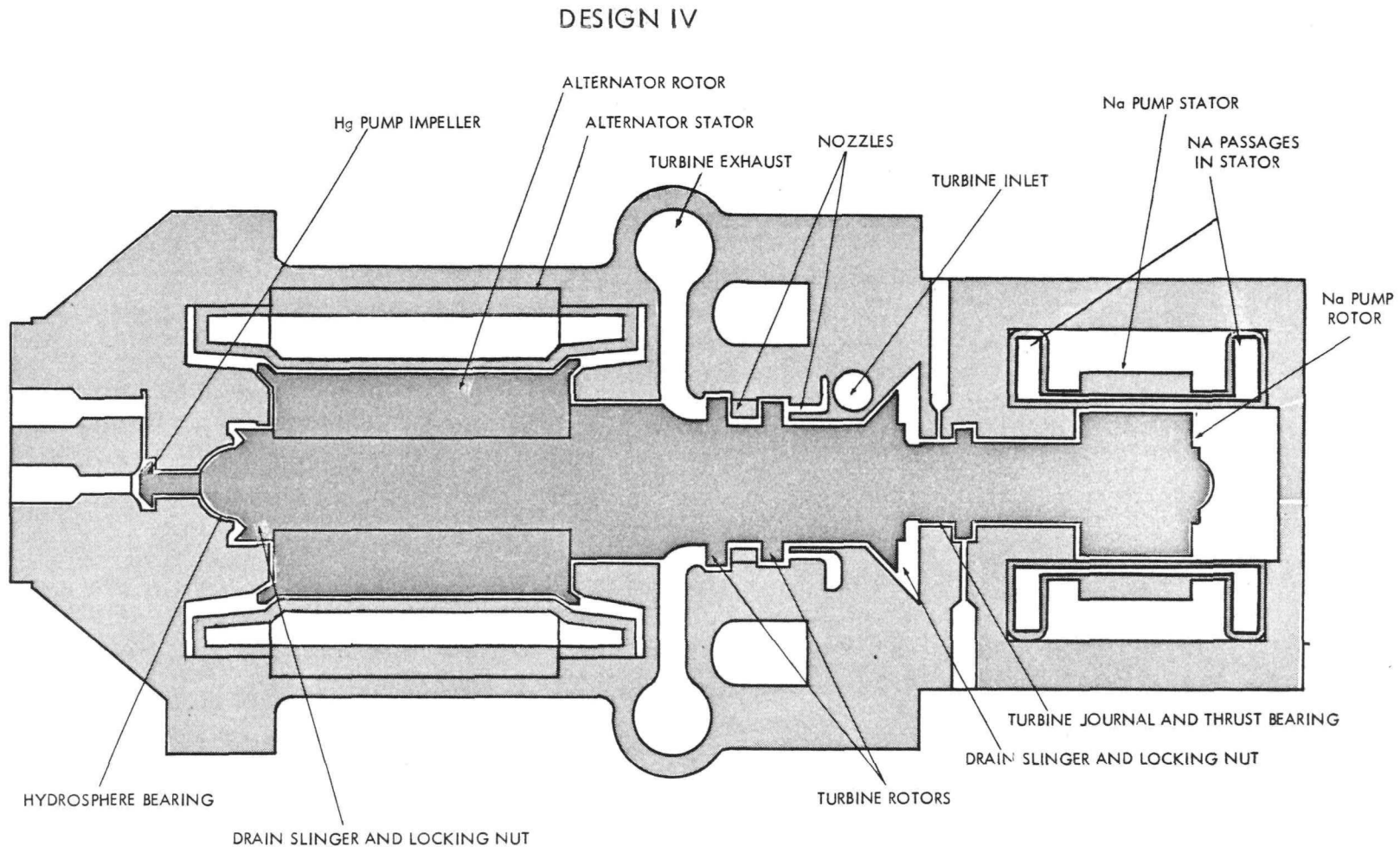
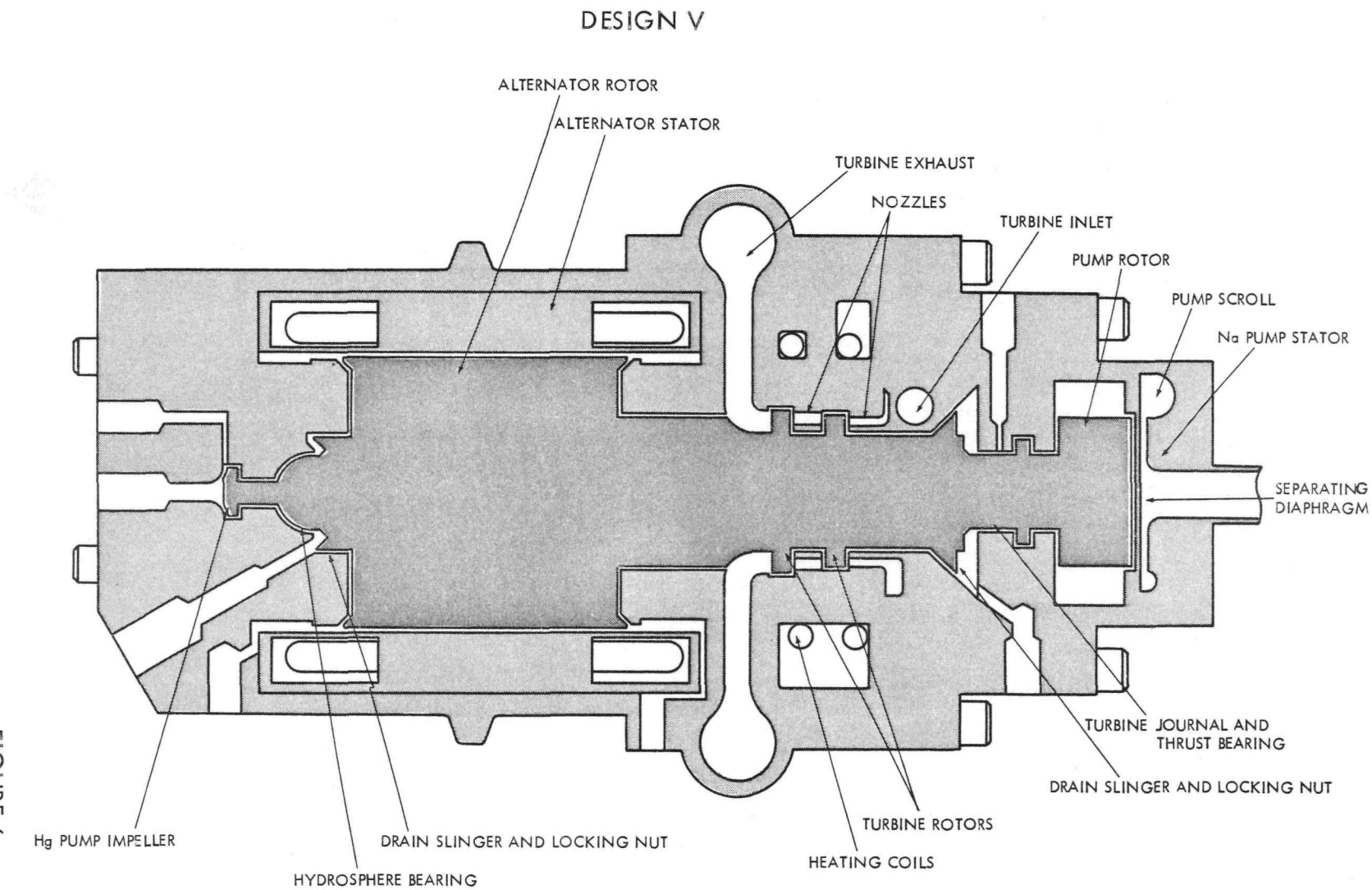


FIGURE 4

FIGURE 5





DESIGN VI

15

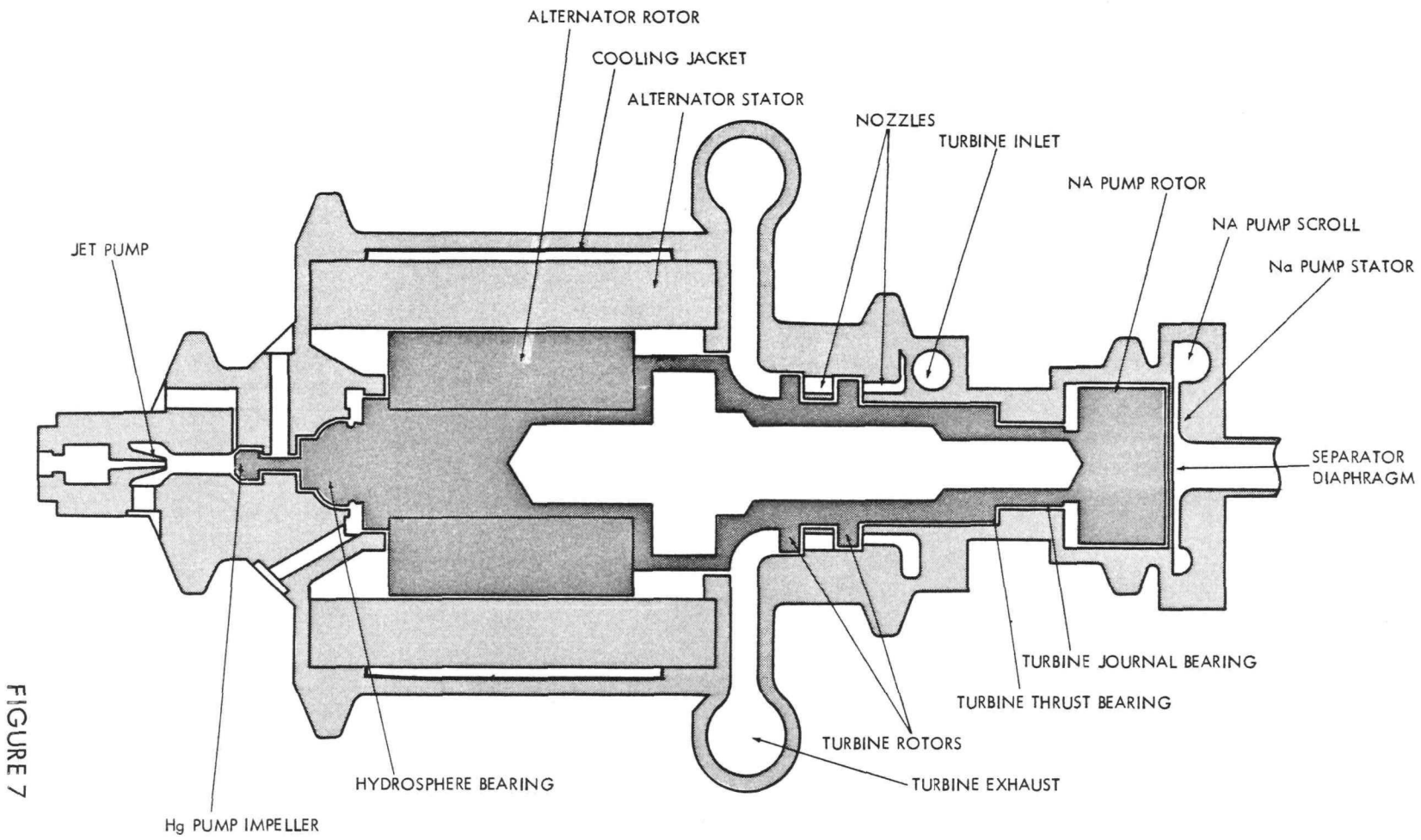
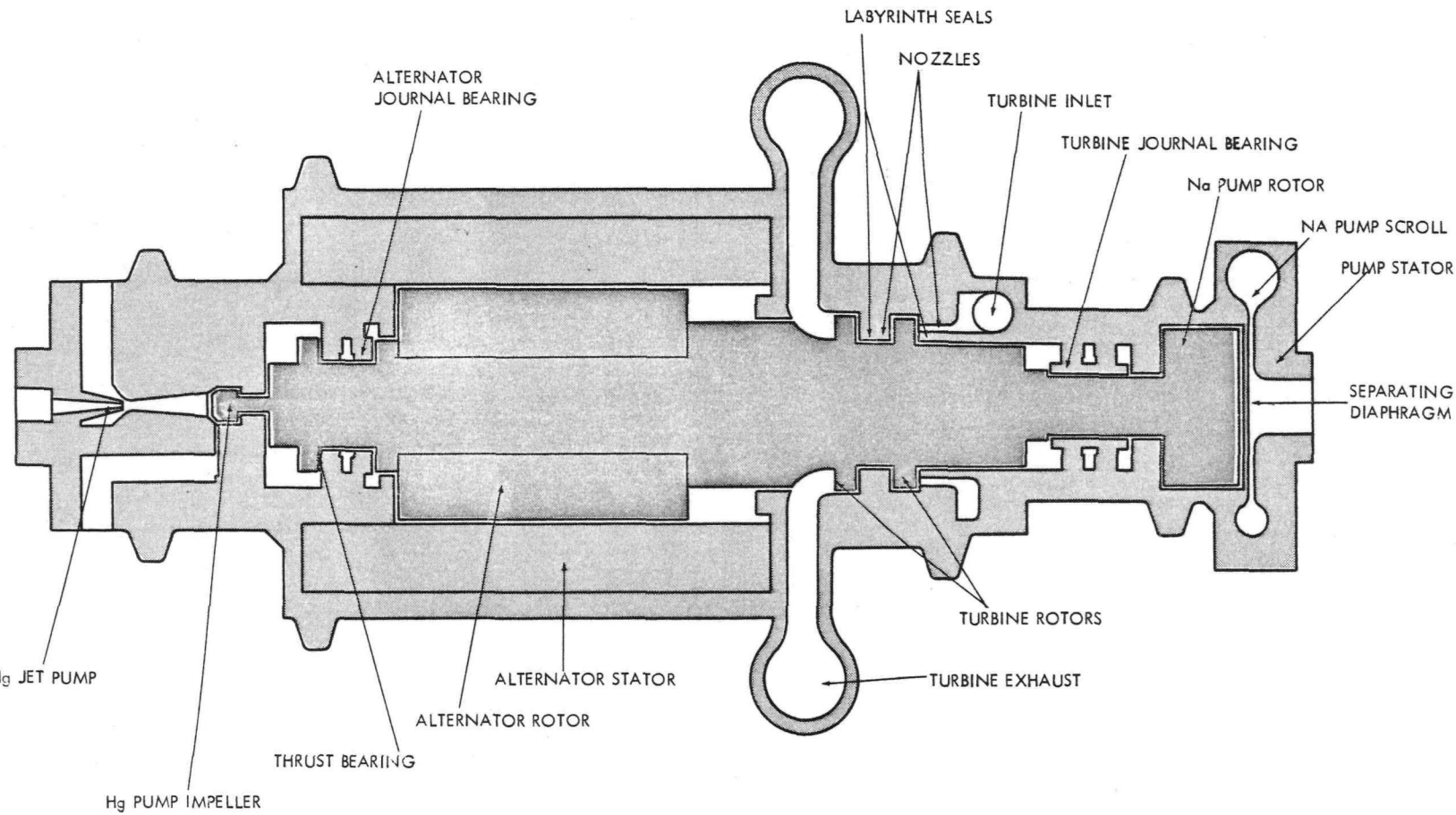


FIGURE 7

DESIGN VII

16

FIGURE 8



seals, fittings, materials, cleaning processes, fabrication, assembly, disassembly, metal treating, bonding, tolerances, clearances, balancing, inspection, testing requirements, and continued component study and experimentation followed Design VII and constituted the preparation for the CRU I design layout. Each CRU required integration of the following major components:

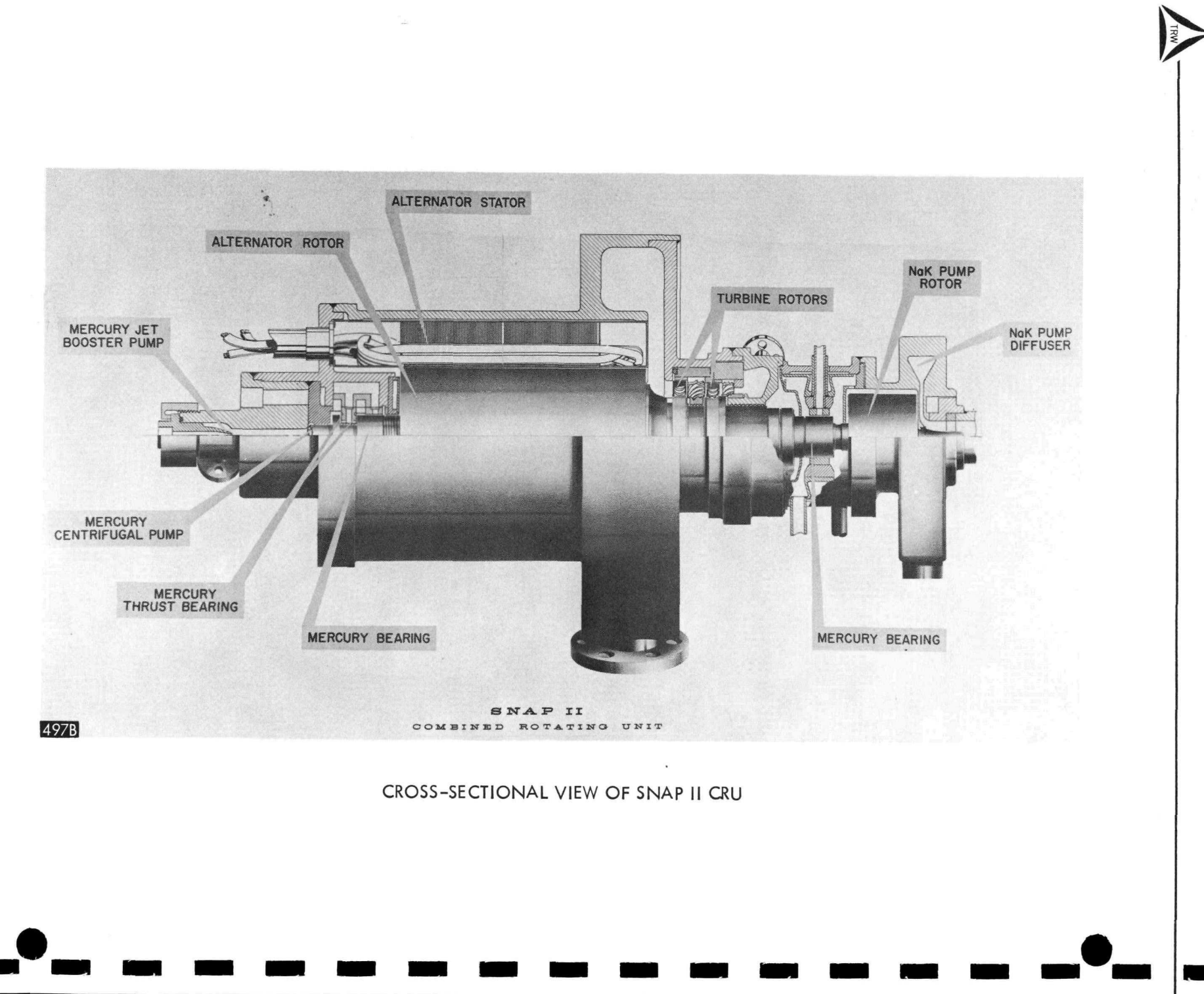
Housing	Alternator
Shaft	Mercury Pump
Bearings	Sodium Pump
Turbine	

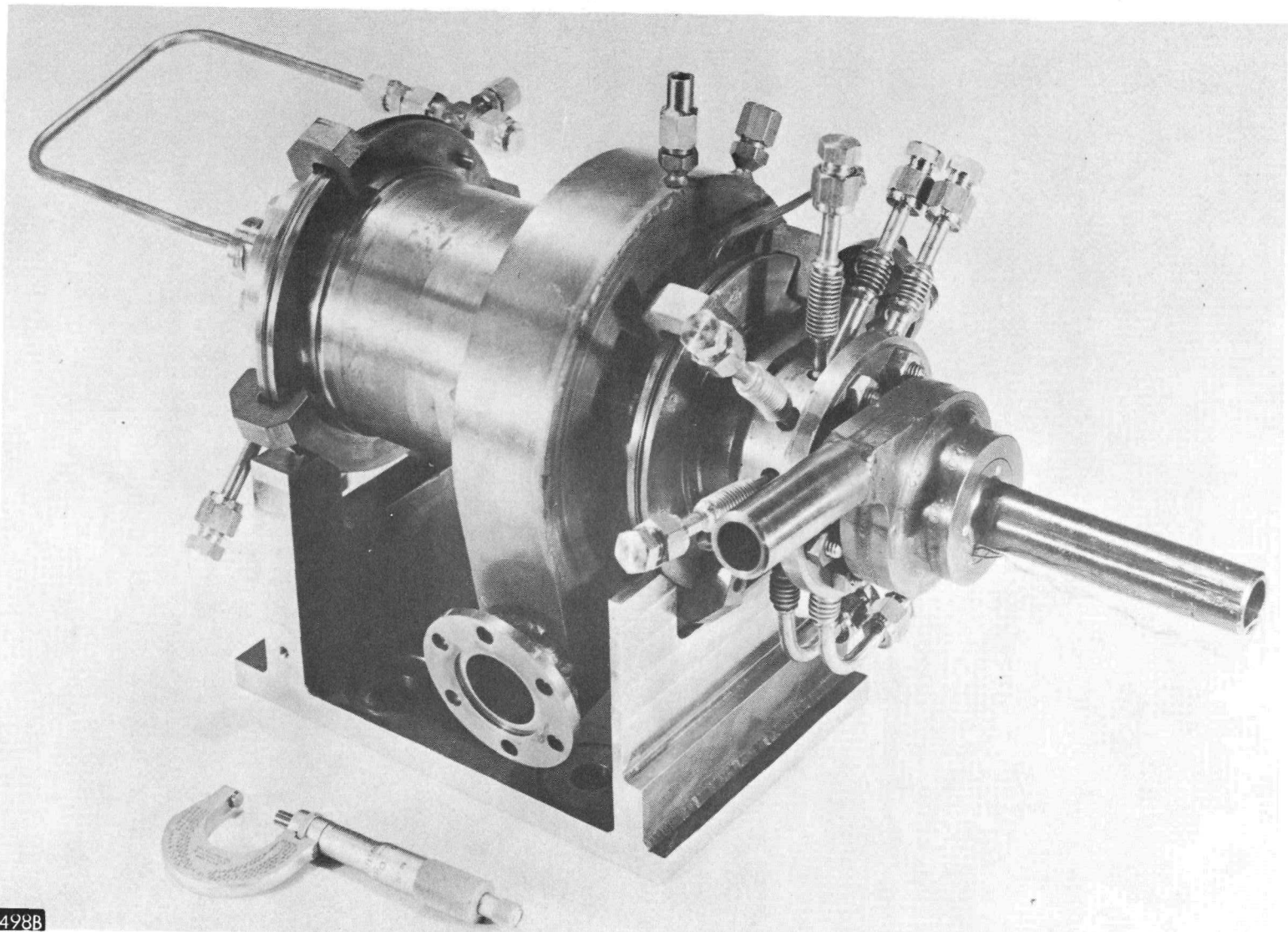
Figures 9, 10, and 11 are views of CRU I. The primary objectives of CRU I were to provide a foundation for further CRU development and to prove the feasibility of operating these components with the required temperature extremes in a single rotating unit.

3.2.1 Housing

The CRU housing encompassed the pump, alternator bearing support, alternator, turbine, and bearing support, and the sodium pump. For CRU I, housings were machined rather than cast to meet development schedules and design flexibility requirements. Parts were welded using the inert-gas-shielded arc method.

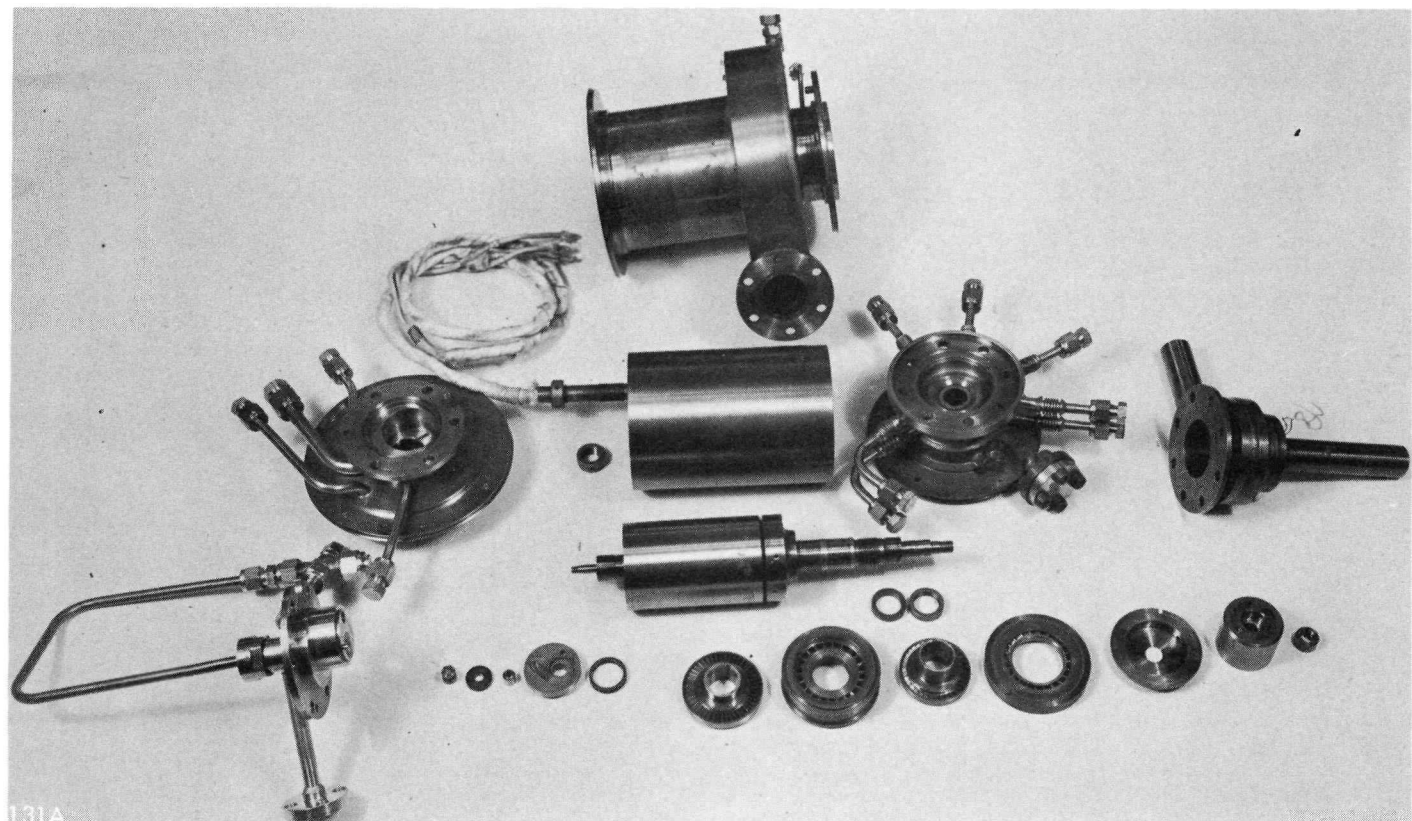
Pilot diameters for the housing components were of short length and close to the inside flange diameter. Dowels were used for greater accuracy. The housing flanges were sealed by metal "O" rings selected for high temperature strength, resistance to creep, thermal expansion coefficient, and availability.





EXTERNAL VIEW OF CRU

TAPCO a division of
Thompson Ramo Wooldridge Inc.



TURBO GENERATOR PARTS PRIOR TO ASSEMBLY

All tubes, the coolant ring of the turbine bearing, the heat shield between the alternator rotor and bearings, and the plugs in the alternator bearing support housing were brazed in place.

The high temperatures of the turbine at 1150°F and sodium pump at 1000°F which flanked the turbine bearing, imposed a severe thermal effect on the lubricant. To overcome this thermal problem, an inner housing, containing an annulus for bearing coolant flow, was incorporated into the turbine bearing housing. Heat shields isolated the bearing discharge area from direct impingement of the hot gases issuing from the high pressure seal and Na pump side. A heat shield also isolated the alternator bearing discharge from the comparatively high temperature of the alternator gap.

3.2.2 Shaft

Critical speed, heat transfer, weight, magnetic properties, thermal expansion, high-temperature strength, corrosion resistance, mercury compatibility, rotating seal leakage, fabrication and assembly influenced the shaft design.

One of the principle factors affecting the shaft design was critical speed. This design requirement was further compounded when the requirements for the rotating components tended to lower the critical speed.

The critical speed considerations penetrated every area of shaft design. A high modulus of elasticity at elevated temperatures became a requirement for the shaft material. Desired length of the alternator rotor required a compromise between critical speed limitations and electrical requirements. Critical speed also influenced turbine geometry, turbine rotor mounting and the sodium pump. A hollow shaft was selected for CRU I to further increase critical speed and simultaneously



minimize shaft weight and angular moment of inertia.

3.2.3 Bearings

The high temperature environment at the turbine end complicated the CRU bearing housing design. To minimize the journal bearing heat load at the turbine end, a flow of mercury through an annulus surrounding the bearing housing was provided. Bearing coolant flow, plus the lubricant flow and the housing structure previously described, helped to maintain a safe temperature in the bearing annulus.

The lubricant flow to the CRU 1 journal bearings was supplied through radial holes in the stationary part of the bearing. One duct supplied both the alternator journal and thrust bearings; the other supplied only the turbine bearing. Coolant flow through the hermetically sealed annulus around the turbine bearing was in series with the mercury boiler inlet flow.

3.2.4 Turbine

Rotor blades and stator vanes presented the major turbine hardware problem. Materials were required to resist corrosion, erosion, high stress concentrations, thermal shock, and dimensional instability. Both rotors and stator were fabricated by cutting airfoil strips of constant section to length to become the blades and vanes. These were inserted into an intermediate holding ring containing holes of corresponding sections. The assembly was completed and locked by inner and outer rings. Rotors were held on the shaft by three pins fitted into axial slots on the rotors and shaft, allowing disassembly and reassembly without disruption of balance. The turbine rotors were retained by two nuts which locked against each other, and fastening torque was fixed slightly beyond retention requirements to preserve shaft balance after reassembly.

3.2.5 Alternator

Achieving the optimum design concept to satisfy the electrical, stress, and critical speed requirements presented the major design problem for the alternator. To increase rotor length and diameter – advantages from an electrical standpoint – meant, respectively, a decrease in critical speed and an increase in rotor stress. The ability of the rotor to withstand stress was diminished by the 700° F temperature of the gap. To compound the problem, materials having good magnetic properties lacked strength, compatibility with mercury, and ease of fabrication.

To ease the rotor stress problem, the magnet was completely enclosed in a can assembled on the magnet by a shrink fit. The can maintained the magnet tensile stress near zero at design speed and temperature, and protected the magnetic materials from mercury corrosion.

Stator requirements for a very thin and precisely dimensioned insulating material at the gap, withstanding high temperatures, and being impenetrable by liquid mercury or vapor also created design difficulties. A sleeve of synthetic mica was initially used to prevent mercury from entering the alternator windings. To keep the total axial length of the shaft at a minimum, the stator also served as part of the turbine exhaust scroll wall.

3.2.6 Mercury Pump

Fabrication and assembly of small intricate parts, high precision, and the arrangement of inlet and outlet lines presented hardware problems in the mercury pump. The centrifugal pump and the thrust bearings demanded tighter dimensioning than the relatively relaxed axial clearances and tolerance for other shaft components; therefore, they were arranged as close together as possible. The critical dimensions were then confined to the cold end. Results were minimum stack-up where tolerances were critical, good control of thermal expansion, and freedom from difficult design problems in accommodating axial shaft expansion



at the turbine end.

In CRU I, stationary parts of both the thrust and alternator journal bearings were assembled directly into the pump housing. The three-point contact of the pump volute plate with the thrust bearing stator allowed the drainage of mercury from the bearing.

3.2.7 Sodium Pump

The sodium pump rotor submitted to straight forward design, fabrication and assembly techniques. The stator, however, contained a thin, poorly supported diaphragm which was required to show good stress resistance and maintain position and flatness at high temperatures. A digital computer controlled milling machine was used to machine the pump diffuser and collector housing. This technique eliminated the use of castings in the critical sodium-mercury diaphragm sections. In CRU I the sodium pump rotor was mounted by a slip fit between the rotor bore and the shaft. Drive was obtained by using the three-pin method used on the CRU I turbine wheels. The rotor retaining nut was restrained from rotation by a key fitted into a slot at the end of the shaft.

3.2.8 Fabrication

Basic objectives were design for fabrication within standard machine limitations and manufacturing procedures and interchangeability of subassemblies. In order to maintain critical dimensions, machining of important mating parts was accomplished after processes such as brazing or welding was completed. In all cases dimensioning took into account the entire range of clearances at conditions ranging from room temperature to operating temperatures. All parts were inspected against chips, metallic stringers, oils, and foreign particles. X-ray and leak inspections were applied for all hermetically sealed assemblies.

3.3 CRU II Design

The objectives of CRU II were,

- (1) design refinement, and
- (2) performance improvement

In CRU II design, the search for compatible materials was intensified and the housing hermetic sealing problem was considered.

3.3.1 Housing

CRU II embodied the initial welding development of the housing. Two of the four flanges were welded together instead of bolted, the goal being the elimination of all "O" rings as external seals.

3.3.2 Shaft

To further improve the critical speed, the CRU II shaft dimensions were modified. Rotating component mounting techniques were refined to provide higher precision, greater facility in balancing, and ease of assembly and disassembly. Dimensioning was modified as a result of continued study of thermal expansions.

3.3.3 Bearings

Because launching conditions imposed upon the bearings were better understood, CRU II bearing design reflected the need for consistent flow of lubricant during launch. The lubricant inlet was placed tangentially to the bearing in CRU II rather than radially as in CRU I. In addition, flows to the thrust and alternator journal bearings were separated in CRU II to provide better flow control than that attained with the common feed line used in CRU I. Mechanical design, fabrication, and assembly techniques were improved to provide positive location and

higher precision.

3.3.4 Turbine

In the CRU II, the turbine pitch diameter was increased to provide a larger ratio for better performance. Profiles were changed in both the first and second-stage turbine blades and in the second-stage nozzle vanes. To accommodate the larger difference in blade height between stages, the approaches to the throat areas of both the second-stage nozzle and the second-stage turbine rotor were tapered.

Labyrinth seals, similar to those over the turbine hubs, were added over the shroud rings to lower axial leakage across the turbine stages. In addition, the exhaust scroll diameter was increased to decrease vapor pressure drop increasing turbine efficiency.

3.3.5 Alternator

Better protection for the alternator stator coil ends was provided by increasing the stator can and corresponding housing length and inserting insulation disks between end plates and coil ends. Mechanical design of both stator and rotor remained essentially that of CRU I.

3.3.6 Mercury Pump

The CRU II mercury pump diameter was increased to achieve the higher discharge pressures required by altered system requirements.

3.3.7 Sodium Pump

The CRU II sodium pump rotor differed from that of CRU I only in minor areas of mechanical design. The pump rotor was concentrically fitted upon circumferential lands. For improved nut retention and assembly, a tab spot-welded onto the outside face of the nut was bent into the groove on the end of the shaft.

3.4 CRU III Design

The results obtained from intensive testing of CRU components, CRU I, and improved system requirements dictated the design objectives for CRU III.

The most significant change in the CRU III design resulted from the change of reactor coolant from sodium to the sodium potassium eutectic (NaK 78). The system change was made to simplify orbital start requirements. The new reactor coolant pump required a larger rotor and over 600 watts of shaft power. The pump flow rate was increased to 72 pounds per minute because of the lower heat capacity of NaK compared to sodium. Efficiency of the pump was reduced because of the increased electrical resistance of NaK compared to sodium.

System changes also required modified mercury pump characteristics. Increased discharge pressure was required to match both bearing and boiler pressure requirements. Pump flow was also increased to provide more turbine power and bearing lubricant.

Alternator power requirements were increased by 350 watts to provide necessary power for the reactor and CRU speed controls.

In order to meet the added power requirements, turbine flow rates and inlet pressure objectives were modified. In addition, inlet and discharge scrolls were improved for the added flow and performance. Basic turbine geometry for the CRU III, however, remained the same as for CRU II. Many design details of the CRU were also improved as a result of continued analysis and development as indicated in the following sections.

3.4.1 Housing

The CRU III housing is a fully welded, hermetically sealed shell. A radial lip design at the



flanges isolated deformation due to welding from critical reference surfaces and bores.

CRU III also introduced alternator cooling. This was accomplished by brazing a coil of flattened cobalt alloy tubing around the alternator housing in series with the flow to the boiler inlet and the bearing coolant.

3.4.2 Shaft

The CRU III shaft assembly embodied the measures taken to increase critical speed with a minimum compromise to rotating component performance as listed below.

- a. Haynes-25 cobalt alloy was chosen as the basic shaft material because of its high modulus of elasticity at high temperatures.
- b. Rotating seal labyrinth were cut into bores instead of on the shaft.
- c. Mounting surfaces were of constant diameter wherever possible.
- d. The second-stage turbine rotor assembly employed the shaft itself as a hub, thus allowing an increase in shaft diameter.
- e. NaK pump and first-stage turbine rotor were keyed by three axial pins to increase shaft stiffness and minimize balancing problems.
- f. Bearing to bearing centerline distance was decreased as far as possible.
- g. Weight distribution for the overhung NaK pump rotor was designed to provide a minimum mass moment.

Table II charts weight, mass moment, and both calculated and experimental critical speeds for CRU I, II and III. The graphical analysis method for calculating critical frequency, with

particular care taken in assuming distribution of masses, was used in determining theoretical critical speeds of CRU II and CRU III shaft assemblies. This method produced a close approximation to experimental results.

TABLE II
WEIGHT, MASS MOMENT AND CRITICAL SPEEDS
FOR CRU'S I, II, AND III

Unit	Weight		Mass Moment	Critical Speed		- Shake Table - Experimental
	Calculated			Hot	Cold	
	Total Unit	Rotor lbs	Rotor lb-in-sec ²	rpm	rpm	
CRU-I	22	4.42	5.94×10^{-3}	44,400	46,500	39,600
CRU-II	30	4.62	6.12×10^{-3}	46,022	48,000	42,000 to 45,000
CRU-III	27	5.74	7.53×10^{-3} (calc) 7.44×10^{-3} (exp)	49,100	51,500	43,200 to 49,800

Figure 12 shows the curves plotted by this method for CRU III. A force polygon was derived from the bending moment diagram. The "EI" product for each shaft section then determined the slopes for the funicular polygon which, in turn, produced the static deflection curve. The data for typical curve is shown in Table III. Thus, using "W" for weight in pounds, "y" for deflection in inches, the following formula yielded critical speed, "N_{cr}". The modulus of elasticity, "E", was corrected for temperature in these calculations:



$$N_{cr} = \frac{60}{2\pi} \left[\frac{\sum w_y}{\sum w_y^2} \right]^{1/2} \text{ RPM}$$

TABLE III
DISTRIBUTION OF CRU III SHAFT ASSEMBLY WEIGHT
AND CORRESPONDING STATIC DEFLECTION
FOR A TYPICAL CRITICAL SPEED DETERMINATION

W POUNDS	γ MICRO-INCHES
1.334	2.8
0.204	5.7
0.267	10.2
0.232	12.4
1.559	12.4
0.309	11.7
0.160	11.3
0.174	11.0
0.195	9.8
0.320	9.4
0.044	8.3
0.169	3.4
0.966	22.4

From Table III,

$$\begin{aligned}\sum W_y &= 6.38 \times 10^{-5} \\ \sum W_y^2 &= 9.326 \times 10^{-10}\end{aligned}$$

Substituting into the equation for critical speed yields:

$$\begin{aligned}N_{cr} &= \frac{60}{2\pi} \left[\frac{386 \times 6.38 \times 10^{-5}}{9.326 \times 10^{-10}} \right]^{1/2} \\ N_{cr} &= 49,074 \text{ RPM}\end{aligned}$$

Table IV charts a set of representative shaft conditions and the consequent critical frequencies.

To satisfy the magnetic needs of the NaK pump in CRU III, an insert of 17-4 stainless steel replaced the non-magnetic L-605 of the shaft under the back iron of the pump rotor. Thus, the shaft is a three-piece weldment with the basic assembly including the second-stage turbine rotor.

Using the mercury pump side of the thrust bearing as a reference plane, the axial growth of the shaft from room temperature to operating conditions is 0.0527 inch. Axial growth of the housing from the same plane is 0.0463 inch. Thus, the total relative expansion of the shaft with reference to the housing, is 0.0087 inch.



TABLE IV
REPRESENTATIVE SHAFT CONDITIONS AND CRITICAL SPEEDS

Bearing & Length	Rotating Wt.	Shaft Mat'l.		(N _{cr}) _{Hot}
1. 7.060	4.931	AMS 5643	.77 # NaK Pump; CRU II Shaft	45,800
2. "	5.20 (approx.)	AMS 5759	" ; CRU II Shaft	48,100
3. "	4.77 (approx.)	Kentanium	" ; CRU II Shaft	62,300
4. "	4.77	AMS 5759	.40 # Na Pump; CRU II Shaft	46,000
5. "	4.552	AMS 5643	" ; CRU II Shaft	43,400
6. 6.90	4.87	AMS 5759	.77 # NaK Pump; Large Bores In Shaft; CRU II Shaft	40,500
7. 6.90	4.99	AMS 5759	.77 # NaK Pump; 1/2" Shaft Bore	43,700
8. 6.81	5.72	AMS 5759	.77 # NaK Pump; Integral Brgs; Solid Shaft CRU III	57,800
9. 6.81	5.72	AMS 5759	As above except removable brgs CRU III	51,400
10. 6.91	6.00	AMS 5759	1.1 # NaK Pump; Solid Shaft CRU III	41,800
11. 6.91	5.84	AMS 5759	.97 # NaK Pump (CRU III)	49,100

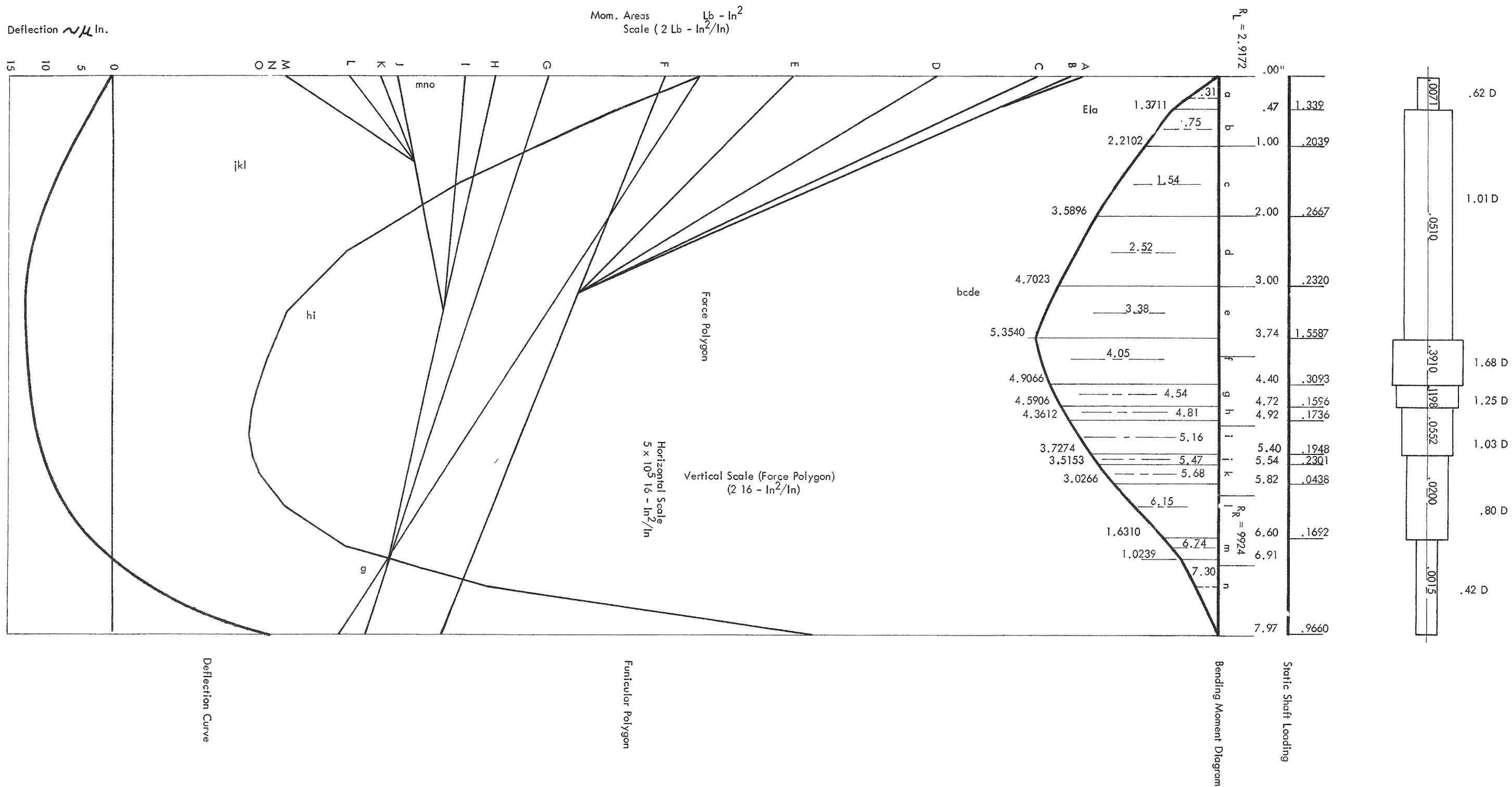


FIGURE 12

3.4.3 Bearings

The CRU III thrust bearing design was improved by the replacement of the three-point contact of the volute plate with a continuous surface having drain holes drilled into the wall of the plate, allowing full contact between the plate and the thrust bearing. The turbine bearing, held axially by a four point contact, was also modified to attain full contact to assure flatness.

Finally, experimentation with the effects of whirl and loading resulted in selection of pad-feed rather than annual-feed type journal bearings.

3.4.4 Turbine

For CRU III, additional investigation dictated an increase of turbine exit scroll minimum diameter. A new turbine construction evolved, increasing the shaft diameter toward improved critical speed. Also, the second-stage rotor hub was eliminated and the shaft was integrated with the rotor assembly. Thus, critical speed was substantially increased.

A new keying device was successfully developed to attain a positive fix of the first-stage rotor and yet allow easy disassembly and reassembly without disrupting balance. The rotor was held in position by a shaft piloted retainer nut bearing precisely upon a rotor surface to insure an evenly distributed locking load. The nut thread was designed so that bearing of the nut and rotor surfaces was accurate to the high degree of precision required for this application. A second locking nut of similar thread and precise mating surface locked the retainer.

3.4.5 Alternator

Since the second-stage turbine wheel in CRU III was an integral part of the basic shaft assembly,



It was necessary to redesign the alternator rotor retainer to allow its removal from the shaft. A split ring which axially positioned the nut could be removed when the nut was loosened, thus allowing disassembly of both the retainer and the rotor. To allow for balancing stock in the heaviest section of the shaft assembly, a balancing lip was added to the rotor can. The end configuration of the rotor can was modified to relieve the combined stress and thermal shock sensitivity of the CRU II rotor.

The problem of providing both a hermetic seal and support for the alternator leads was resolved by using a tube welded to the alternator housing. The external seal was made by welding the alternator lead connector to the external tube.

3.4.6 Mercury Pump

The CRU II pump required only minor refinements for use in CRU III. The greatest change, involving the pump plate, was dictated by mechanical design of the thrust bearing assembly rather than by pump performance.

The pump volute plate, which fixed the thrust bearing axially, was originally designed to bear on the thrust washer at three points. In order to distribute the loading on the thrust bearing uniformly, full contact replaced the three-point contact and holes were fabricated into the wall of the volute plate to allow bearing drainage.

3.4.7 NaK Pump

The decision to employ NaK instead of sodium as the heat transfer fluid forced the change to a larger rotor and a corresponding change in the volute and pump housing. A minimum rotor

weight with no sacrifice of pump performance was required to attain a safe critical speed.

To provide an optimum magnetic path it was necessary to use magnetic stainless steel for that part of the shaft which supported the rotor; the remainder was the non-magnetic cobalt alloy. The CRU III shaft proper was made from cobalt alloy divided by a section of stainless steel.

The NaK rotor was mounted on the shaft by a device identical in principle to that of the CRU III first-stage turbine rotor. To reduce turbulence at the NaK Inlet, a 12-inch long run of straight pipe entered the pump.

4.0 CRU TEST AND DEVELOPMENT

Design, fabrication and instrumentation of CRU test rigs, testing of CRU's, and data reduction and analysis of test results accompanied CRU design. The test and development of one CRU I and two CRU II units are described in the following sections.

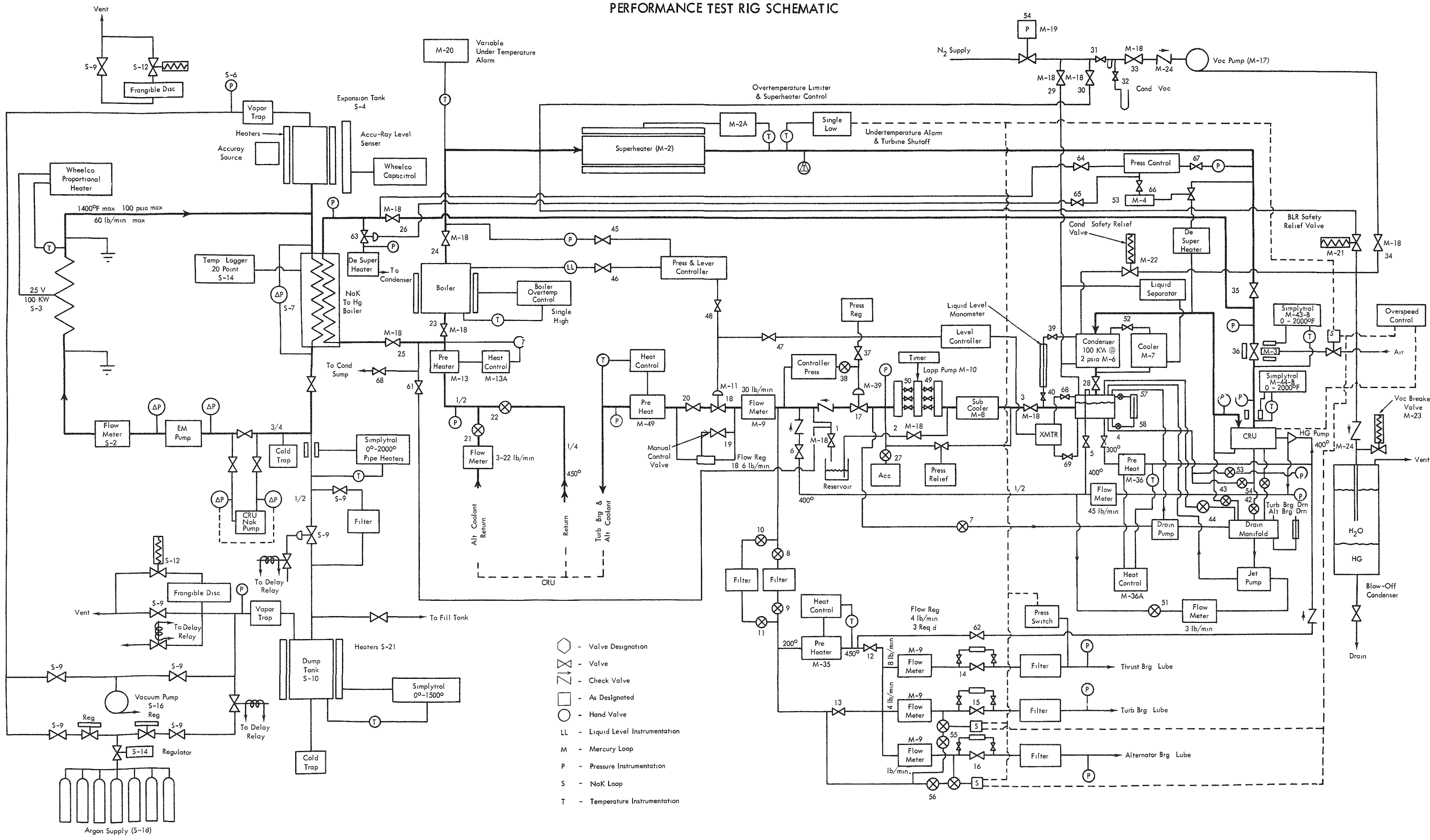
4.1 Test Equipment

The Performance Test Rig, shown schematically in Figure 13, was designed for performance and endurance tests of the CRU's, for evaluating procedures and techniques for startup, shutdown, and operation, and for testing component performance and CRU control dynamics. Figures 14-16 are photographs of rig components. Table V lists the capabilities of this rig.

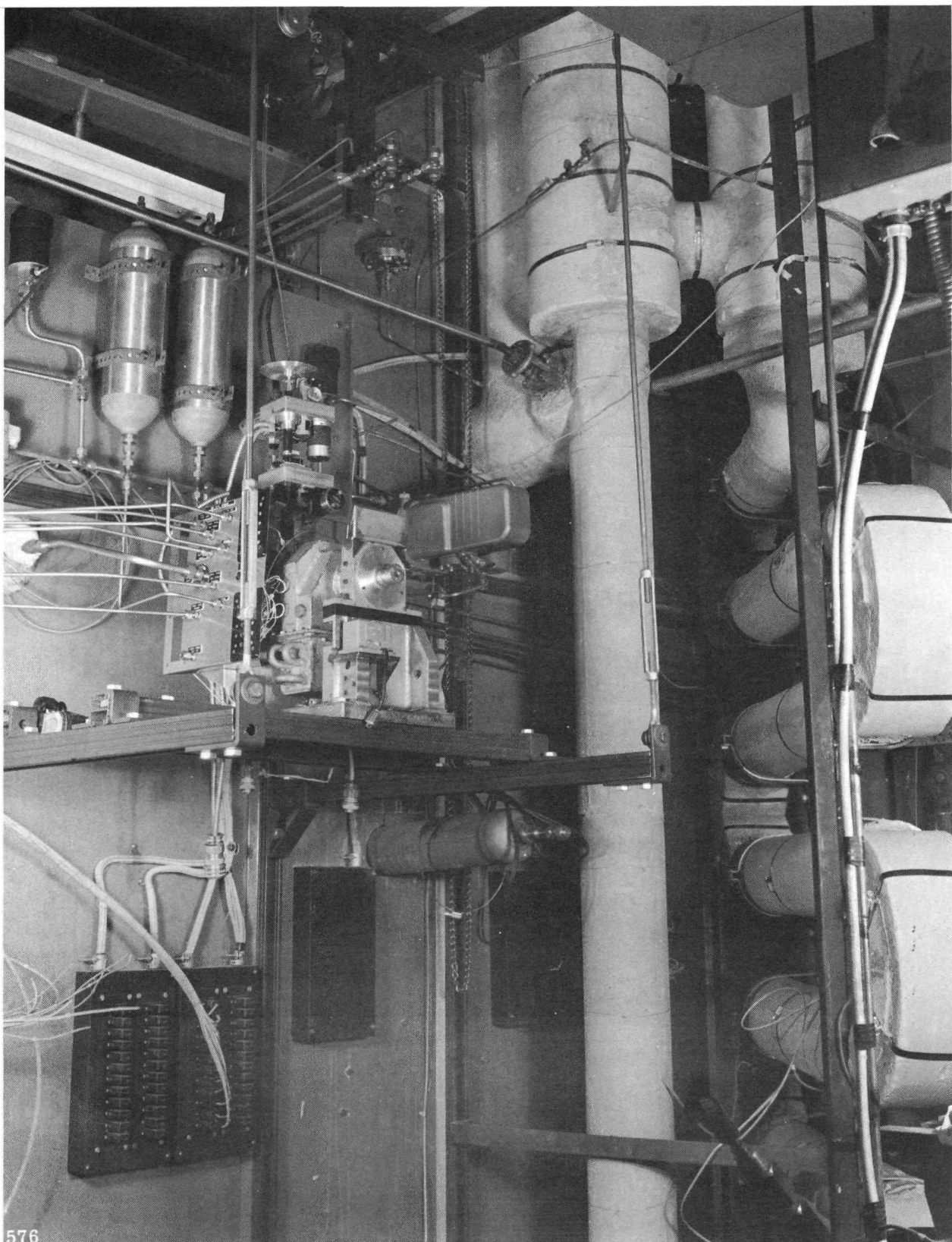
The wide band of operating conditions available on the Performance Test Rig are listed below:

1. Turbine inlet pressure and temperatures, as well as condenser pressure, could be varied to establish a complete performance map of turbine operation.
2. Alternator load could be infinitely varied between 0 and 5 kw to establish any desired speed or load condition on the Combined Rotating Unit.
3. Mercury pump inlet temperature and pressure could be varied along with pump discharge pressure to establish pump performance characteristics over a wide flow range.
4. Bearing supply temperatures and pressures could be varied to determine bearing performance at design and off-design conditions.

PERFORMANCE TEST RIG SCHEMATIC

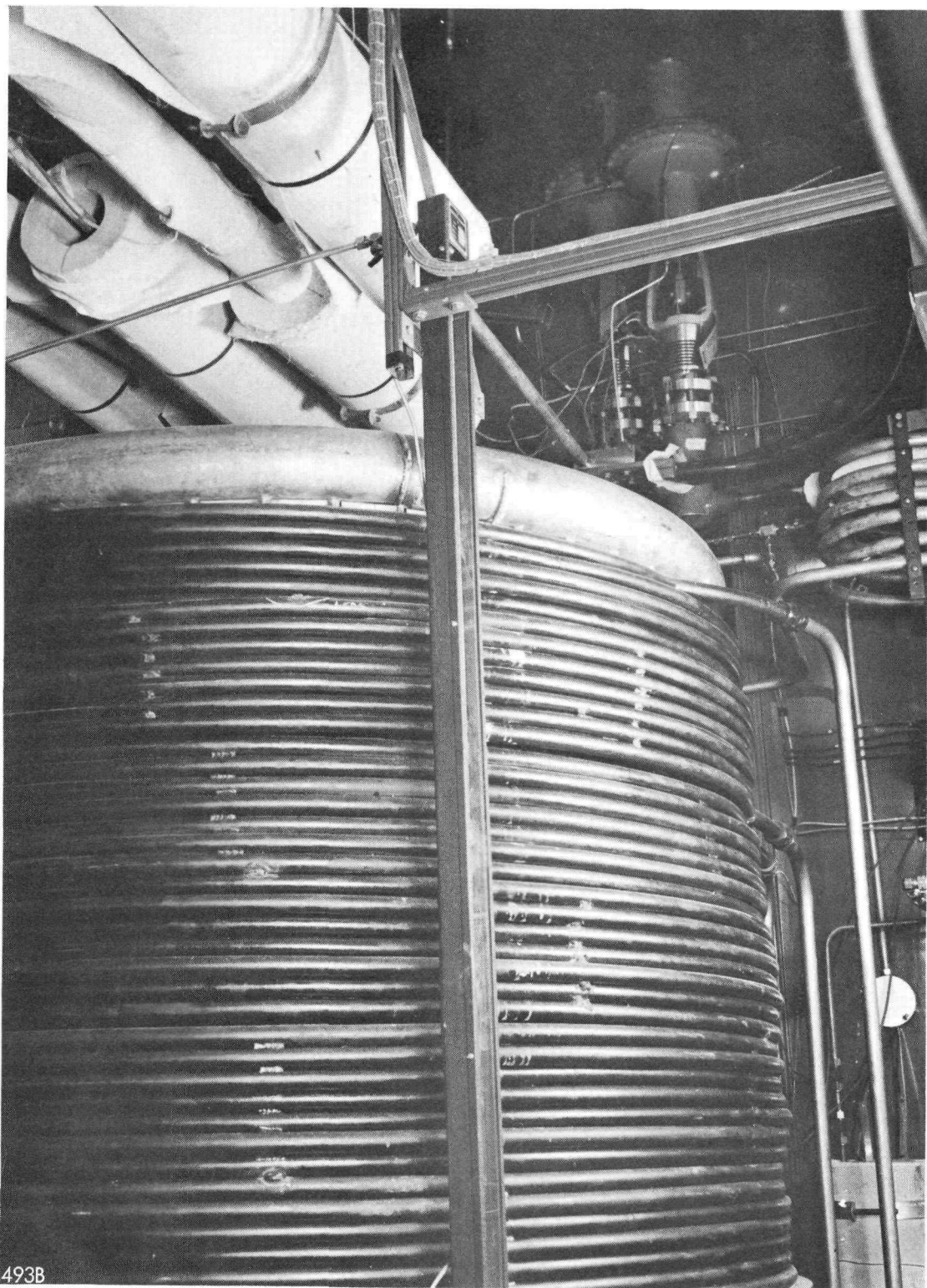


BLANK



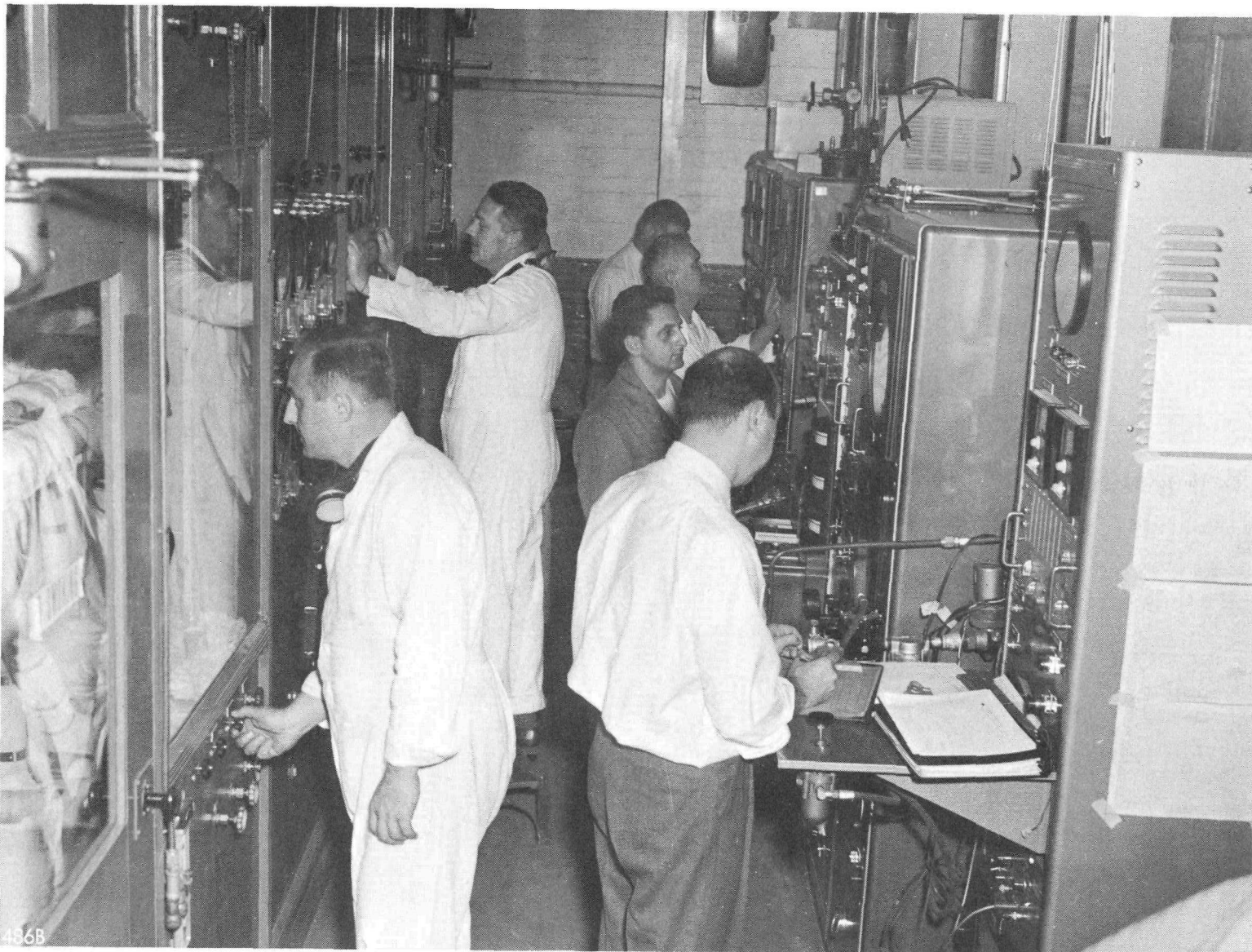
576

VIEW OF COMPONENTS LOCATED IN CRU BOOTH



VIEW OF COMPONENTS LOCATED IN CONDENSER BOOTH

FIGURE 15



CONTROL CONSOLE FOR SNAP II PERFORMANCE RIG

TAPCO a division of
Thompson Ramo Wooldridge Inc.

Automatic controls on the test rig protected the development hardware from inadvertent test rig malfunctions. For example, a device which closed the turbine inlet valve if the frequency of the alternator output exceeded a set value or if the signal was lost, protected the CRU from overspeed in the event of an electrical short or open circuit. Failure of the lubricant supply to maintain a pre-set minimum pressure would close the turbine valve.

Low turbine inlet temperature also would close the turbine inlet valve, thus guarding the turbine against excessively wet vapor. Although the possibility of mercury contamination by sodium was extremely remote, the consequences could have been serious. Therefore, a sodium-in-mercury detector would ring an alarm and divert any contaminated mercury to an isolated reservoir. An over-temperature alarm would ring should the alternator stator exceed a pre-set maximum temperature. Vibrations were amplified to both audibility and visibility, so changes in sound or in the vibration pattern served as an indication of CRU status and warned against impending failure. The NaK loop was constructed to minimize fire hazard, and fire-fighting and sodium disposal equipment were provided.

Instrumentation for the Performance Test Rig was designed to record performance without compromising design and to allow easy separation and reduction of meaningful data. Wherever possible, primary elements were placed outside the rotating package. This eased probe requirements, removed additional design variables, and assured greater facility in handling rotating units in the test cell.

To minimize duplication of data and quantity of instruments, individual component test records were included in the body of data whenever pertinent.

TABLE V
 PERFORMANCE TEST RIG CAPABILITIES

Mercury System -	vapor capacity	25 lb/min
	pressure	300 psia
	temperature	1300°F
NaK System -	flow	85 lb/min
	pressure	100 psia
	temperature	1400°F
NaK or Mercury System Input Power		100 kw maximum
Condenser Water		40 gpm
Instrumentation		
	Pressures	Static: Bourdon gages, manometers Dynamic: strain gage transducers
	Hg Flow	Manometer and differential pressure transducers
	NaK Flow	Electromagnetic Flowmeter
	Temperatures	Logger type potentiometers
	Speed	Digital counters
	Alternator Output	Volts, amperes, and watts from 25 to 2000 cps (2 phase)
Controls		System Pressure Controller Rig Boiler Liquid Level Controller Condenser Liquid Level Controller Auxiliary pump discharge pressure controller NaK Boiler inlet temperature controller

Figure 17 is an example of initial test rig instrumentation. For CRU I, chromel alumel thermocouples were used for all temperature probes. Pressures were read out on dial gauges and manometers, and fluid flows were recorded by manometers and flowmeters. CRU I internal probes were limited to turbine inlet and exhaust temperatures and pressure, turbine interstage static pressure, alternator stator can temperature, and alternator windings temperature.

The CRU instrumentation, outlined as data columns in Figure 18, indicated that the instrumentation was separated according to component designation for ease of data collection and correction. Figure 18 also shows the data categories for rig performance.

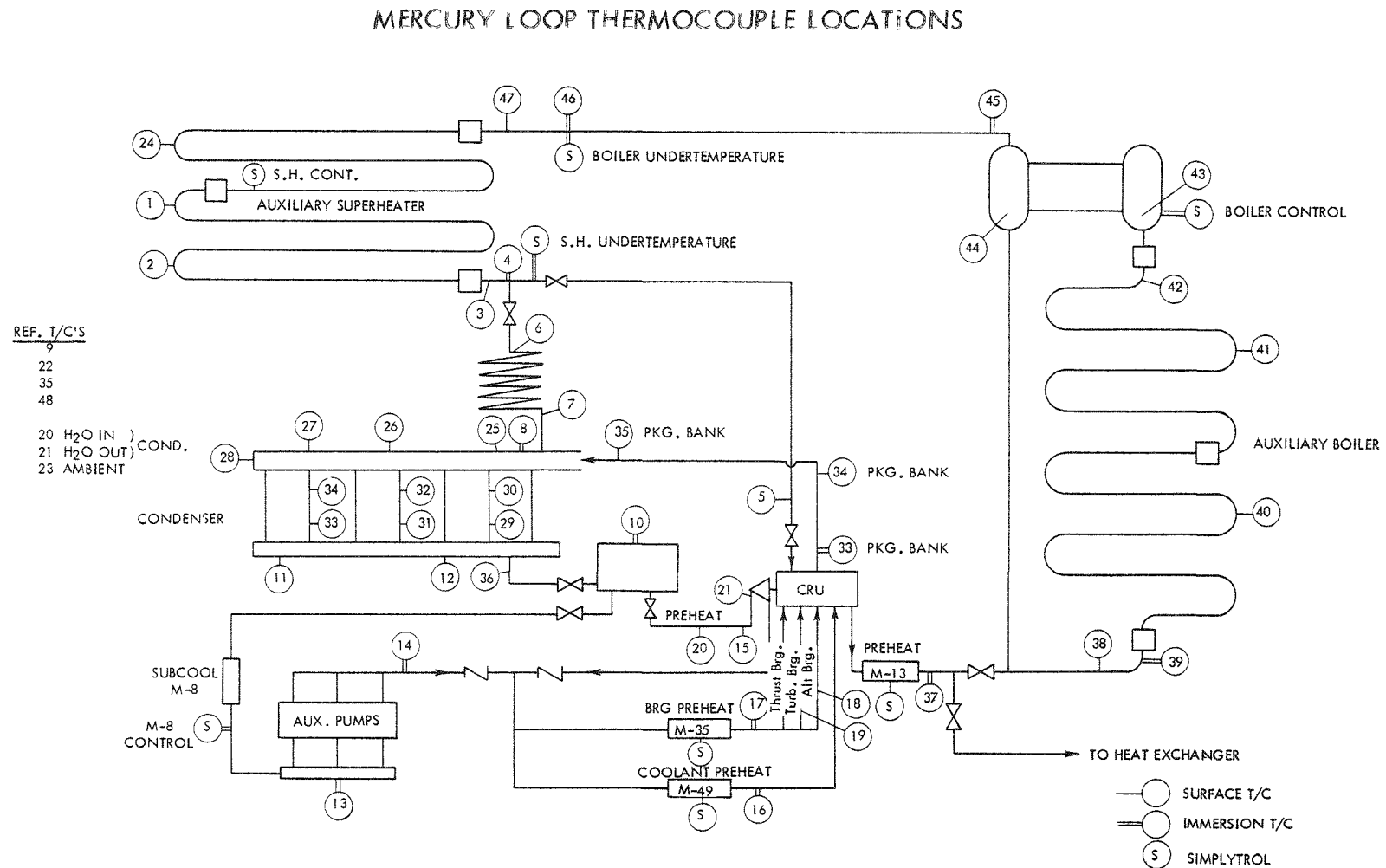
Extensive vibration tests were conducted on an MB Electronics C-10D Exciter with power capabilities of 1200 g-lb force for a frequency range of 5 to 3000 cps with a maximum peak-to-peak displacement of one inch.

4.2 Data Analysis Techniques

Performance tests were evaluated during and after actual test. Performance estimates based upon design criteria were calculated to serve as a comparison for generated data. From inspection of fabricated parts, actual dimensions were tabulated to provide an exact basis for analysis. During test, evaluation of results served to maintain safety, determine patterns of behavior, and suggest changes in test procedure and objectives. After each test, overall CRU performance, as well as component performance, was determined from the reduced data.

A heat balance and a power balance were made to verify component performance estimates. The heat balance was based on temperature difference across each fluid line.

FIGURE 17



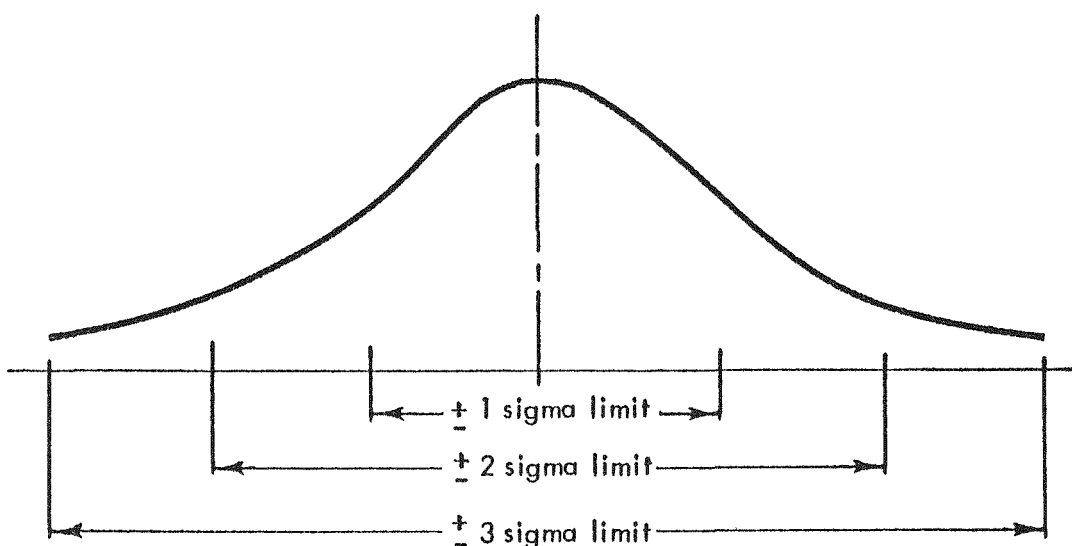


TEST RIG DATA CATEGORIES

DATE				AUX. PUMPS				BOILER DATA					CONDENSER DATA							SIMPLYTROL TEMPS. (F)																														
RUN NO.				TIME	INLET PRESS. PSIG	DISCH. PRESS. PSIG	CONT. PRESS. PSIG	FLOW		LEVEL INCHES	POWER KW	CONTROL TEMP. °F	LEVEL CONT. INCHES	SUMP LEVEL INCHES	COND. LEVEL IN.	INLET PRESS. "HG VAC	SUMP PRESS. "HG VAC	MANOMETER "HG VAC	H ₂ O FLOW GPM	BOILER UNDER TEMP.	S. H. UNDER TEMP.	S. H. CONTROL TEMP.	PRE-HEAT M-13A	PRE-HEAT M-35	PRE-HEAT M-49	SUB-COOL M-8	SUB-COOL M-14	S.H. POWER KW	SYSTEM PRESS. PSIG	VAPOR METER																				
								"HG	S/MIN.																																									
HG PUMP DATA				BEARING DATA																									ALT. STATOR CONTROL																					
				NO.	TIME	SHAFT SPEED CPS	PUMP FLOW IN. HG	PUMP FLOW #/MIN.	PUMP DISCH. PRESS. PSIG	COND. LIQUID LEVEL IN.	COND. PRESS. IN.-HG	COND. LIQUID LEVEL IN.-HG	PUMP INLET HEAD IN.-HG	TURB. BEARING FLOW IN.-HG	TURB. BEARING FLOW #/MIN.	ALT. BEARING FLOW IN. - HG	ALT. BEARING FLOW #/MIN.	THRUST BEARING FLOW IN. - HG	THRUST BEARING FLOW #/MIN.	ALT. COOL. IN FLOW IN. - HG	ALT. COOL. IN FLOW PSIG	TURB. BEARING SUPPLY PRESS. PSIG	ALT. BEARING SUPPLY PRESS. PSIG	THRUST BEARING SUPPLY PRESS. PSIG	TURB. BEARING COOL. PRESS. PSIG	BOILER INLET PRESS. PSIG	DRAIN MANIFOLD PRESS. PSIG	DRAIN SUMP LEVEL INCHES	BOILER INLET FLOW IN. - HG	BOILER INLET FLOW #/MIN.	ALT. HSG. PRESS. IN. - HG	N ₂ FLOW SCFH																		
DATE OF LAST GAGE CALIBRATION																																																		
TURBINE DATA				ALTERNATOR DATA																									SPEED CONTROL																					
				NO.	TIME	SHAFT SPEED CPS	TURB. INLET PRESS. PSIG	INLET SCROLL PRESS. PSIG	INTER STAGE PRESS. PSIG	EXH. SCROLL PRESS. IN.-HG	TURB. CAVITY PRESS. IN.-HG	VOLTAGE VOLTS	CURRENT L ₁ - N METER READING	POWER METER READING	TAP SW SETTING L ₁	CURRENT L ₁ - N	POWER METER READING	VOLTAGE L ₂ - N METER READING	CURRENT L ₂ - N	POWER METER READING	TAP SW SETTING L ₂ - N	CURRENT L ₂ - N	POWER METER READING	TOTAL ALT. POWER WATTS	GANG CONTROL	FINE CONTROL	FINE CONTROL	CURRENT AMPS	POWER D.C. MILLIAMP	LEFT	CENTER	RIGHT																		
DATE OF LAST GAGE CALIBRATION							PSIG	PSIG	PSIG	IN.-HG	IN.-HG	IN.-HG	IN.-HG	°F	°F	°F	°F	°F	°F	°F	°F	°F	°F	°F	°F	°F	°F	°F	MA	MA	MA																			
CRU DATA CATEGORIES																																																		
HG PUMP				ALT. BEARING				TURBINE BEARING					THRUST BRG.	TURBINE					ALTERNATOR					NA OR NAK PUMP				MISCELLANEOUS																						
NO.	TIME	SHAFT SPEED CPS	JET NUT SKIN	DISCH. °F	BEARING BEARING °F	BEARING BEARING °F	BEARING HOUSING SKIN	BEARING SUPPLY °F	BEARING HOUSING SKIN	BEARING CAVITY NA	BEARING CAVITY °F	BEARING TURB. °F	COOL-ANT IN °F	COOL-ANT OUT °F	BEARING SUPPLY °F	BEARING DRAIN °F	CASING SKIN °F	INLET LINE SKIN °F	INLET LINE IMMER. °F	EXH. SCROLL SKIN °F	EXH. SCROLL IMMER. °F	CAVITY °F	HSG. SKIN °F	STATOR COOL. IN °F	STATOR COOL. OUT °F	GAP HGP END °F	PUMP DIA- PHRAGM °F	PUMP FLANGE SKIN °F	PUMP CAP SKIN °F	PUMP DIA+ PHRAGM °F	MTG. "V" BLOCK SKIN °F	BOX FRT. TURB. FACE SKIN °F	EXH. ELBOW (STREAM) °F																	
LOGGER POINT				2	3	4	5	6	7	8	9	10	11	12	13	15	16	17	18	19	20	21	22	23	24	25	26	28	29	30	31	32	33																	
LOGGER KEY				1												2											3																							

Heat loss from the housing was estimated by analysis. The power balance utilized spindown data, previous component test results, and CRU operational data. Spindown eliminated the turbine as a power source, wherein the component drag torques must equal the product of the angular deceleration and the shaft moment of inertia. Removing fluids or loads from any selected set of components produced an accurate power determination for those components which were operating with fluids or loads. Thus, by testing various combinations, a set of simultaneous equations was obtained. Solution of the simultaneous equations, component data, and heat balance data provided a good analysis of component performance.

The sigma limit method of data analysis was used in data reduction for the CRU I test. The sigma limit assumed that the data fell into a Gaussian distribution (Bell curve), with the number of observations on the high side equal to the number of observations on the low side. Thus the ± 1 sigma limit included 68.26% of the observations, the ± 2 sigma limit included 95.46% of the observations and the ± 3 sigma limit included 99.73% of the observations as shown below.



The shape of the above curve or sigma limit range depended upon the accuracy and number of observations. Errors might be introduced through instrument resolution, reading repeatability, hysteresis, human error, instrument location error, fluid and thermodynamic error. An overall accuracy of $\pm 5\%$ was an instrumentation objective.

To decrease the deviation band caused by instrumentation inaccuracies during the analysis of test data, statistical approaches were used. First, instrumentation was required to measure each parameter with an accuracy ranging between 0.5 and 3%, depending on the parameter being measured. Then, after a test had been performed, a statistical model (as shown in Figure 25, Section 4.3) was prepared for the input parameters. Because the possible errors mentioned earlier caused deviations much greater than normally desired if the 3 sigma limit (approximately 99%) was used, the statistical model was based on that data which fell within the 1 sigma limit of the statistical model. This reduced the total deviation band by two-thirds and the number of observations by one-third.

4.3 CRU I Tests

Figure 19, a schematic drawing of the CRU I test package, shows the paths of fluid flow through the system. This package was installed in the CRU test enclosure (Figure 20), which had been designed to provide ease in installing and removing the turbomachinery portion of the system. The enclosure insulated the CRU, thereby permitting accurate determination of housing temperatures.

Figures 21 and 22 are cross-sectional and external views, respectively, of the CRU I. During test, temperatures were recorded on the drawing at each point indicated to provide a CRU temperature profile.

PERFORMANCE TEST RIG FLOW DIAGRAM

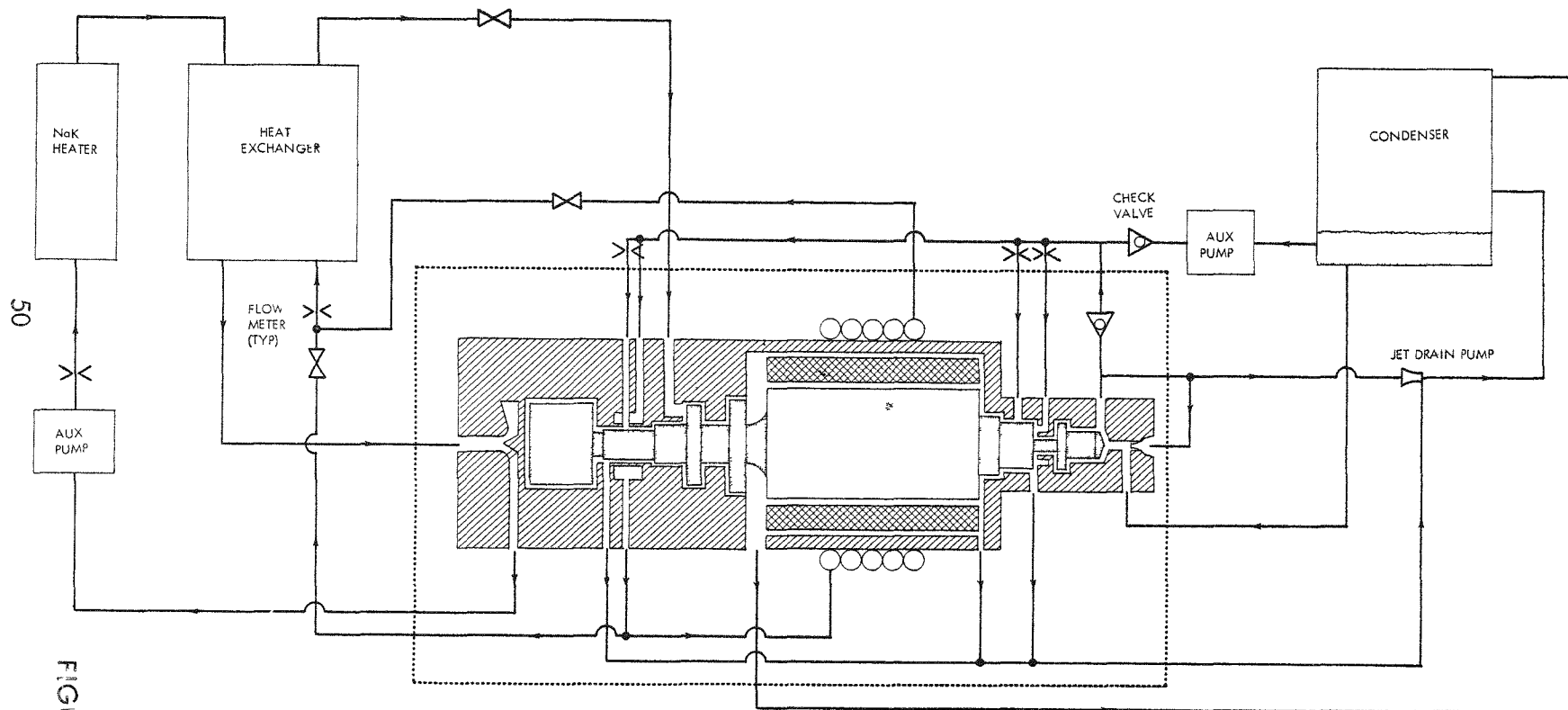
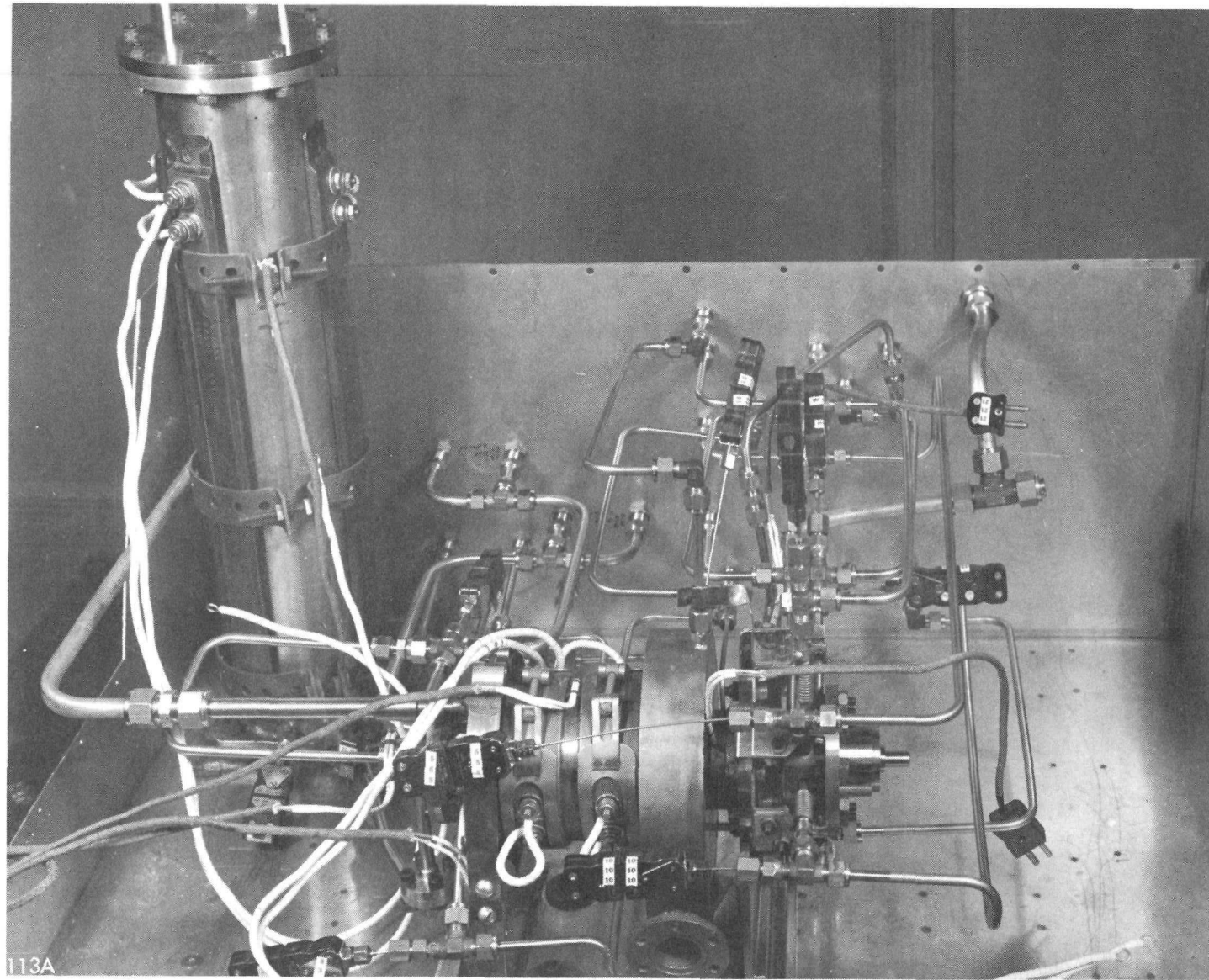


FIGURE 19

51

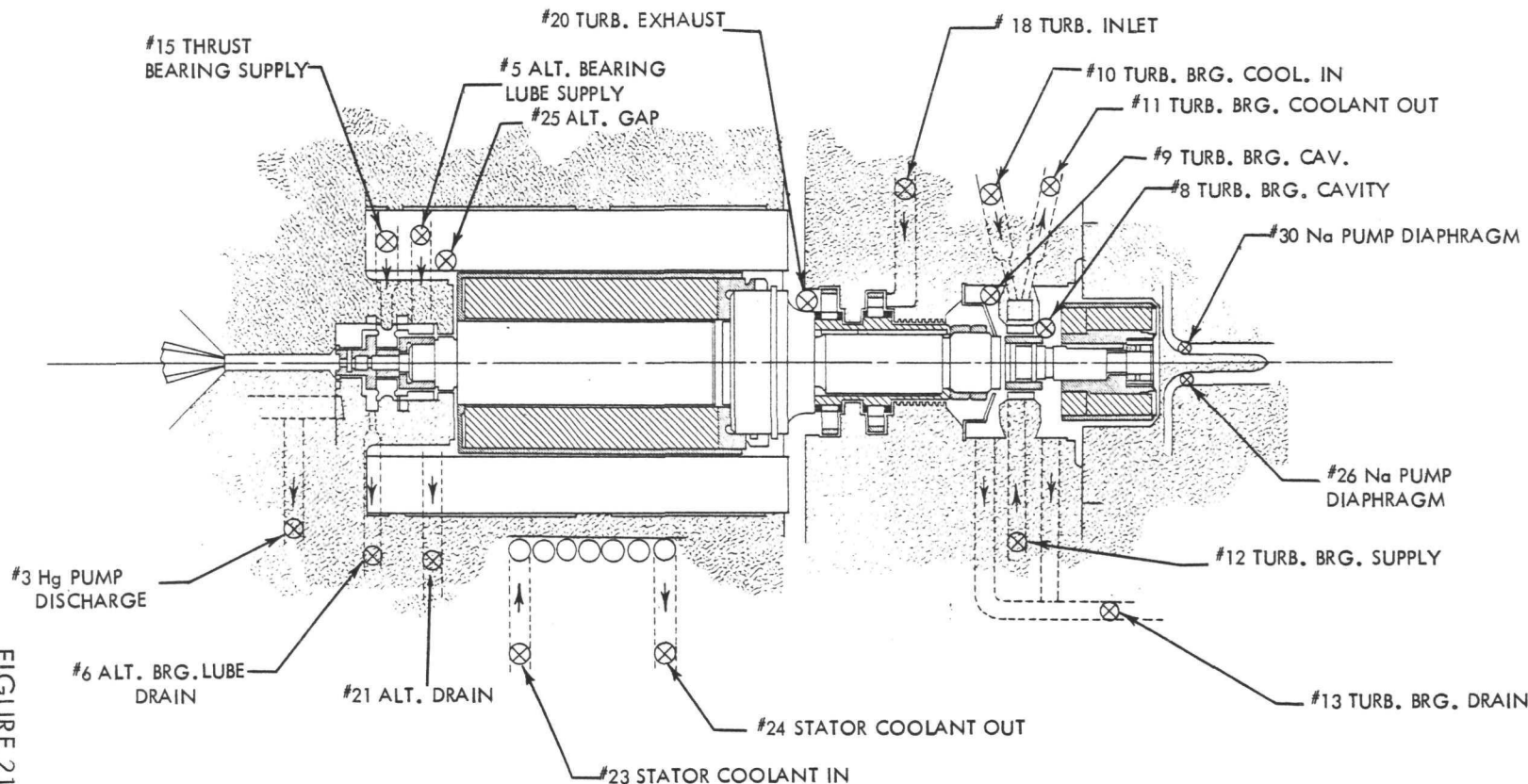


VIEW OF CRU TEST ENCLOSURE

FIGURE 20

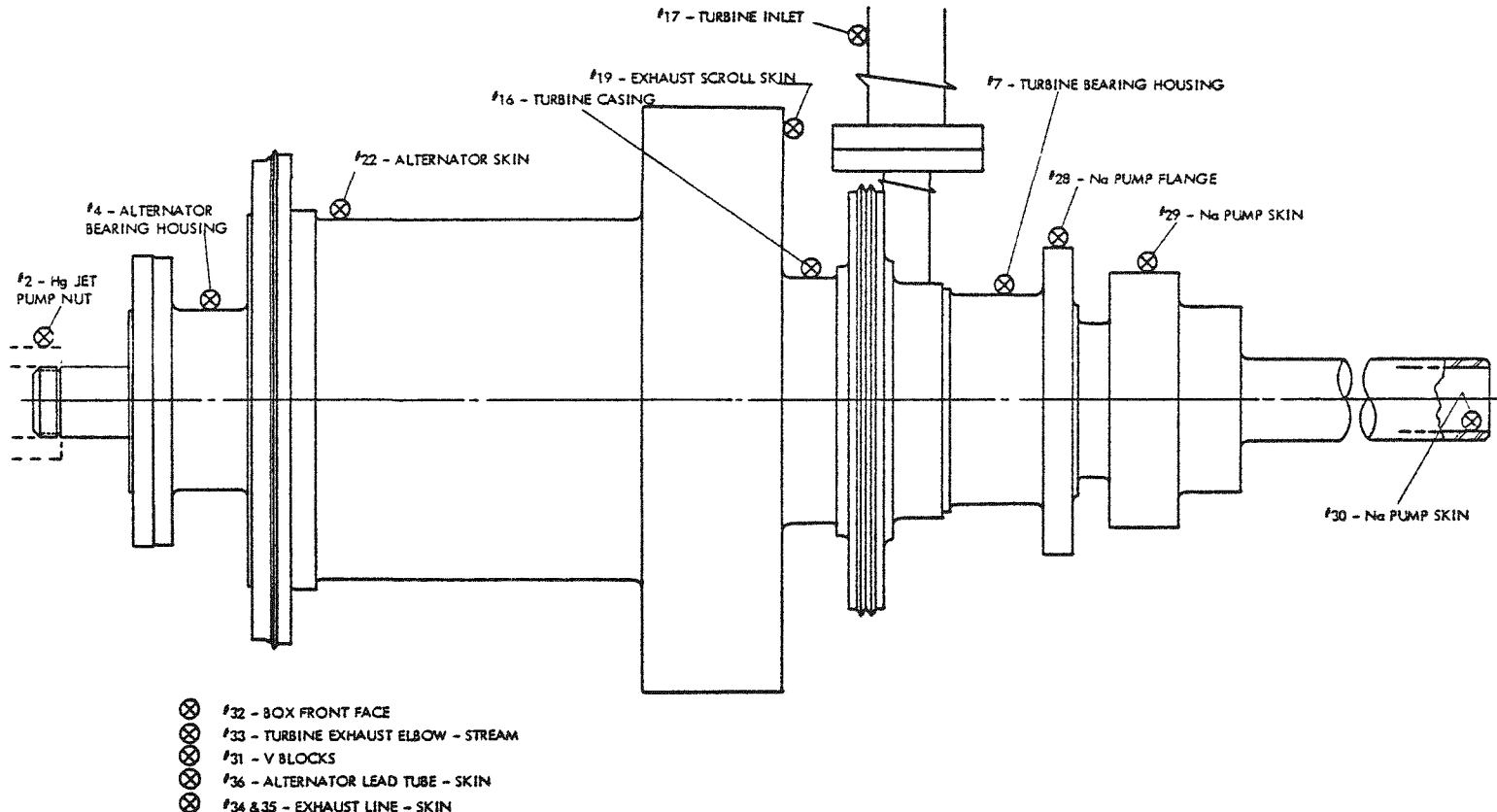
FIGURE 21

LOCATION OF CRU INTERNAL TEMPERATURE PROBES
(NUMBER AT T/C LOCATION IS TEMPERATURE LOGGER REFERENCE)



LOCATION OF CRU EXTERNAL TEMPERATURE PROBES

(NUMBER AT EACH T/C LOCATION IS TEMPERATURE LOGGER REFERENCE)



4.3.1 Critical Speed Test Results

The most significant early test result from CRU I was the indication of a shaft critical speed nearly coincident with design speed. These data were obtained by plotting CRU vibration (measured in a plane perpendicular to the shaft axis) versus shaft speed. Although an absolute value for shaft vibration amplitude was not obtained, relative vibration amplitude (Figure 23) conclusively showed the existence and point of critical speed. Had there been no critical point, the vibration amplitude curve would have simulated the dotted line in Figure 23.

CRU I testing also uncovered magnetic asymmetry in the permanent magnet material for the alternator rotors. This asymmetry caused CRU shaft radial loads large enough to prevent normal CRU startup. Rigid specifications and quality control measures were instituted to overcome this difficulty. One further result of the early CRU I tests was excessive heating in the area of the sodium pump mounting flange. Review of the data revealed that eddy-current heating was being induced by the flux leakage from the sodium pump rotor. This energy loss was reduced by using a non-magnetic material for the affected part.

An extremely significant CRU I test was a continuous 483 hour test, initiated in December, 1959. This 20-day endurance run made on CRU I most closely approached design operating conditions. During the test, operating conditions were as follows:



TABLE VI
OPERATING CONDITIONS
CRU I 20-DAY ENDURANCE RUN

<u>Parameter</u>	<u>Tested</u>	<u>Design Condition</u>
<u>Turbine</u>		
1. inlet pressure	94.7 psia	105 psia
2. inlet temperature	1145°F	1150°F
3. exhaust pressure	9.6 psia	6 psia
4. turbine flow	15.0 lb/min	17.0 lb/min
5. turbine efficiency	44%	55%
6. turbine speed	35,000 rpm	40,000 rpm
<u>Alternator</u>		
1. Output watts	2127 watts	3100 watts
2. Voltage	89.0 volts	110.0 volts
3. Current	25 amps	28.0 amps

The primary design operating conditions which were not fulfilled during this test were those of turbine speed, inlet pressure and exhaust pressure, but turbine speed and inlet pressure were only 10% away from design. Turbine exhaust pressure was more than 50% away. System speed was limited by the short span between critical speed and design speed. The accumulation of non-condensables in the condenser prevented maintenance of the design point of 6 psia in the condenser.

VIBRATION AMPLITUDE VERSUS SHAFT SPEED

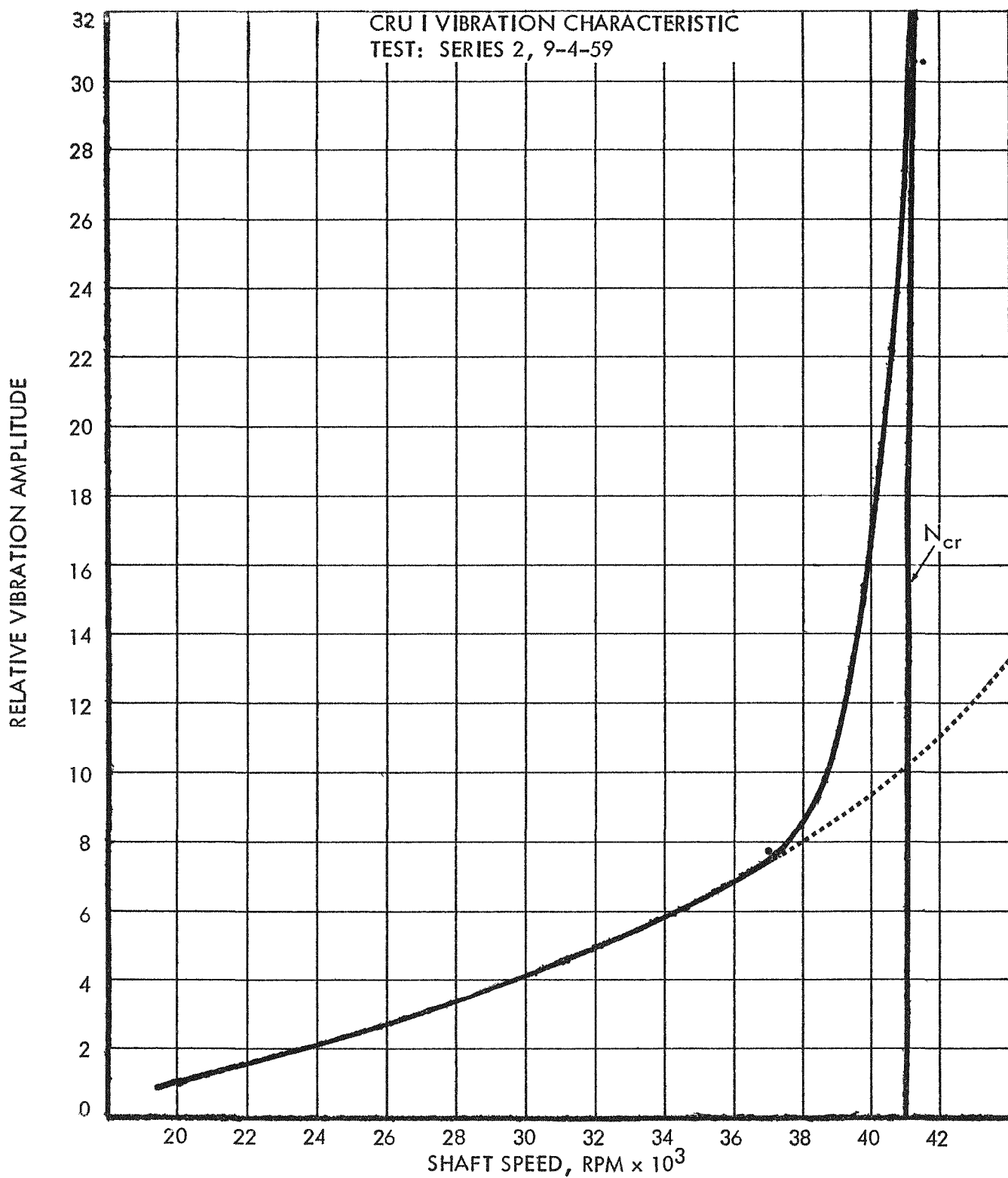


FIGURE 23

Alternator output of CRU I at design speed and turbine pressure, based upon extrapolated test data, was 2900 watts.

A plot of significant data taken during this test is presented in Figure 24. This plot shows that the performance of the CRU during this test remained constant, except for known external disturbances. Over 30,000 data observations were made during this test period. This large quantity of data at constant turbine speed and inlet conditions allowed use of the standard deviations (sigma limit) program. This program was put on a Burroughs 205 digital computer. The results of some 46 different parameters are shown in Figures 25 and 26, and in Table VII.

The 483 hour CRU I test was terminated by a short circuit in the alternator output instrumentation. As a result of the short circuit and the use of manual speed control instead of the automatic frequency control, the CRU speed increased to the critical speed with excessive bearing loads estimated at 400 pounds. Subsequent bearing seizure stopped the CRU 40 seconds after the short circuit was applied. Disassembly inspection of the hardware revealed no excessive erosion or damage from the hot mercury operation. CRU damage was limited to the turbine bearing which was scored and the alternator bearing which was scored and welded following lubricant film breakdown.

4.3.2 Vibration Testing

As a first step in qualifying the CRU for satellite launching, a program to evaluate the effect of vibration on the CRU I was next undertaken. The shaft assembly, bearings, and alternator stator bore seal were independently analyzed. Vibrations resulting from sources such as engine

PILOT OF SIGNIFICANT PARAMETERS CRU I-1B

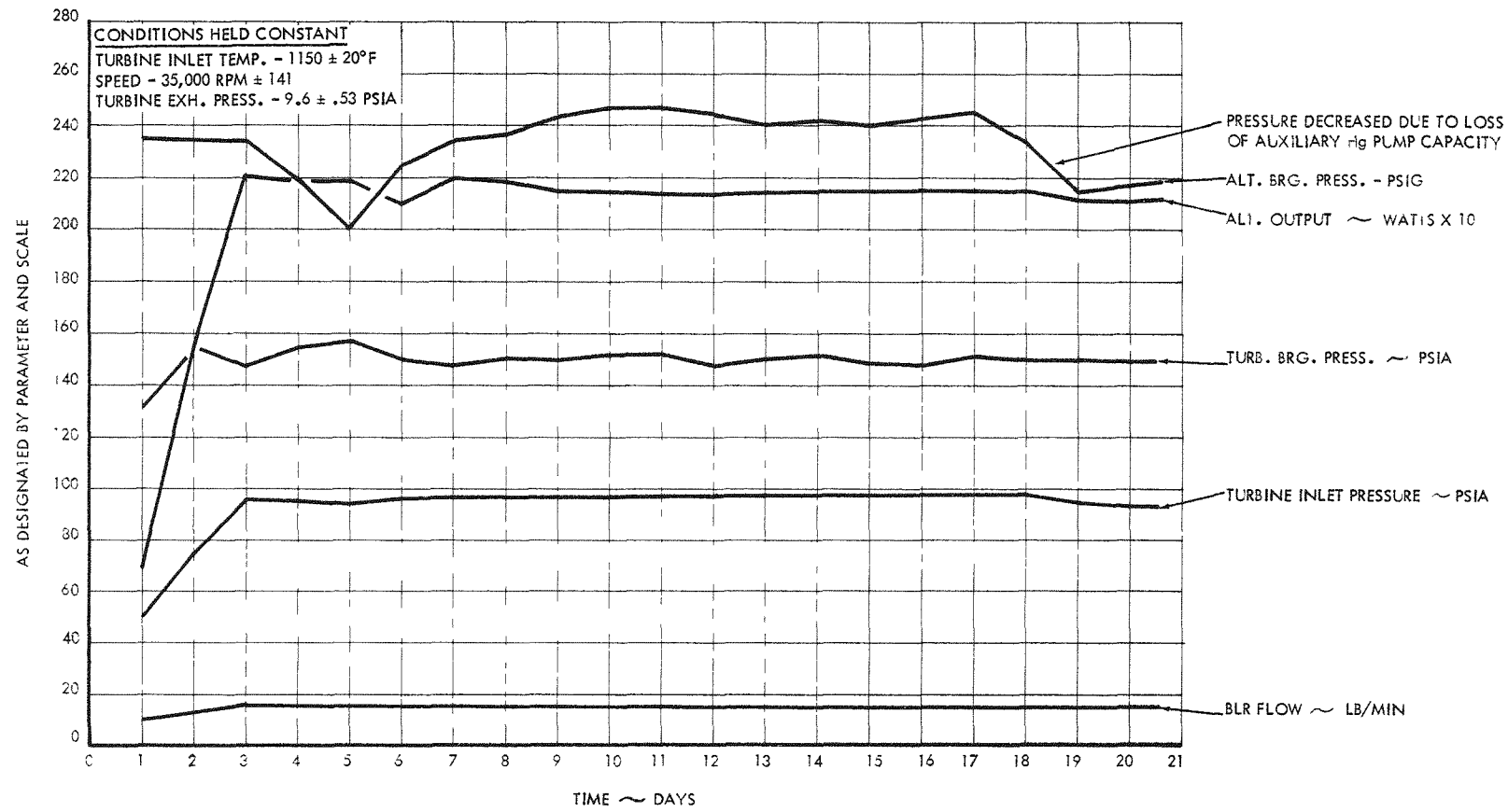
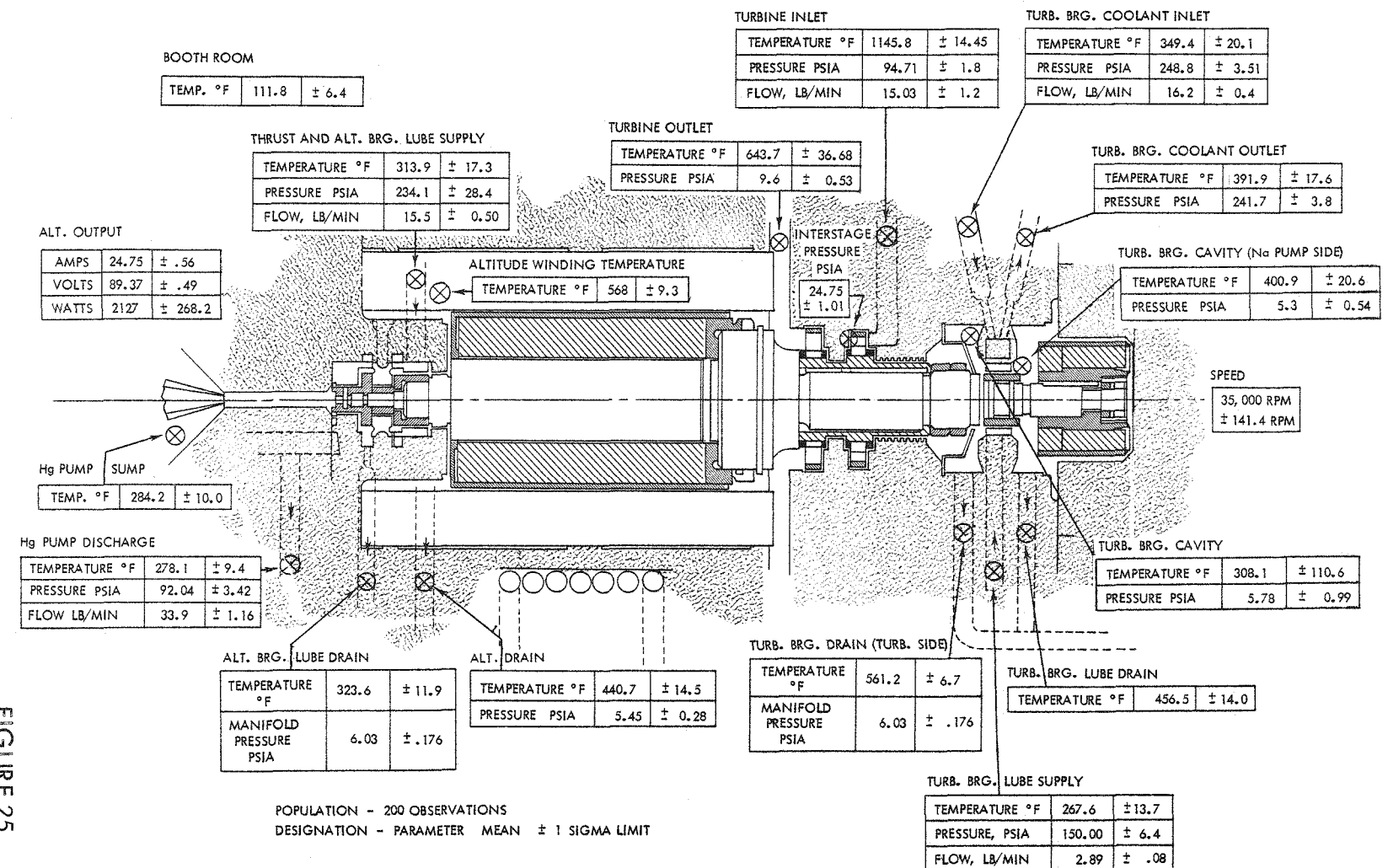


FIGURE 24

STATISTICAL RESULTS OF CRU I - 1B - 1

59



STATISTICAL HOUSING TEMPERATURE RESULTS (CRU-1B-1)

(NUMBER AT EACH T/C LOCATION IS TEMPERATURE LOGGER REFERENCE)

60

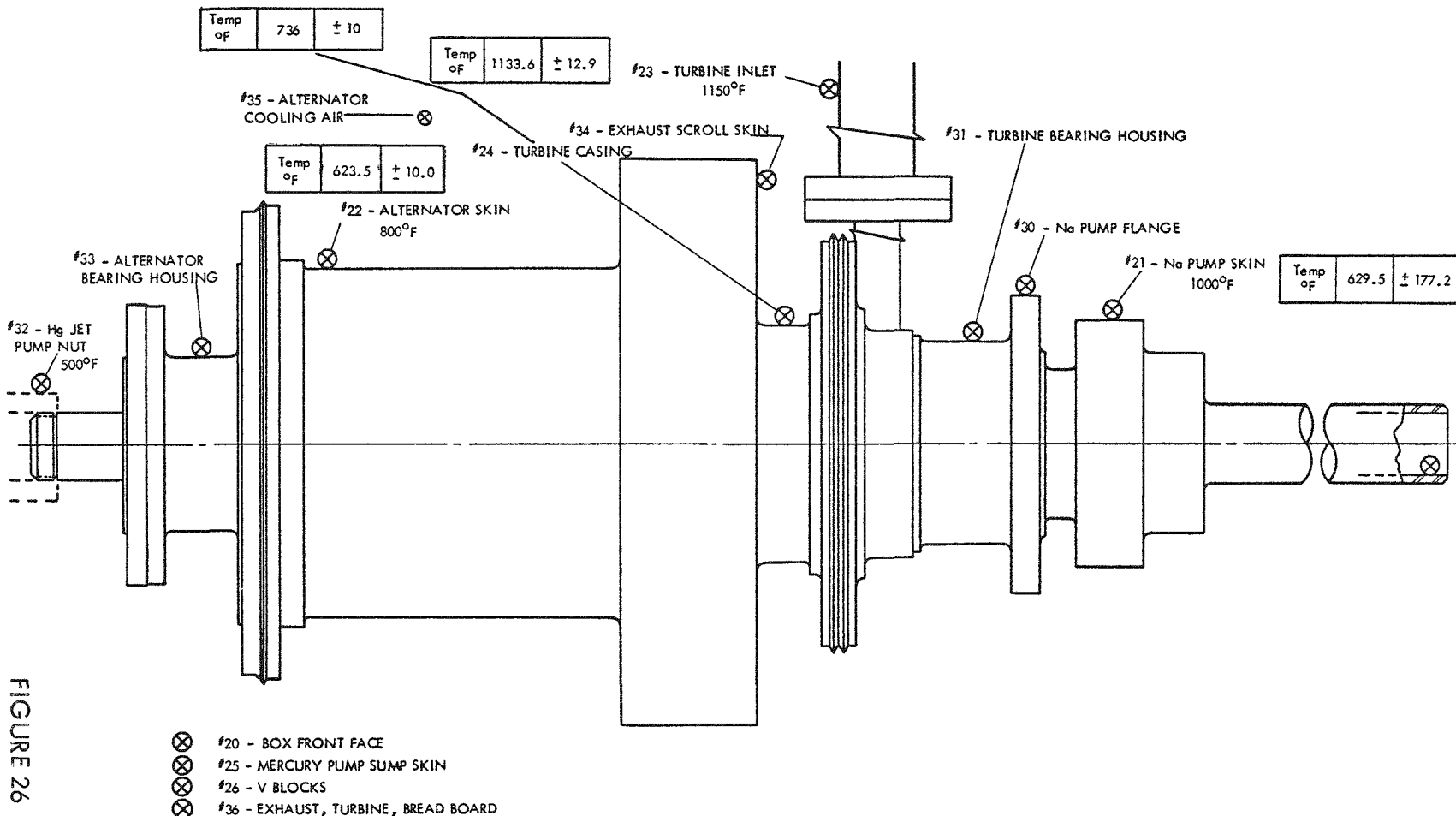


FIGURE 26



TABLE VII
SUMMARY OF CRU '73-1 TEST RESULTS

Parameter	Mean	± 1 Sigma
Turbine Bearing Lube Supply Temperature, °F	267.6	13.7
Alt. Bearing Lube Supply Temperature, °F	313.9	17.3
Alt. Bearing Lube Drain Temperature, °F	323.6	11.9
Hg Pump Sump Temperature (Inlet), °F	284.2	10.0
Turbine Bearing Coolant (Out) Temperature, °F	391.9	17.6
Bearing Coolant Inlet Pressure, Psia	248.8	3.5
Alt. Drain Vac. Pressure, Psia	5.45	0.28
Turb. Brg. Lube Drain (Na Pump) Temp., °F	456.5	14.1
Turb. Brg. Cavity (Na Pump) Temp., °F	400.9	20.6
Turb. Brg. Coolant Inlet Temperature, °F	349.4	20.1
Bearing Cavity (Na Pump) Pressure, Psia	5.28	0.54
Turbine Bearing Cavity Temperature, °F	308.1	110.6
Turb. Brg. Lube Drain Temperature, °F	561.2	6.7
Alt. Winding Temperature, °F	568	9.3
Bearing Coolant Outlet Pressure, Psia	241.7	3.8
Drain Manifold Vac. Pressure	6.03	0.176
Turbine Bearing Flow, Lb/Min	2.89	0.08
Alt. Bearing Flow, Lb/Min	15.5	0.50

TABLE VII (Continued)

Parameter	Mean	± 1 Sigma
Turbine Speed, Rpm	35000	1414
Boiler Inlet Flow Lb/Min	15.03	1.2
Alt. Output, Watts	2127	268
Turbine Inlet Pressure, Psia	947	1.8
Turbine Discharge Pressure, Psia	9.6	0.53
Turbine Interstage Pressure, Psia	24.8	1.0
Turbine Inlet Temperature, °F	1145.8	14.5
Turbine Exhaust Temperature, °F	643.7	36.7
Hg Pump Flow, Lb/Min	33.9	1.2
Bearing Cavity Turbine Pressure, Psia	5.78	1.0
Hg Pump Sump Pressure, Psia	16.37	0.34
Alt. Bearing Lube Pressure, Psia	234.1	28.4
Hg Pump Discharge Pressure, Psia	92.0	3.4
Turbine Bearing Lube Pressure, Psia	150	6.43
Hg Sump (Pump Outlet) Temperature, °F	278.1	9.4
Turbine Inlet Skin Temperature, °F	1133.6	12.9
Turbine Casing Skin Temperature, °F	736	10.7

TABLE VII (Continued)

Parameter	Mean	± 1 Sigma
Bearing Coolant Flow, Lb/Min	16.2	0.4
Hg Pump Sump N ₂ Pressure, Psia	1.64	0.479
Condenser Pressure, Psia	9.1	0.57
Booth Room Temperature, °F	111.8	6.38
Alt. Drain Temperature, °F	440.7	14.5
Na Pump Skin Temperature, °F	629.5	177.2
Alt. Skin Temperature, °F	623.5	9.98
Alt. Volts	89.4	0.5
Hg Pump Skin Temperature, °F	279.6	9.4
Turbine Valve N ₂ Pressure, Psia	16.12	0.134
Alt. Current	24.8	0.56

and equipment operation on the ground and in flight were considered in arriving at the specified sinusoidal vibration level. The specified vibration program is shown in Figure 27. In addition, components having resonant frequencies between 5 and 24.5 cps were required to withstand sinusoidal vibration at such resonant frequencies for a period of 15 minutes at amplitudes of 0.5 inch (peak to peak).

During testing, the non-operating CRU 1 was exposed to sinusoidal and random or white noise vibration with the use of an M. B. Electronics C-10D Exciter for a frequency range of 5 to 3000 cps with a maximum 15 G vibration or 0.5 peak to peak displacement. The sinusoidal or random noise signal was produced by an M.B. console as pictured to the right of Figure 28. The exciter is in the left foreground. The amplified accelerometer outputs were recorded during test with a 12-channel Century recorder, and the control console frequency output was monitored on the Century recorder as a DC shift with the use of a converter. This test recording equipment is shown in Figure 29.

Special fixtures were designed and constructed to accurately locate the CRU on the vibration exciter in both the lateral and longitudinal planes. Figures 30-31 indicate the fixturing required for the CRU 1 lateral and longitudinal vibration tests.

Inspection checks were made on the hardware prior to and after vibration testing. During the vibration test, the unit was void of mercury and not rotating to simulate the non-operating launch requirement. Inspection of tested units adhered to the following procedures:

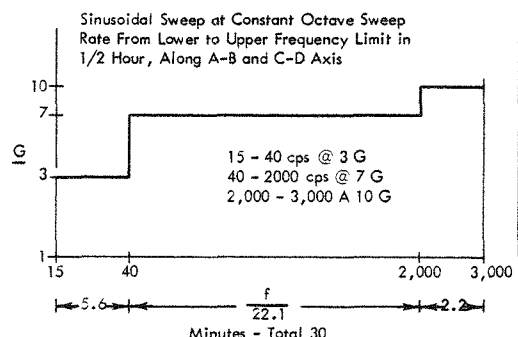
1. Shaft Assembly

- a. All mating parts were scribe lined.
- b. Critical areas were photographed ten times actual size.

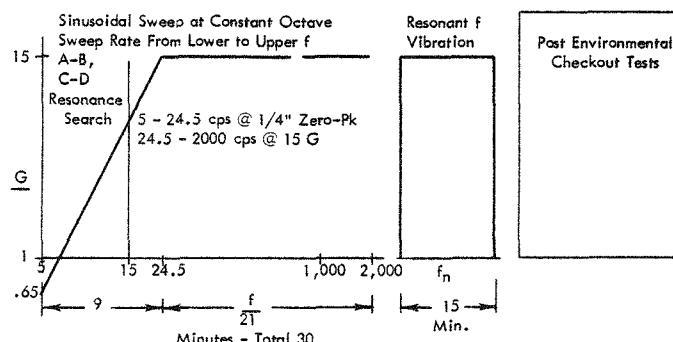
VIBRATION TEST FLOW SCHEMATIC

SINUSOIDAL VIBRATION

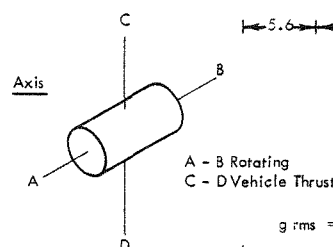
Engine Phase



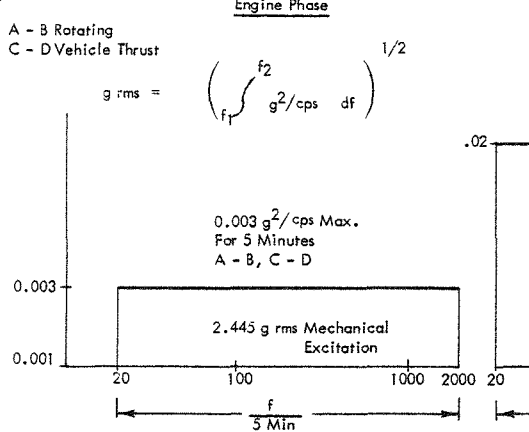
Boost Phase



WHITE NOISE VIBRATION



Engine Phase



Boost Phase

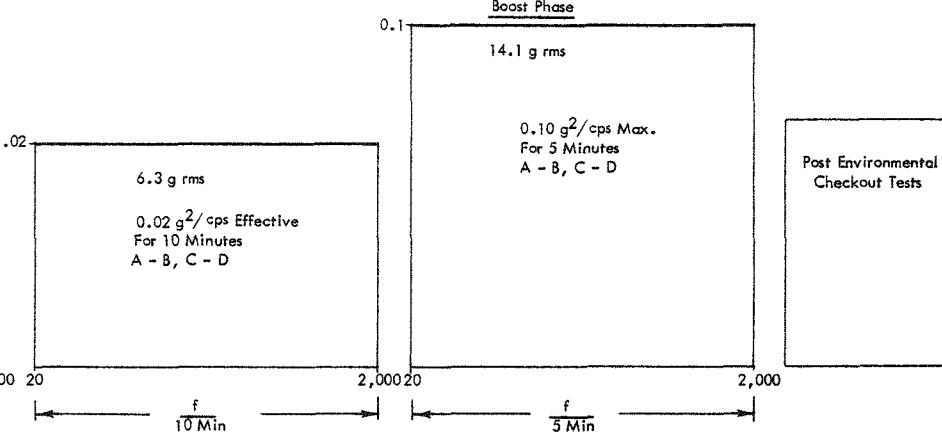
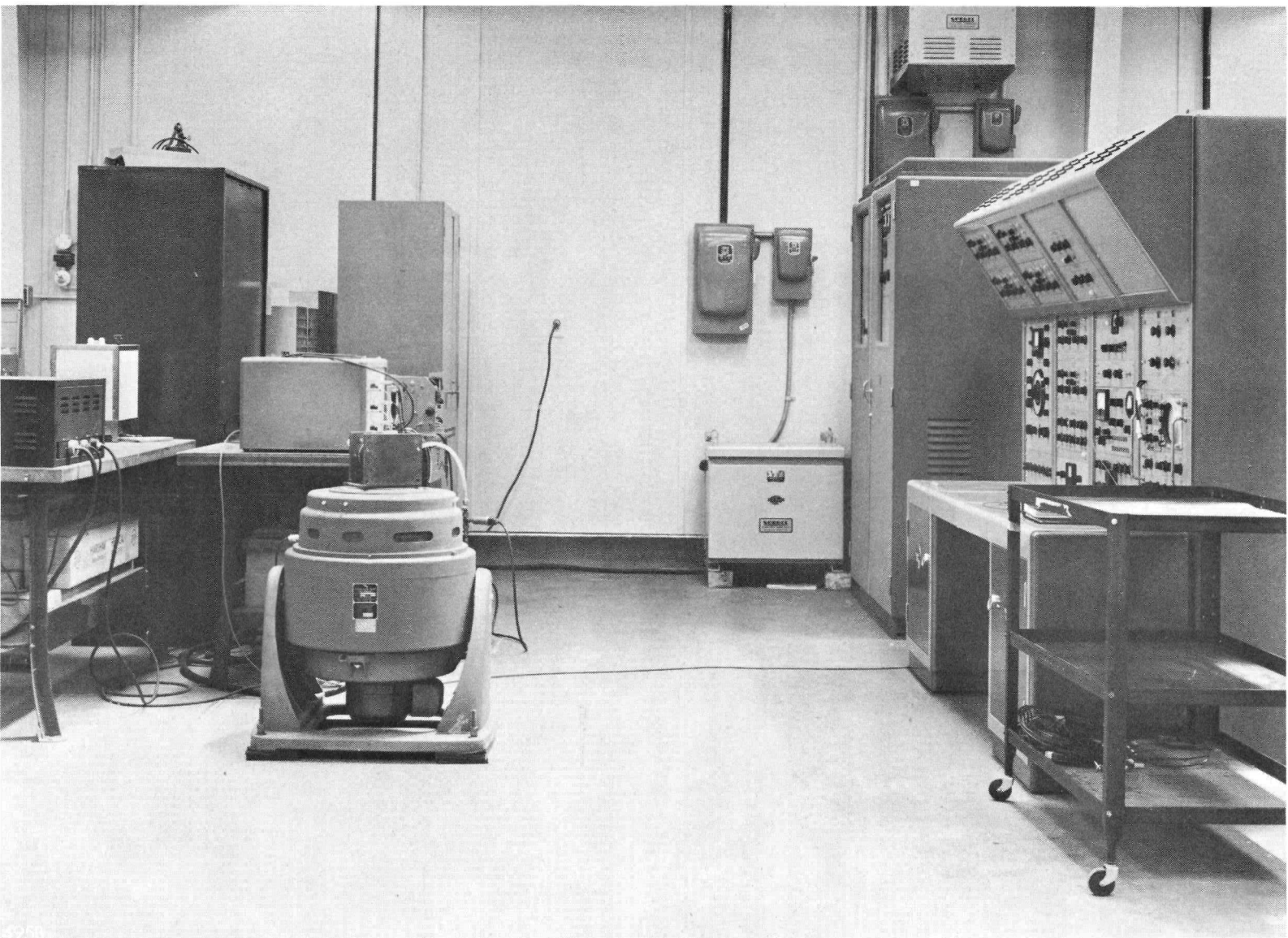


FIGURE 27



VIEW OF MB CONSOLE AND EXCITER TEST FACILITY

FIGURE 28

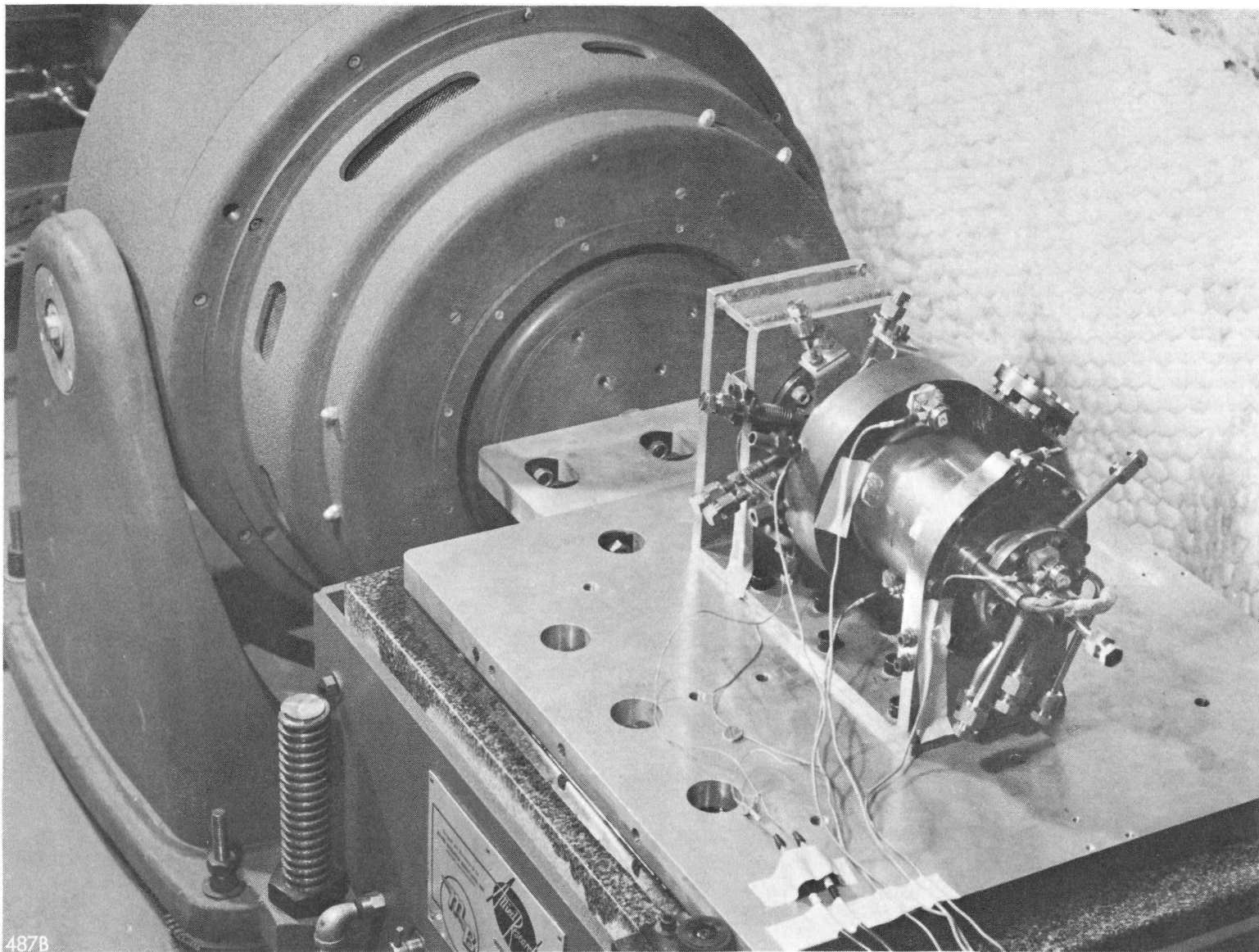
66

TAPCO a division of
Thompson Ramo Wooldridge Inc.

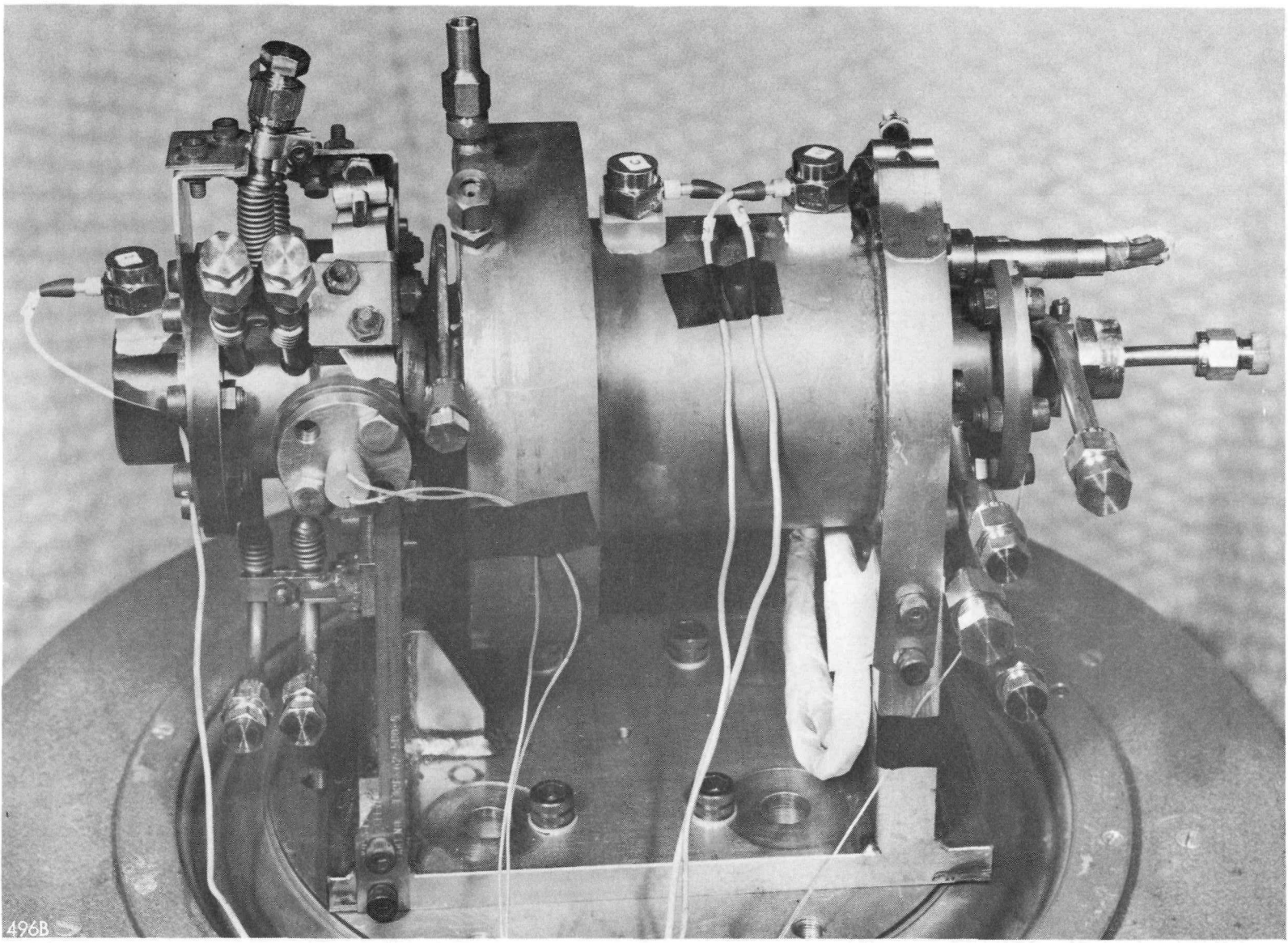


489B

TEST RECORDING EQUIPMENT



LATERAL FIXTURING REQUIRED FOR CRU I



LONGITUDINAL FIXTURING REQUIRED FOR CRU-1

- c. Indi Ron charts were made as an indication of bearing roundness.
- d. Static and dynamic balance of assembly was checked for variations from initial balancing.

2. Assembly and Disassembly of CRU

- a. All dimensions were checked.
- b. Any parts or welds were zyglo tested for fatigue.
- c. Axial and radial shaft assembly clearances with respect to housing were recorded.
- d. In the alternator stator assembly, the resistance of stator windings was checked and the stator can assembly tested for leakage.

Figure 32 presents a historical summary of CRU I vibration testing.

Three control accelerometer points were used for the CRU I in the following locations:

1. Directly to the housing shaft on the centerline of the CRU I over the center of gravity of the package.
2. On the bracket mounting leg adjacent to the alternator stator flange.
3. On the center of gravity of the bracket adjacent to the exciter table.

These locations were used to differentiate between the imposed "G" load of the exciter and the actual "G" level of the specimen, as the system under test progressed through its resonant frequency points. The accelerometer outputs also served as a basis for locating the portion of the system which is subjected to extreme resonance for future flight mounting vibration isolation.

HISTORICAL SUMMARY OF CRU I

	January	February	March	April	May	June
ENVIRONMENTAL TEST					D G	K
ASSEMBLY					C E	I
DISASSEMBLY					B E	H
PREPARATION			A			J

A - Unit to be assigned to environmental testing. Center of gravity determined, special fastening brackets for tube ends fabricated, mounting fixture reworked, straps designed and fabricated, and vertical positioning bracket for vibration tests designed.

B - Unit disassembled for inspection prior to sinusoidal vibration tests. Bearing photos, indi-ron maps, geometry recorded.

C - Unit reassembled - no modifications to assembly "C". New unit designation CRUI-D.

D - Unit subjected to 1G sinusoidal vibration, 5 to 300 cps for 30 minutes.

E - Unit disassembled. Not affected by 1G vibration.

F - Unit reassembled. Now CRUI-E.

G - Unit subject to engine phase in horizontal position for 30 minutes. No damage during test.

H - Unit disassembled. No mechanical damage.

I - Unit reassembled. Now CRUI-F in vertical fixture for engine phase test. No modifications to unit.

J - Component testing preparation - termination of CRU I environmental testing.

K - Subassembly testing. Alternator stator unit subjected to engine phase in vertical position for 30 minutes. Loose line damage.

A visual examination of the disassembled CRU I was made after both lateral and longitudinal tests were completed. Photographs of the shaft assembly, such as Figure 33, an enlarged view of the turbine bearing surface, indicated only minor dullness on the bearing in the areas under surface contact. The bearing dimension remained intact in spite of the severe contact pressures. Dimensionally, the remainder of the package showed no deviation from the original.

4.3.3 CRU Component Testing - (Alternator Stator Assembly)

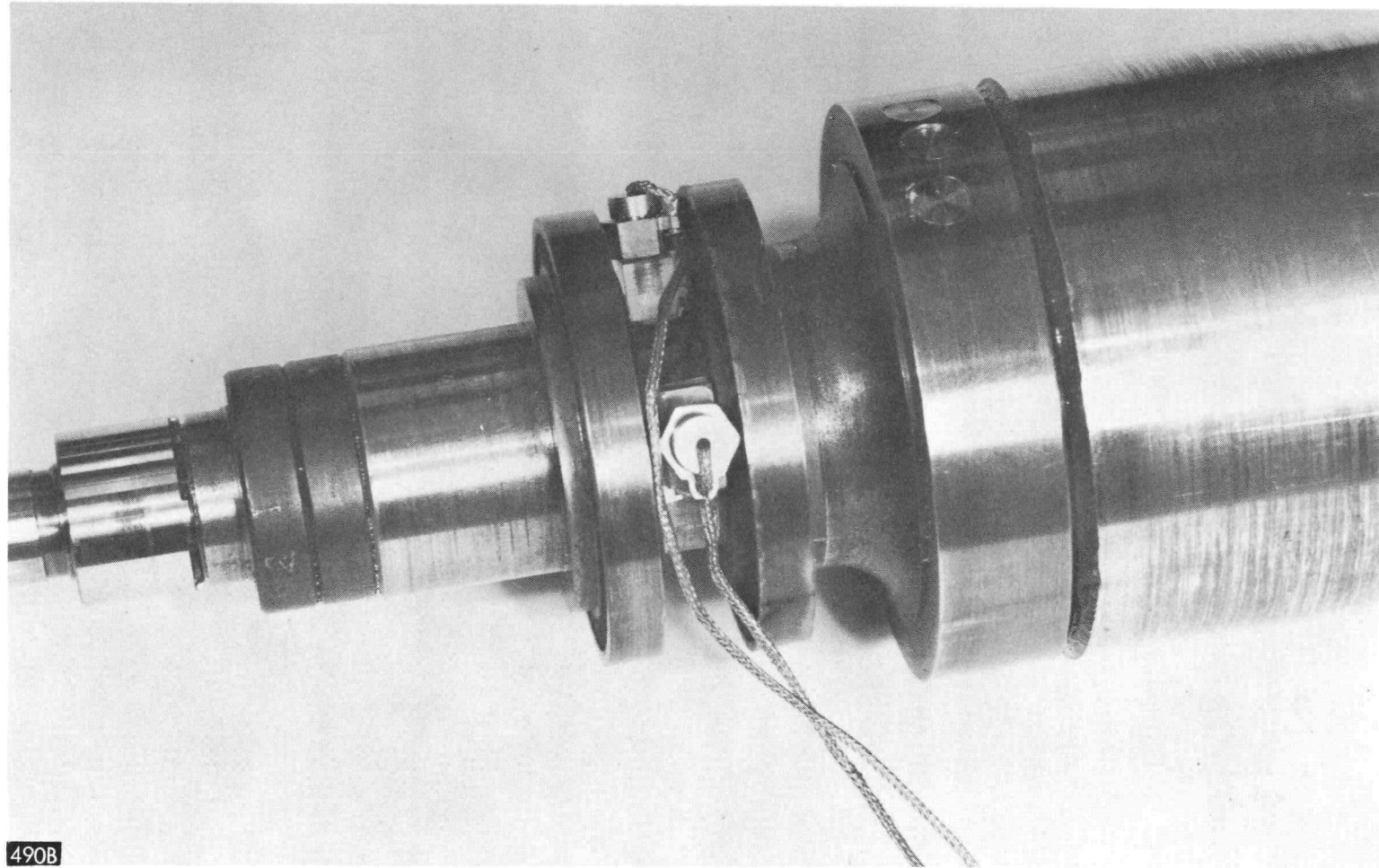
An alternator stator assembly, a CRU component, was tested in accordance with the procedures outlined earlier in Figure 27. The purpose of this testing was to determine:

1. Whether vacuum seal of the assembly was susceptible to any given frequencies, and
2. The effect of sinusoidal and random "G" loading on the sealed windings contained in the package.

To determine when and where damage occurred, a constant 20 micron vacuum was maintained in the assembly during testing.

Figures 34 and 35 show the alternator stator assembly mounted to the exciter table in the lateral fixtures. To simulate actual conditions, the internal bracket dimensions were the same as those of the CRU housing.

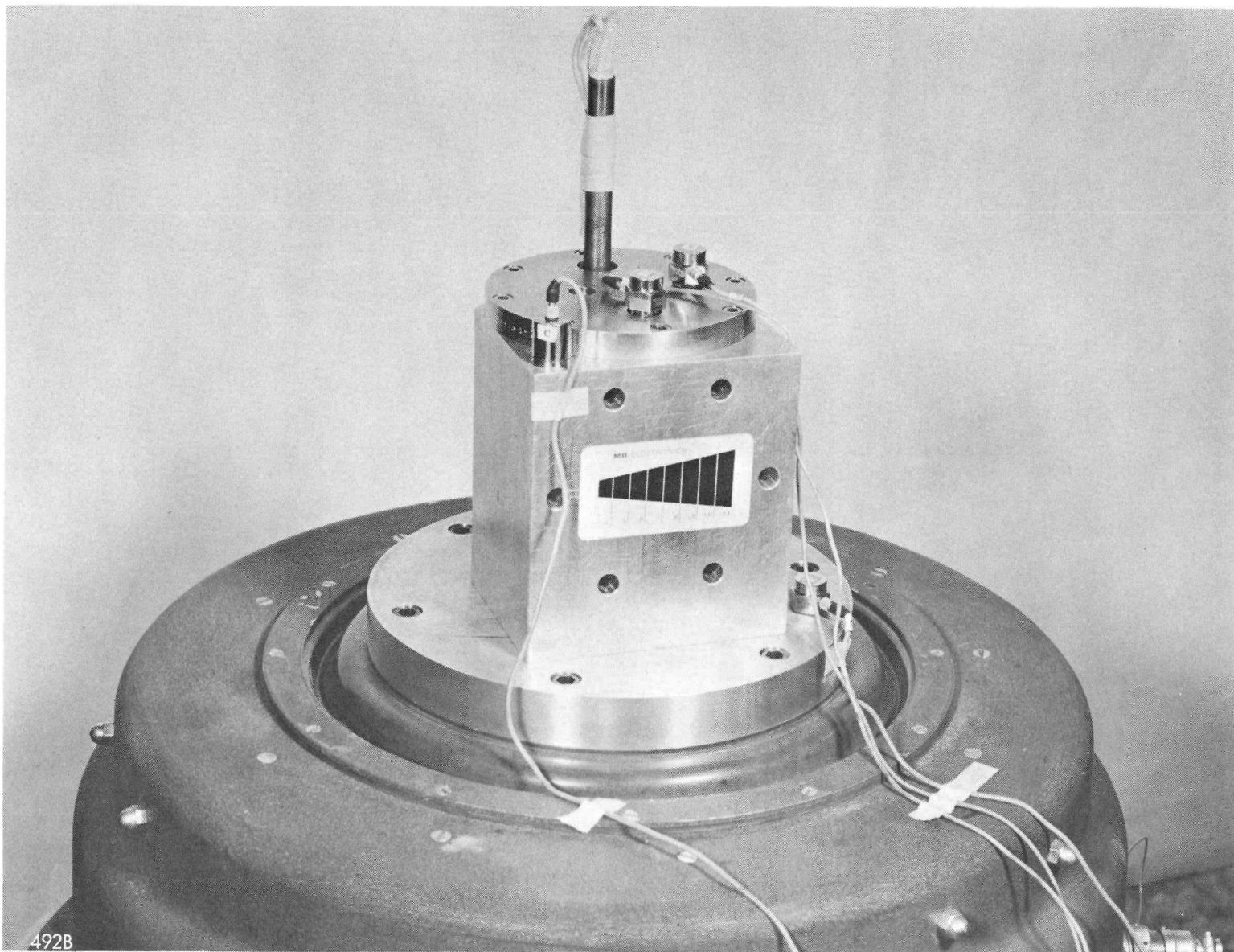
Two accelerometers were mounted to the fixture and stator assembly to indicate the actual applied "G" levels. The alternator stator retained its seal throughout the vibration test. Electrical and dimensional properties remained unchanged although the assembly was subjected to 20 G's at critical frequencies.



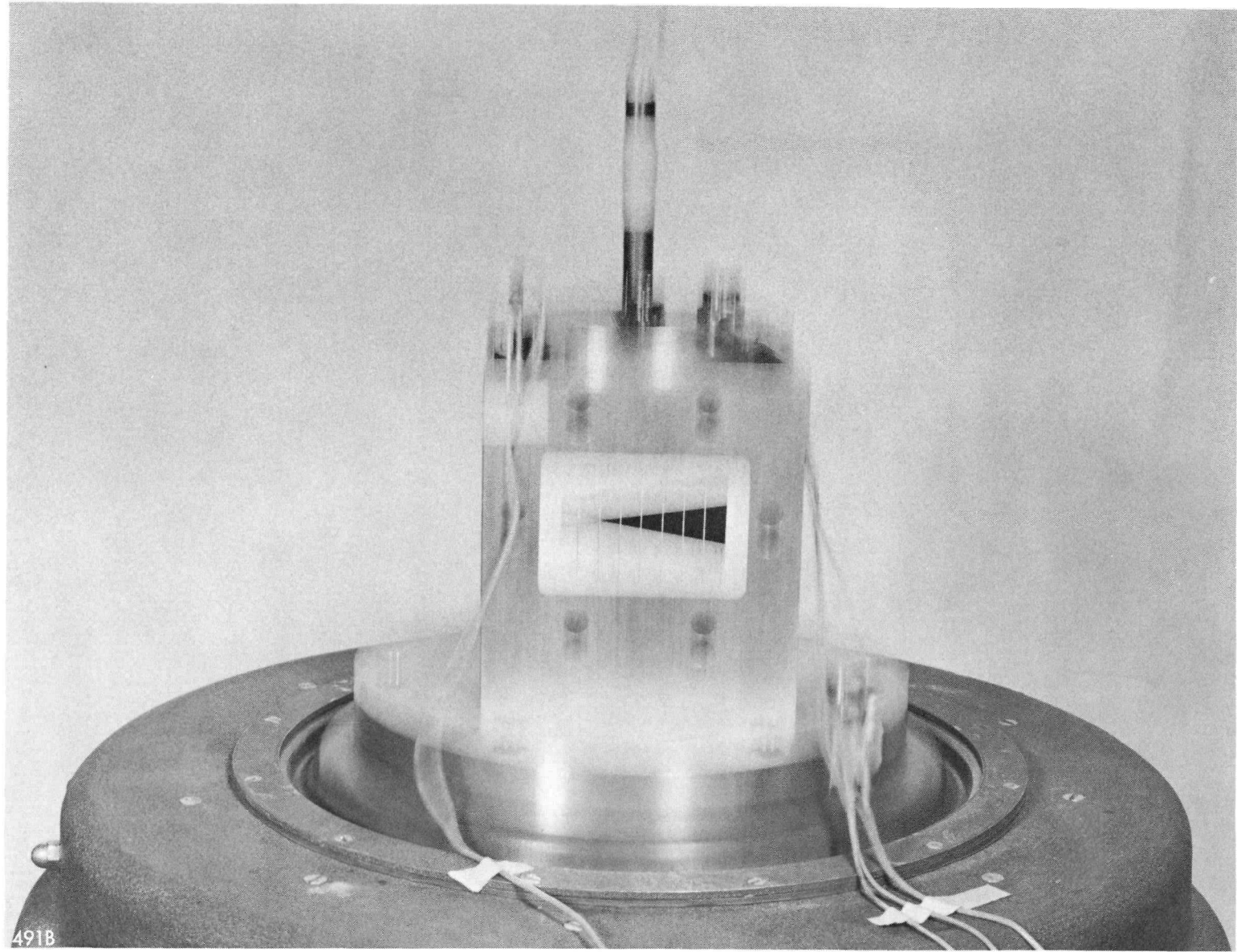
VIEW OF TURBINE BEARING SURFACE

73

FIGURE 33



VIBRATION TEST OF ALTERNATOR STATOR



VIBRATION TEST OF ALTERNATOR STATOR
(CONSTANT DISPLACEMENT PORTION)

4.3.4 Shock Testing - (Alternator Stator)

Preliminary shock tests were conducted on the ceramic materials used in the alternator stator.

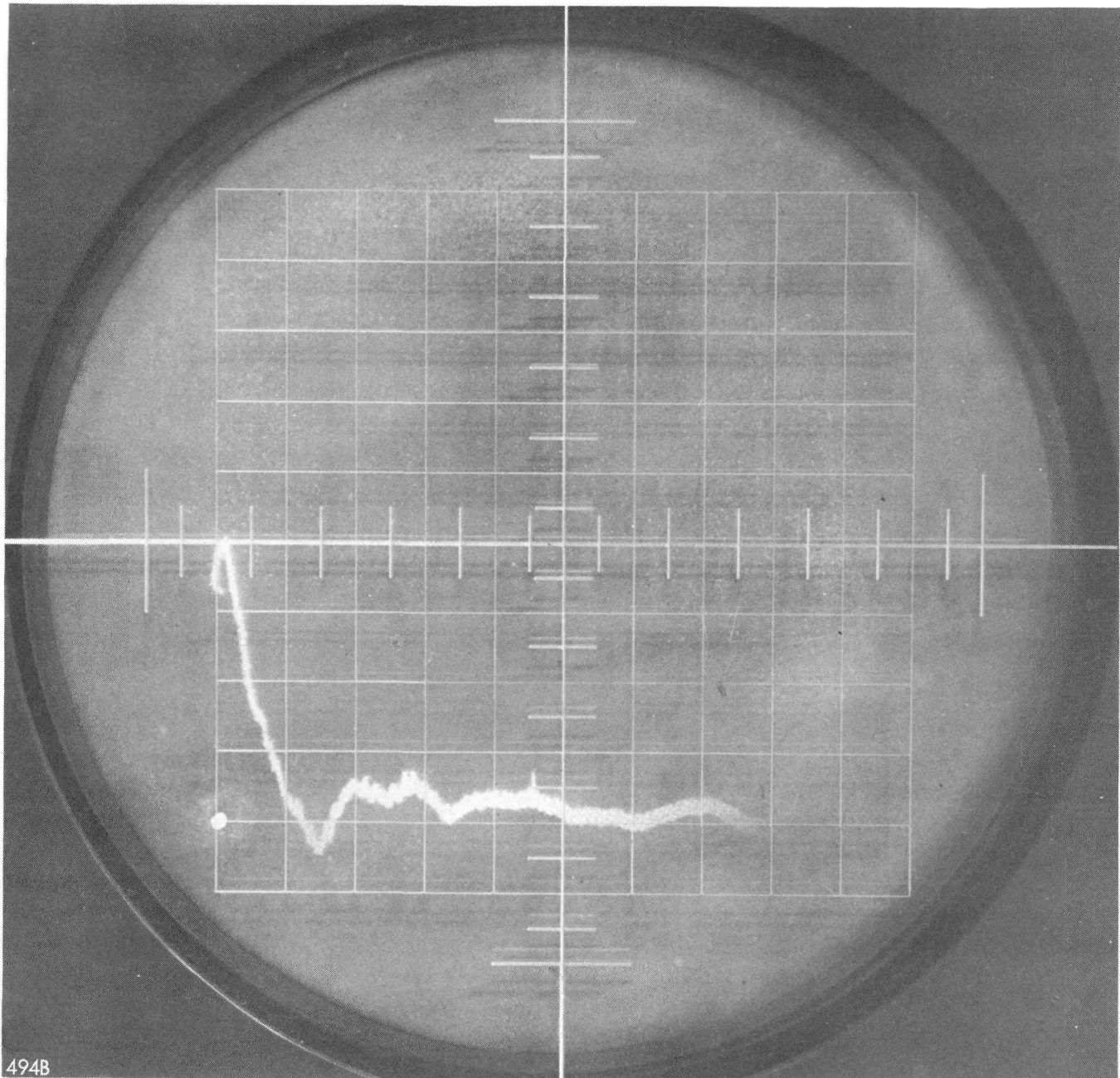
Initial specifications required a boost phase shock of 40 G's with a dwell time of 6×10^{-3} seconds and an engine phase shock of 30 G's with a dwell time of 2×10^{-3} seconds. In each of the above tests, the rise time was 2×10^{-3} seconds.

The alternator stator was mounted in a fixture representative of the CRU housing and subjected to shock to meet the specification. In the course of testing, shocks in excess of 40 G's and 6×10^{-3} seconds were achieved. A typical shock test trace pattern is shown in Figure 36. Although the stator was able to withstand initial shock tests, repeated testing resulted in hose seal fractures. In order to improve the shock capability, the alternator stator mounting was redesigned to provide a friction damping device within the CRU housing. During the period this modification was in process, the shock test specifications were reduced because of an altered vehicle configuration.

The alternator stator with the improved mounting was shock tested to the following revised specifications:

Longitudinal shock

Peak G Level	8 G
Shock wave form	1/2 sine wave
Dwell time (1/2 sine wave period)	6×10^{-3} seconds



STATOR SHOCK TEST OSCILLOSCOPE PATTERN

Lateral Shock

Peak G Level	2.5 G
Shock Wave Form	1/2 sine wave
Dwell time (1/2 sine wave period)	6×10^{-3} seconds

No damage to the stator could be found after the longitudinal and lateral tests, which equalled or exceeded the maximum G-level or the dwell time. The shock test fixture is shown in Figure 37.

4.4 CRU II Tests

CRU II was also tested in the SNAP II Performance Test Rig described in Section 4.1.

The objective was twofold:

1. Evaluation of the improved CRU package design, and
2. Establishment of direction and scope of additional component performance improvements.

The need for increased alternator output to meet additional electrical control requirements and improved component performance estimates altered the CRU II input parameters as indicated in Table VIII.

In testing and data analysis, the turbine performance was the most difficult measurement problem. In order to derive turbine shaft power from total electrical output, it was necessary to know the performance characteristics of the other CRU components. Extensive component testing at design and off-design conditions was performed to provide the required data for CRU analysis.



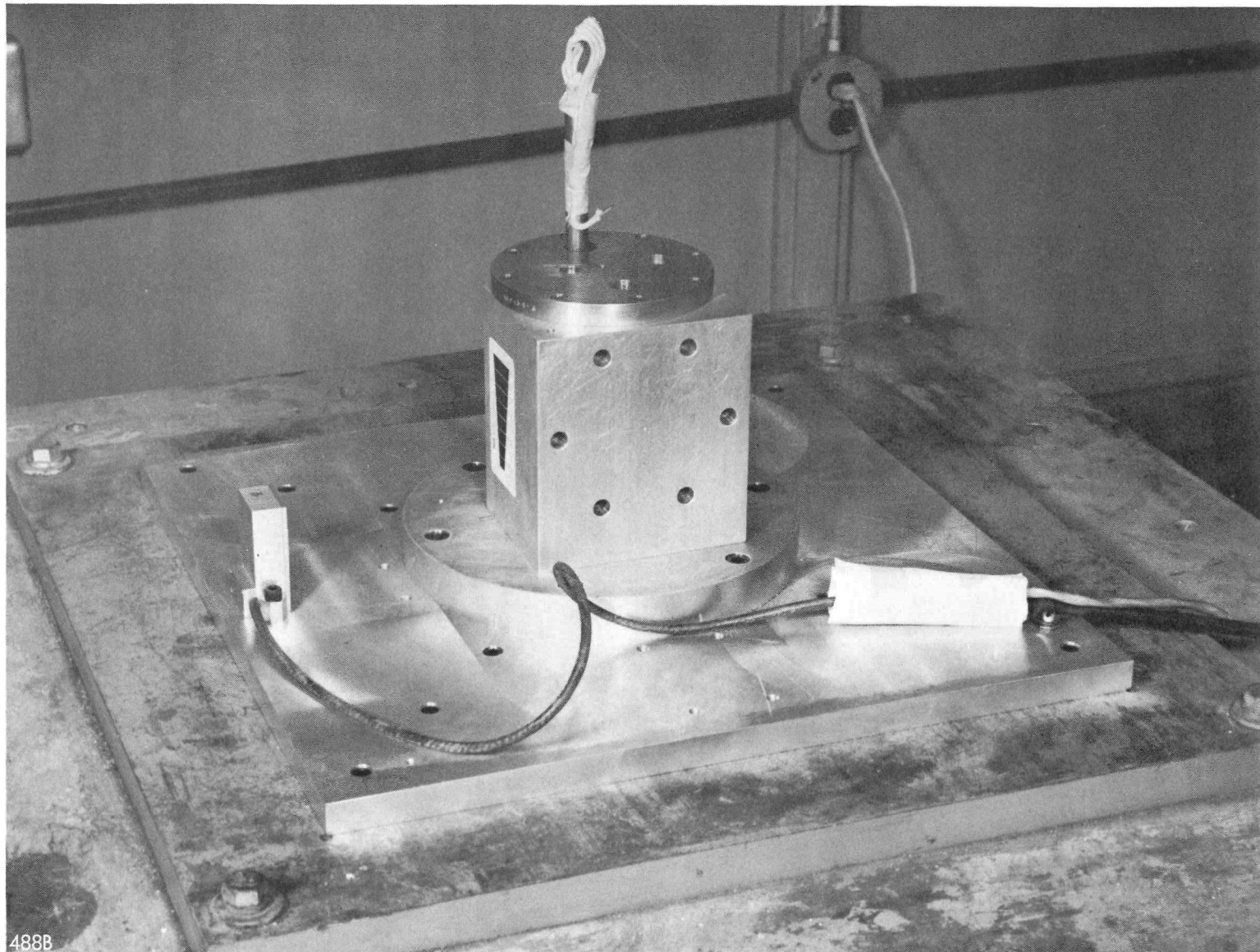
TABLE VIII
CRU II ALTERED INPUT PARAMETERS

<u>Parameter</u>	<u>CRU I Requirements</u>	<u>CRU II Requirements</u>
Turbine inlet pressure	105 psia	115 psia
Turbine inlet temperature	1150°F	1150°F
Turbine exhaust pressure	6 psia	7 psia
Turbine flow	16.7 lb/min	18.6 lb/min

The component power losses at various speeds are shown below for the CRU II-2 unit:

TABLE IX
COMPONENT POWER CONSUMPTION

<u>Component</u>	<u>10,000 rpm</u>	<u>20,000 rpm</u>	<u>30,000 rpm</u>	<u>40,000 rpm</u>
1. Alternator losses (including windage and friction)	40 watts	90	175	275 (unloaded) 383 (loaded)
2. Bearings	35	138	309	550
3. Pump (Hg)	2	14	46	111
4. Na Pump				
a. Shell Losses	4	13	34	60
b. Windage and friction	<u>1</u>	<u>4</u>	<u>13</u>	<u>30</u>
Total	82	259	577	1026
				1134



ALTERNATOR STATOR SHOCK TEST FIXTURE

As indicated in the above table, the mercury pump was operated at an off-design condition, thereby consuming only 111 watts as compared to 140 watts estimated at design. The sodium pump during the test was demagnetized, accounting for the low power consumption of 90 watts. Figure 38 shows the results of the above table plotted in an unloaded condition with and without the alternator power consumption.

To verify the power consumption of the components, the spindown technique was again employed. Spindown testing procedures with the CRU, although simple in principle, were difficult to accomplish in operation. The assumption that input energy was removed from the turbine during the spindown process was not entirely accurate under actual operating conditions. For example, liquid mercury in the cooler portions of the turbine inlet pressure line would vaporize as the pressure decayed, thus providing flow to the turbine after the turbine inlet valve had closed. It was also difficult to obtain immediate closure of the valve in the turbine inlet line at the required high temperatures. For this reason, most of the successful spindown testing was accomplished with nitrogen as the working fluid. With the CRU preheated to design temperatures, the error introduced by using a different working fluid was negligible, and experimental results of much greater consistency and accuracy were obtained.

Additional correlation on component power consumption was made using the Willans method. (Ref 2) Using this method, data taken at constant turbine speed, turbine inlet temperature, and turbine back pressure was plotted to obtain a turbine inlet pressure vs alternator output curve. Extrapolation of this curve to the abscissa yielded the total parasitic shaft power. Figure 39 shows three data points of alternator output versus nozzle inlet pressure plotted for a turbine speed of 40,000 rpm, exhaust pressure of 7.36 psia, and inlet temperature of 1050°F. Extending the

COMPONENT POWER LOSSES AT NO LOAD VERSUS SPEED

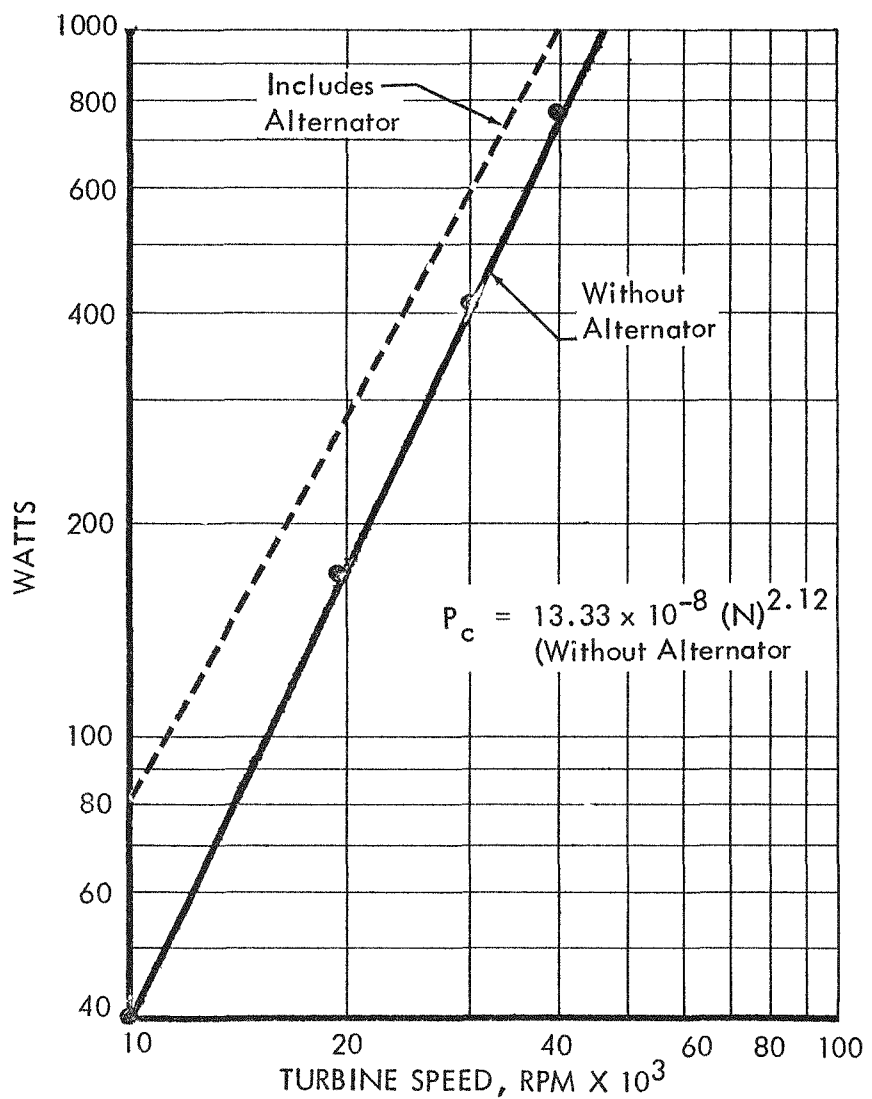
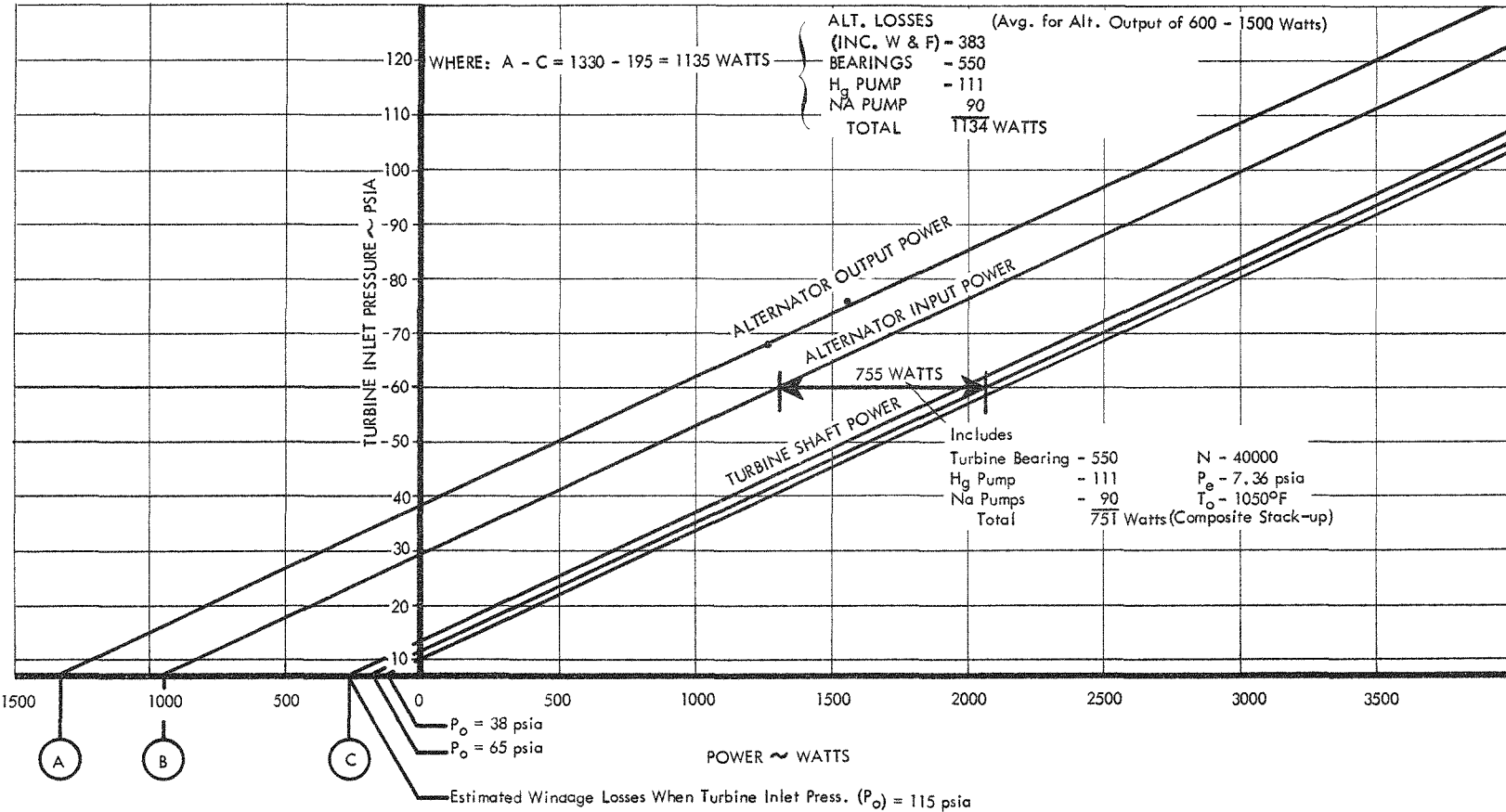


FIGURE 38

FIGURE 39

WILLIANS LINE CRU II 2-2



curve passing through the three points to the abscissa indicated that total parasitic power requirements equal 1330 watts @ 40,000 rpm, including turbine windage losses.

Summarized below are the parasitic power requirements (excluding turbine viscous losses), determined by the three methods.

NO-LOAD LOSS AT 40,000 RPM

Component Power Estimates	Spindown Power Using Alternator Calibration Curve	Willans Line
1134 watts (loaded)	1089 watts (loaded)	1135 watts (loaded)

Extracting the alternator no-load, windage, and friction power as listed earlier from the component power losses at speeds of 10,000, 20,000, 30,000, and 40,000 rpm enabled the formulation of a general component power equation for the bearings, mercury pump, and NaK pump.

$$P_c = 13.33 \times 10^{-8} (N)^{2.12}$$

It was desirable to obtain the above relationship without the influence of the alternator since normally, alternator calibration curves contained windage and friction.

Initial tests for CRU II were at turbine inlet conditions of 75 psia pressure and 1150°F. In order to determine what would be expected at the design conditions of 115 psia and 1150°F, a performance map was constructed.

Figure 40 shows the flow diagram used in preparing the program for the Burroughs digital computer. Alternator output was obtained for speeds between 20,000 and 60,000 rpm in

increments of 2000 rpm, for turbine inlet pressure of 30 to 140 psia in increments of 10 psi.

The results of this program were plotted as a performance map (Figure 41). The program also determined the turbine shaft power as a function of speed and turbine inlet pressure (Figure 42). Although a limited range of performance data was available when the performance map was prepared, later test data at design turbine inlet conditions verified the performance map.

The CRU II tests indicated improvements in the following areas of the CRU package:

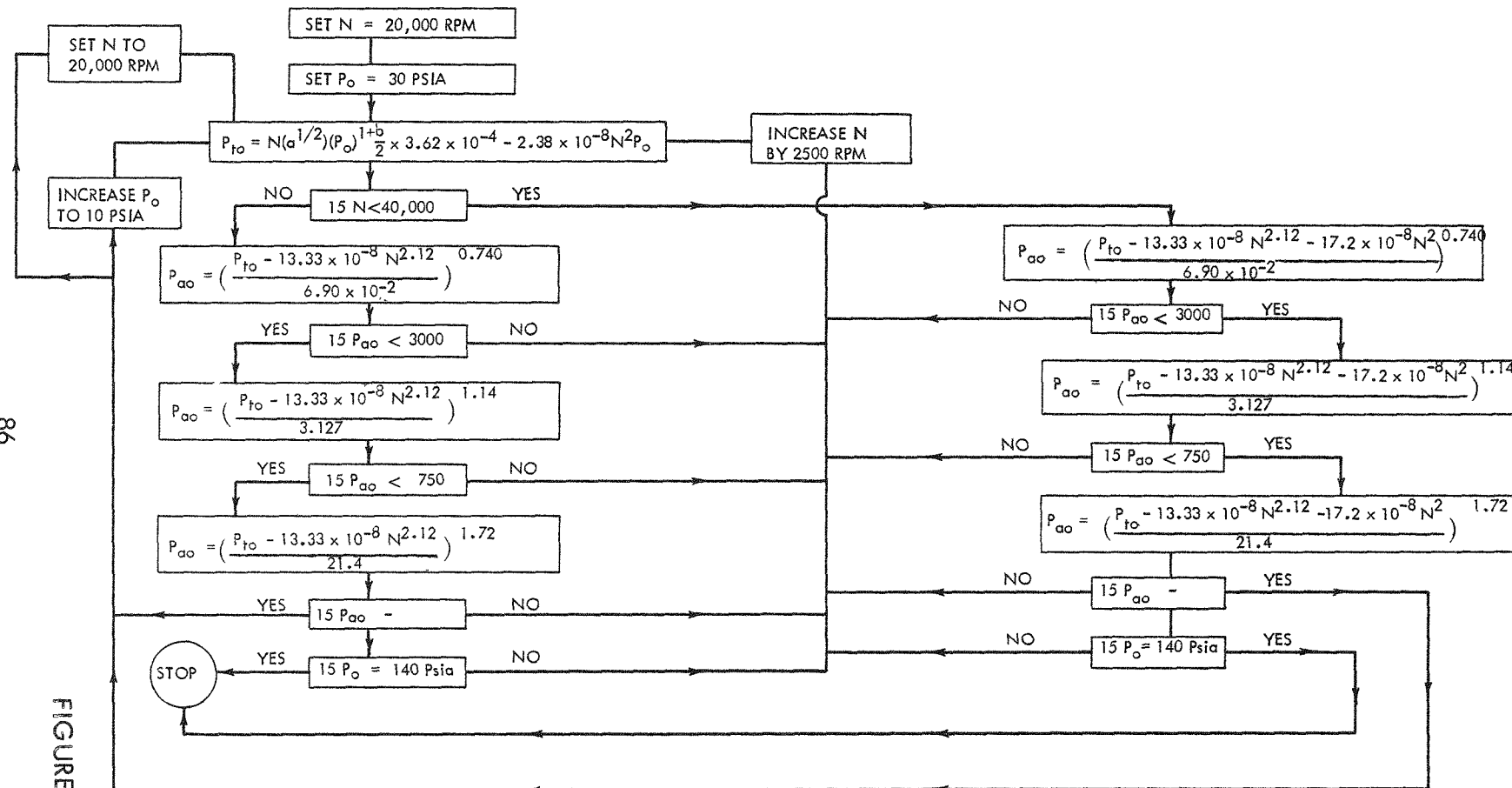
1. Alternator rotor magnetic symmetry.
2. Turbine inlet scroll.
3. Turbine exhaust scroll.
4. Turbine output power.
5. Critical speed.
6. Alternator bore seal integrity.
7. Alternator efficiency.

4.5 CRU Test Summary

A complete summary of tests conducted to August 1, 1960 on the CRU I and two CRU II units is provided in Table X. Endurance testing of CRU II was not conducted in this test series because of the system change from sodium to NaK and the availability of CRU III units by August 1, 1960.

Table XI compares the objectives for CRU I, II, and III. Representative performance for the CRU I and CRU II units were also tabulated for comparison. Na pump test results were not

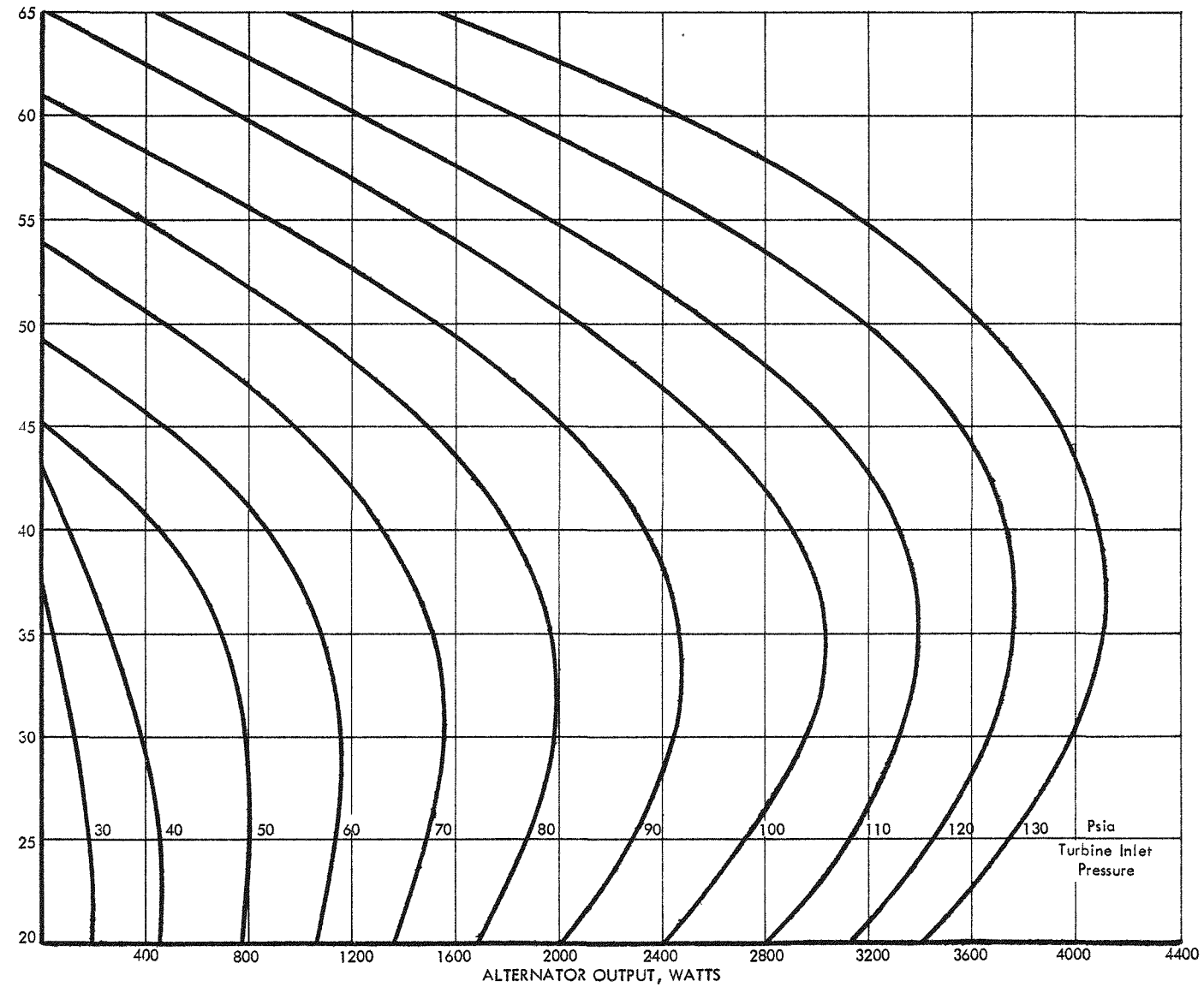
COMPUTER FLOW DIAGRAM



P_{ao} - Alternator Output Power
 P_{t0} - Turbine Shaft Power
 P_o - Turbine Inlet Pressure
 N - Speed in RPM

PERFORMANCE MAP CRU II

FIGURE 41

Turbine Conditions

- P_1 - Nozzle Inlet (As Listed)
- T_1 - Nozzle Inlet = 1150°F
- P_e - 7 Psia
- P_e - Turbine Exhaust Pressure

SHAFT POWER VERSUS TURBINE INLET PRESSURE FOR CRU II

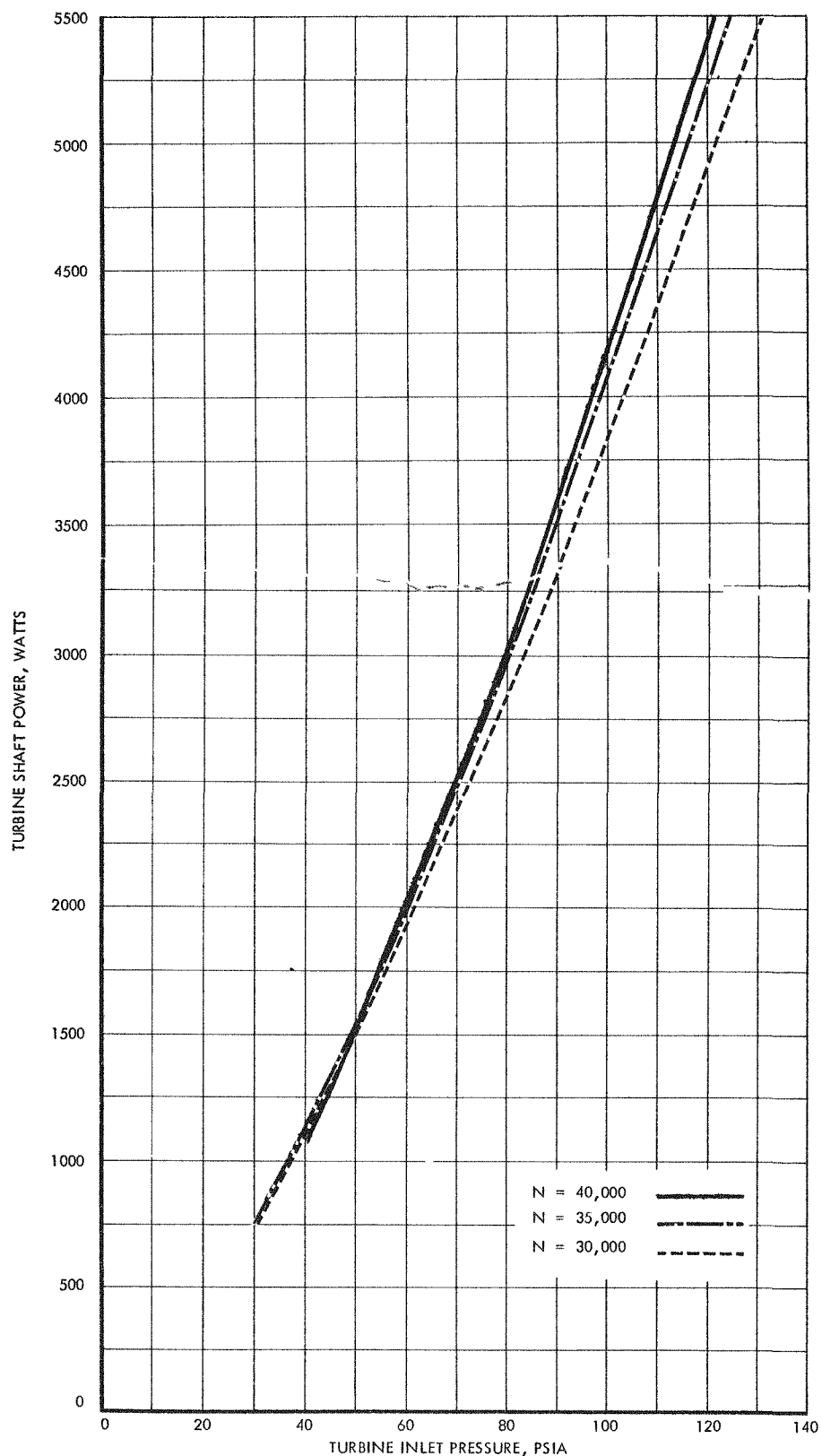


FIGURE 42

shown for CRU I and CRU II units, since the sodium pump was not operative for these tests. An electrically heated end cap was used to simulate the 1000°F sodium influence on the CRU, and in some tests the sodium pump rotor was magnetized to provide some of the power loss associated with the pump.

TABLE X

CRU I - II

SUMMARY OF TESTING

TEST NO.	DATE	TEST OBJECTIVE	RUN TIME	MAX SPEED	MAX ALT OUTPUT	REASON FOR SHUTDOWN
CRU I-1-1	8-3-59	Cold Gas Performance	0	0	0	NaK Rotor Interference
CRU I-1-2	8-4-59	" " "	0	0	0	Rotor Assymetry
CRU I-1-3	8-5-59	" " "	1 hr 21 min	35,000 rpm	500 watts	Turb. bearing heat shield overheating due to Na Rotor leakage flux
I-1B-1	9-4-59	Cold Gas Critical Speed Search	2 hr 36 min	41,000	500	Operation at critical speed resulted in bearing failure
I-1C-1	12-19-59	Hot Vapor Test	483 hr	41,500	2,100	Alternator instrumentation short circuit
I-1D	5-16-60	Non-operating shake and shock tests	-	-	-	Continuous test effort thru 1960
II-1-1	11-2-59	Cold Gas and Hot Vapor Performance	4 hr	40,000	684	Superheat low temperature shutoff with alternator seal distortion
II-1A-1	11-20-59	Hot Vapor Performance	10 hr	40,000	600	Turbine labyrinth rub
II-1B-1	6-20-60	" " "	1 hr	30,000	2,520	Turbine 2nd stage wheel rub
II-1C-1	7-6-60	Perf with Prototype Boiler	12 min	30,000	600	Turbine inlet pressure fluctuations
II-1C-2	7-8-60	Perf with Prototype Boiler	14 min	30,000	600	Turbine inlet pressure fluctuations

TABLE X (Continued)

TEST NO.	DATE	TEST OBJECTIVE	RUN TIME	MAX SPEED	MAX ALT OUTPUT	REASON FOR SHUTDOWN
II-1C-3	7-9-60	Hot Vapor Performance	21 hr	40,000 rpm	3,480 watts	Automatic shutdown due to instrument malfunction. Thermal shock cracked alt rotor can
II-2-1	4-26-60	Start-Stop Tests and CRU operation with speed control	1 hr 15 min	40,000	1,600	Test rig turbine inlet valve inoperative after 5 start stops
II-2-2	5-4-60	Start Stop Tests and CRU Performance	7 hr 50 min	40,000	1,600	Alt rotor fracture after 6 start stops

TABLE XI
CRU I - II - III
SUMMARY OF TESTING

COMPONENT	CRU NO. 1		CRU NO. 2		CRU NO. 3	
	Objective	Actual or Experimental CRU I-1B-1	Objective	Experimental CRU II-1C-3	Objective	
<u>MERCURY TURBINE</u>						
Speed (rpm)	40,000	35,000	40,000	40,000	40,000	
Mercury Vapor Flow Rate (lb/min)	15.2	15.03	17.0	17.9	18.6	
Power Output (kw)	4.39	3.46	5.16	4.63	5.67	
Turbine Shaft Efficiency (%)	55	48.7	55	46.8	55.0	
Exhaust Pressure (psia)	6.2	9.6	6.2	7.0	7.0	
Inlet Pressure (psia)	105	94.7	105	115	115	
Inlet Temperature (°F)	1150	1146	1150	1150	1150	
<u>ALTERNATOR</u>						
Speed (rpm)	40,000	35,000	40,000	40,000	40,000	
Electrical Output (kw)	3.10	2.13	3.40	3.30	3.40	
Frequency (cps)	2000	1750	2000	2000	2000	

TABLE XI (Continued)

	CRU No. 1	CRU No. 2	CRU No. 3
Voltage (volts)	115	89.4	115
Voltage Variation with Freq. Regulation of $\pm 1\%$ (volts)	$115 \pm 5\%$	-	same
Load Power Factor	1.0 to .8 lagging	1.0	same
Efficiency (%)	80	73	80
<u>SODIUM PUMP</u>			NaK Pump
Speed (rpm)	40,000	-	40,000
Flow Rate (lb/min)	45.2	-	45.2
Shaft Power Req'd - Less Windage (kw)	0.143	-	0.143
Pressure Rise (psi)	3	-	3
Efficiency (%)	6	-	2.5
<u>MERCURY PUMP</u>			
Speed (rpm)	40,000	35,000	40,000
Shaft Power Required (kw)	0.12	0.085	0.140
Net Flow Rate (lb/min)	37.0	33.9	37.0
Inlet Pressure (psia)	5.5	16.4	6.0
Outlet Pressure (psia)	138	92.0	240
			120.0
			175.0

TABLE XI (Continued)

	CRU No. 1	CRU No. 2	CRU No. 3
Efficiency (%)	15	15	25
Inlet Temperature (°F)	420	284	420
Outlet Temperature (°F)	430	278	430
BEARINGS			
Speed (rpm)	40,000	35,000	40,000
Mercury Lubricant Flow (lb/min)	16.0	17.4	16.0
Lubricant Supply Pressure (psia)	138	105	240
Lubricant Drain Pressure (psia)	6.5	6.03	6.5
Shaft Power Consumption (kw)	0.60	0.425	0.600
0.550			0.600

* Estimated power with magnets at part strength

5.0 CONCLUSIONS

As a result of the CRU design and test efforts conducted to date, the following conclusions were drawn:

1. Operation of a combined rotating unit containing a mercury vapor turbine, an alternator, a mercury pump and a primary fluid pump on a common shaft has been demonstrated.
2. Bearings utilizing the working fluid mercury have been satisfactorily employed to support the CRU shaft.
3. Component performance in the CRU configuration, at various speeds and loadings, has been found to have a reasonable relationship to the performance achieved in the component test rigs.
4. Component performance improvements of the turbine, alternator, and pumps are required to achieve overall CRU performance design objectives.
5. Continued CRU development is required to increase reliability of both the rotating unit and the associated system. The 483 hour run of the first SNAP II CRU design and the 2500 hour run of the SNAP I CRU, however, demonstrate the endurance capability of this type of system.
6. Environmental tests on the initial design offer reasonable likelihood that the CRU can successfully withstand the vehicle launch. Following establishment of the final design, additional test work will be required for verification of operability after launch.

REFERENCES

1. Burlington, R. S. and May, D. C., Jr. Handbook of Probability and Statistics with Tables. Sandusky: Handbook Publishers, Inc., 1953.
2. Church, E. J. Steam Turbines, 3rd ed., McGraw Hill Book Company, 1950.

SNAP II DISTRIBUTION LIST

Advanced Research Projects Agency 2

Advanced Research Projects Agency
The Pentagon
Washington 25, D.C.
Attn: Fred A. Koether

Aerojet General, Azusa 1

Bureau of Naval Weapons Representative
Aerojet-General Corp.
6352 North Irwindale Avenue
Azusa, California

Aerospace Technical Intelligence Center 1

Commander
Aerospace Technical Intelligence Center
Wright-Patterson Air Force Base, Ohio
Attn: H. Holzbauer, AFCIN-4Bla

AiResearch Manufacturing Co. of Arizona 2

AiResearch Manufacturing Co. of Arizona
Division of Garrett Corp.
402 South 26th Street
Phoenix, Arizona
Attn: Myric H. Currey

Air Force Ballistic Missile Division 5

Air Force Ballistic Missile Division
Hq. Air Research and Development Command
Air Force Unit Post Office
Los Angeles 45, California
Attn: Lt. Col. Melvin M. Burnett, WDAT

Air Force Special Weapons Center 6

Commander
Air Force Special Weapons Center
Technical Information and Intelligence Office
Kirtland Air Force Base, New Mexico
Attn: Delmer J. Trester



Air University Library

1

Air University Library
Maxwell Air Force Base, Alabama
Attn: Major Lee C. Free, AUL 3T-7143

Argonne National Laboratory

1

Argonne National Laboratory
9700 South Cass Avenue
Argonne, Illinois
Attn: Dr. Hoylande D. Young

Army Ballistic Missile Agency

1

Commanding General
Army Ballistic Missile Agency
Redstone Arsenal, Alabama
Attn: ORDAB-RPEF

Atomic Energy Commission, California Patent Group

1

U.S. Atomic Energy Commission
San Francisco Operations Office
2111 Bancroft Way
Berkeley 4, California
Attn: William E. Elliott
California Patent Group

Atomic Energy Commission, Washington

5

U.S. Atomic Energy Commission
Technical Library
Washington 25, D.C.

Battelle Memorial Institute

1

Battelle Memorial Institute
505 King Avenue
Columbus 1, Ohio
Attn: Dr. H.W. Russell

Bureau of Naval Weapons

2

Chief, Bureau of Naval Weapons (RRNU)
Department of the Navy
Washington 25, D.C.

Bureau of Ships

2

Bureau of Ships
Code 1500
Navy Department
Washington 25, D.C.
Attn: Melvin L. Ball

Bureau of Yards and Docks

1

Chief, Bureau of Yards and Docks
Department of the Navy
Washington 25, D.C.
Attn: Code D-440

Canoga Park Area Office

2

Canoga Park Area Office
Box 309
Canoga Park, California
(Return to AI)

Chicago Operations Office

2

U.S. Atomic Energy Commission
Chicago Operations Office
9800 South Cass Avenue
Argonne, Illinois
Attn: Chief, Office Services Branch

Chicago Patent Group

1

U.S. Atomic Energy Commission
Chicago Operations Office
9800 South Cass Avenue
Argonne, Illinois
Attn: George H. Lee
Chicago Patent Group

Chief of Naval Operations

1

Office of the Chief of Naval Operations (OP-75)
Department of the Navy
Washington 25, D.C.



Defense Atomic Support Agency, Sandia

1

Commander
Field Command
Defense Atomic Support Agency
Sandia Base
Albuquerque, New Mexico
Attn: F.C. Technical Library, Cohee W. Merritt

Department of the Army

1

Chief of Research and Development
Department of the Army
Washington 25, D.C.
Attn: Atomic Division

Director of Defense Research and Engineering (OABCW)

1

Office of Atomic, Biological and Chemical Warfare
Room 3E1071, Pentagon
Washington 25, D.C.
Attn: John E. Jackson, Director

Jet Propulsion Laboratory

2

Jet Propulsion Laboratory
California Institute of Technology
4800 Oak Grove Avenue
Pasadena 3, California
Attn: Irl E. Newlan, Supervisor
Technical Reports Department

Lawrence Radiation Laboratory

1

University of California
Lawrence Radiation Laboratory
Technical Information Division
P.O. Box 808
Livermore, California
Attn: Clovis G. Craig

Lockheed Aircraft Corp., California Division

1

Lockheed Aircraft Corporation
Dept. 01-14
Burbank California
Attn: Dr. James Everett Lipp For: Frank E. Rand, Jr.

Lockheed Missiles and Space Division 3

Lockheed Missiles and Space Division
3251 Hanover Street
Palo Alto, California
Attn: Miss Kathleen P. Nolan

Los Alamos Scientific Laboratory 1

Los Alamos Scientific Laboratory
P.O. Box 1663
Los Alamos, New Mexico
Attn: Report Librarian

National Aeronautics and Space Administration, Ames 1

National Aeronautics and Space Administration
Ames Research Center
Moffett Field, California
Attn: Director

National Aeronautics and Space Administration, Goddard 1

National Aeronautics and Space Administration
Goddard Space Flight Center
Glenn Dale Road
Greenbelt, Maryland
Attn: Librarian

National Aeronautics and Space Administration, Lewis 2

National Aeronautics and Space Administration
Lewis Research Center
21000 Brookpark Road
Cleveland 35, Ohio
Attn: Librarian

National Aeronautics and Space Administration, Langley 1

National Aeronautics and Space Administration
Langley Research Center
Langley Field
Hampton, Virginia
Attn: Associate Director



National Aeronautics and Space Administration, Marshall 2

National Aeronautics and Space Administration
George C. Marshall Space Flight Center
Publications Engineering Section
Huntsville, Alabama
Attn: Librarian, M-MS-IP

National Aeronautics and Space Administration, Washington 5

National Aeronautics and Space Administration
1520 H Street, N.W.
Washington 25, D.C.
Attn: Associate Director for Technical Information

National Aeronautics and Space Administration,
Western Operations Office

1

Director NASA Western Operations Office
150 Pico Blvd.
Santa Monica, California
Attn: Mr. John S. Keeler

Naval Ordnance Laboratory

1

Commander
U.S. Naval Ordnance Laboratory
White Oak
Silver Spring, Maryland

Naval Radiological Defense Laboratory

1

Commanding Officer and Director
U.S. Naval Radiological Defense Laboratory
San Francisco 20, California
Attn: Dr. Eugene P. Cooper

Naval Research Laboratory

2

Director
U.S. Naval Research Laboratory, Code 1572
Washington 25, D.C.
Attn: Classified Material Control Branch

New York Operations Office

U.S. Atomic Energy Commission
New York Operations Office
376 Hudson Street
New York 14, New York
Attn: Reports Librarian

Nuclear Development Corp. of America

2

Nuclear Development Corp. of America
5 New Street
White Plains, New York
Attn: Library

Oak Ridge National Laboratory

1

Union Carbide Nuclear Company
X-10 Laboratory Records Department
P.O. Box X
Oak Ridge, Tennessee

Office of the Chief of Ordnance, DOFL

1

Commanding Officer
Diamond Ordnance Fuze Laboratories
Washington 25, D.C.
Attn: ORDTL 06.33, Mrs. Elizabeth W. Channell

Office of Naval Research

2

Office of Naval Research
Department of the Navy, Code 735
Washington 25, D.C.
Attn: E.E. Sullivan

Office of Technical Information Extension,
USAEC, Oak Ridge, Tennessee

30

U.S. Atomic Energy Commission
Office of Technical Information Extension
P.O. Box 62
Oak Ridge, Tennessee



Power Information Center, University of Pennsylvania

1

University of Pennsylvania
The Institute for Cooperative Research
3400 Walnut Street
Philadelphia 4, Pennsylvania
Attn: Dr. Donald S. Murray, Security Officer
TO BE OPENED BY ADDRESSEE ONLY

Project RAND

1

Los Angeles Air Procurement District
1700 Main Street
Santa Monica, California
Attn: Administrative Contracting Officer
For: Frank R. Collbohm

Rome Air Development Center

1

Commander, Rome Air Development Center
Griffiss Air Force Base, New York
Attn: J.L. Briggs Jr.
Directorate of Engineering

School of Aviation Medicine

1

Commandant
School of Aviation Medicine
USAF Aerospace Medical Center (ATC)
Brooks Air Force Base, Texas
Attn: Chief Radiobiology Branch

The Martin Company

3

The Martin Company
P.O. Box 5042
Middle River, Maryland
Attn: AEC Contract Document Custodian

Thompson Ramo Wooldridge Inc., Cleveland

3

Thompson Ramo Wooldridge Inc.
P.O. Box 1616
Cleveland 4, Ohio
Attn: D.L. Southam

University of Washington, Applied Physics Laboratory 3

Applied Physics Laboratory
University of Washington
1013 East 40th Street
Seattle 5, Washington
Attn: Joseph E. Henderson, Director

Wright Air Development Division 3

Commander
Wright Air Development Division
Wright-Patterson Air Force Base, Ohio
Attn: WWAD-ANP

Brookhaven National Laboratory 1

Brookhaven National Laboratory
Technical Information Division
Upton, New York
Attn: Purchasing Department

Atomics International Library 20

Atomics International Library
Box 309
Canoga Park, California